

**Generation of locomotor activity
in fin motoneurons of the lamprey
during „fictive locomotion“**

**INAUGURAL-DISSERTATION
zur
Erlangung des Doktorgrades
der Mathematisch-Naturwissenschaftlichen Fakultät
der Universität zu Köln**

vorgelegt von

**Alexander Krause
aus Remagen**

Köln 2005

**Berichterstatter: Prof. Dr. A. Büschges
Prof. Dr. P. Kloppenburg**

Tag der mündlichen Prüfung: 13. 12. 2005

The Socialist Lamprey

If I'm not much to look at and you dislike my way of life
Remember that my childhood was full of woe and strife;
'Cos I was squeezed out of my Mum by an ultravigorous Dad
And dumped right on the gravel - it's all so very sad.

And if that wasn't bad enough my parents went and died
And left me orphaned in this stream, an insult to my pride;
But, when I'm a little older - some say four or five -
I'm going to change my colours and really come alive.

You may think I'm only kidding but inside my notochord
I feel these changes coming and teeth growing like a horde;
I'll live on social welfare and I'll suck you good and dry
A daily blood transfusion should keep me feeling spry.

Never mind your blood group - just let me hitch a ride
Roll over if you wish to - I'll latch on to either side
I'm not worried by your morals or your very numerous scales
Board and lodgings quite enough - I've no interest in your tails!

Your pelagic upper class has had it good to long
Don't forget we're not just suckers for you to string alone
And now I've made my mark and it looks as if you're dying
I'm off to spawn upriver, to keep the red flag flying.

Roger Lethbridge

Contents

Zusammenfassung	IV
Abstract	V
1. Introduction	1
1.1 The spinal motor system organization in lamprey	3
1.2 Two different types of motoneurons in the lamprey spinal cord	6
1.3 Questions and aims of this thesis	7
2. Material and Methods	8
2.1 Preparations	8
2.1.1 Intracellular retrograde staining of fin motoneurons	8
2.1.2 Spinal cord/notochord preparation.....	9
2.1.3 Isolated spinal cord preparation	10
2.1.4 Lesions of the spinal cord	10
2.2 Electrophysiology	11
2.2.1 Extracellular recordings.....	11
2.2.2 Intracellular recordings.....	12
2.3 Data analysis	13
3. Results	17
3.1 Two different types of fin motoneurons	17
3.1.1 Type I fin motoneurons	18
3.1.1.1 Morphological and electrophysiological description	18
3.1.1.2 Phase dependency of membrane potential oscillations	20
3.1.1.3 Temporal dependency of membrane potential oscillations	21
3.1.2 Type II fin-motoneuron	22
3.1.2.1 Morphological and electrophysiological description	22
3.1.2.2 Phase dependency of membrane potential oscillations	24
3.1.2.3 Temporal dependency of membrane potential oscillations	25

3.1.3 Comparison of both types of fin motoneurons	27
3.1.3.1 Membrane potential oscillation	27
3.1.3.2 Phase dependency	29
3.1.3.3 Temporal dependency	31
3.2 Different types of membrane potential oscillations in fin motoneurons	32
3.2.1 Different membrane potential oscillations within one period	32
3.2.1.1 Statistical classification of cells with different shape of membrane potential distribution within one period	35
3.2.2 Different membrane potential oscillations over time	38
3.2.2.1 Statistical classification of cells with different shape of membrane potential distribution over time	41
3.2.3 Electrophysiological comparison of the newly classified groups of fin motoneurons	43
3.3 Excitatory and inhibitory influences from other neurons to fin motoneurons	48
3.3.1 Synaptic input to fin motoneurons of type I	49
3.3.2 Synaptic input to fin motoneurons of type II	52
3.3.3 Synaptic input to fin motoneurons of type III	55
3.3.4 Statistical analysis and comparison of the results of current injection to the three different types of fin motoneurons	57
3.4 Lesion experiments	62
3.4.1 Extracellular recordings	62
3.4.1.1 Sagittal lesion experiments	62
3.4.1.2 Sagittal plus transversal lesion experiments	64
3.4.1.3 Summary of the results of extracellular lesion experiments	65
3.4.2 Intracellular recordings	66
3.4.2.1 Sagittal lesion experiments	67
3.4.2.2 Transversal lesion experiments	68
3.4.2.3 Sagittal plus transversal lesion experiments	70
3.4.2.4 Comparison of intact and lesioned fin motoneuron properties	70

3.4.2.4.1 Peak-to-peak amplitude	71
3.4.2.4.2 Phase of membrane potential maxima and minima	72
3.4.2.4.3 Burst duration and cycle period	75
4. Discussion	77
4.1 Different types of fin motoneurons in lamprey	77
4.1.1 Two morphological different types of fin motoneurons	77
4.1.2 Two electrophysiological different types of fin motoneurons	79
4.1.3 Different types of fin motoneurons after hierarchical clustering	80
4.2 Synaptic input to the three different types of fin motoneurons	82
4.3 Connectivity of fin motoneurons	84
4.4 Possible mechanisms for controlling fin motoneurons	86
5. References	93
Danksagung	106
Teilpublikationen	108
Erklärung	109
Lebenslauf	110

Zusammenfassung

Das Neunauge „*Lampetra fluviatilis*“ verfügt über zwei verschiedene Muskelarten für die Fortbewegung. Für die undulatorische Vorwärtsbewegung des Tieres im Wasser dient die lateral im Körper liegende myotomale Muskulatur, die antiphasisch aktiv ist. Gesteuert wird diese Muskulatur durch die myotomalen Motoneurone. Zur Kontrolle der Lage im Wasser bedient sich das Neunauge der Rückenflosse, die durch spezielle Motoneurone (Rückenflossenmotoneurone) aktiviert wird. Beide Typen von Motoneurone sind im Rückenmark des Neunauges lokalisiert. Intrazelluläre Ableitungen von myotomalen- und Rückenflossenmotoneuronen zeigten, dass letztere während der Fortbewegung immer in Antiphase zur myotomalen aktiv sind.

Hauptaufgabe in dieser Arbeit war die Frage dieser antiphasischen Koordination zu klären. Alle Versuche wurden am „fiktiv schwimmenden“ Tier durchgeführt. Als erstes wurde versucht die Rückenflossenmotoneurone morphologisch und elektrophysiologisch zu charakterisieren. Außerdem wurde durch Strominjektion in die abgeleiteten Rückenflossenmotoneurone der phasische erregende und inhibitorische Einfluß anderer Neurone ermittelt. Durch Läsionen am Rückenmark wurde versucht den kontralateralen, bzw. ipsilateralen synaptischen Eingang zu ermitteln, den die gemessenen Motoneurone erhalten.

Es konnte gezeigt werden, dass mindestens zwei morphologisch verschiedene Typen von Rückenflossenmotoneurone im Neunauge existieren, beide gekennzeichnet durch eine vielleicht für jeden Typ eigenständige Modulation des Membranpotentials.

Nach Klasseneinteilung der Membranpotentialmodulation aller abgeleiteten intrazellulären Ableitungen mit Hilfe der Methode des „hierarchical clustering“ konnte gezeigt werden, dass neben den zwei oben erwähnten Mustern noch ein drittes existiert, welches bis dato noch keinem morphologisch untersuchten Rückenflossenmotoneurontyp zuzuordnen ist. Das bedeutet, dass es in *Lampetra fluviatilis* mindestens drei verschiedene Modulationsmuster des Membranpotentials in Rückenflossenmotoneuronen gibt und diese eventuell auf ebensoviele verschiedene Zelltypen hinweisen.

Durch Injektion von Chlorid-Ionen durch negativen Strom in Zellen dieser drei verschiedenen Typen konnte für zwei Typen gezeigt werden, dass während der Oszillation des Membranpotentials

eine aktive phasische Inhibition und Erregung der Rückenflossenmotoneurone vorliegt. Für den dritten Typ reichen die Ergebnisse im Moment nicht aus um eine gesichert Aussage zu treffen.

Lesionen am Rückenmark zeigten, dass nach einem sagittalen- wie auch nach einem transversalen Schnitt das Modulationsmuster des Membranpotentials unverändert blieb, jedoch wurde die Gesamamplitude des Membranpotentials tangiert. Es konnte gezeigt werden, dass nach einem sagittalen Schnitt die Amplitude geringer wird, während sie nach einem transversalen (egal ob rostral oder kaudal von dem abgeleiteten Neuron durchgeführt) anstieg. Das bedeutet, dass Rückenflossenmotoneurone einen erregenden kontralateralen Eingang erhalten, während sie von benachbarten ipsilateralen Segmenten einen hemmenden Einfluß erhalten.

Auf Grund der ermittelten Ergebnisse und mit Hilfe der vorhandenen Literatur wurde dann ein mögliches Modell entwickelt, um zu zeigen welche Neurone Rückenflossenmotoneurone beeinflussen können und wie eine antiphasische Koordination von myotomalen- und Rückenflossenmotoneuronen im Rückenmark möglich sein könnte.

Abstract

The river lamprey (*Lampetra fluviatilis*) possesses two different types of muscles responsible for swimming. For propulsion of the animal during undulatory movement the lateral, in the trunk of the lamprey located, myotomal musculature is responsible, that is antiphasically active. These muscles are controlled by myotomal motoneurons. For controlling of the horizontal position of the lamprey, the fin of the lamprey is used, controlled by fin motoneurons. Both types of motoneurons are located in the spinal cord. Intracellular recordings of myotomal and fin motoneurons showed during swimming that the latter ones are antiphasic activated compared to myotomal motoneurons. The main aim of this thesis was to find the answer of the question how this antiphasic activation is controlled. Therefore all experiments were performed on the „fictive swimming“ animal. First it was tried to characterize fin motoneurons morphologically and electrophysiologically. Then it was resolved by current injection to the recorded fin motoneurons if they get a phasic inhibitory or excitatory drive from other neurons. Lesion experiments were used to identify whether fin motoneurons receive contralateral or ipsilateral synaptic input and whether this input was inhibitory or excitatory.

It could be shown that there are at least two morphological distinct types of fin motoneurons in the spinal cord of the lamprey, both characterized by a probably specialized shape of membrane potential oscillation. After classification of the different shapes of the membrane potential oscillations of all recorded fin motoneurons using „hierarchical clustering“ it could be shown that there is a third different membrane potential pattern, besides the two mentioned before. This third shape could not be allocated to the morphological fin motoneurons so far. The results show that there are at least three different patterns of membrane potential oscillations in the fin motoneurons of *Lampetra fluviatilis* and therefore this could be a hint that there are also three different types of cells located in the lamprey spinal cord.

After injection of negative current to these three different types of fin motoneurons it could be shown for two types of them that they receive phasic inhibitory and excitatory input during membrane potential oscillations. The data for the third type are not enough yet to confirm this result.

After sagittal and transversal lesions performed on the spinal cord of *Lampetra fluviatilis* showed that the shape of the membrane potential oscillation of fin motoneurons still persisted, but that the peak-to-peak amplitude was affected. It could be shown that after performing a sagittal lesion the peak-to-peak amplitude decreased significantly whereas a transversal lesion (rostral or caudal to the recorded cell) showed a significant increase of the peak-to-peak amplitude. This means that fin motoneurons receive excitatory drive from the contralateral hemisegment and that they receive inhibitory drive from ipsilateral located segments.

According to all the collected results and based on known literature a possible model was developed to show which neurons, located in the spinal cord, could be involved for coordinating and controlling fin motoneurons and their antiphasic activation compared to myotomal motoneurons.

1. Introduction

Locomotion is a complicated motor act requiring the coordination of different muscles in all types of animals. Be it walking, running, hopping or swimming, this coordination is performed by several neural systems that control propulsion, balancing, steering and, in legged animals, the positioning of feet accurately on the ground during each step. Both, vertebrates and invertebrates, have a similar type of neural control structure for the generation of different patterns of motor behaviour, despite the fundamental differences in anatomical organization between their neural systems. In higher vertebrates (mammals), the nervous system is very complex in nature and therefore rather difficult to analyze. It was therefore desirable to develop experimental models in which the principles of motor behaviour on the cellular level could be addressed. Such models allow us to improve our insight in the intrinsic operation of these networks, i.e. increase our understanding of how the concerted action of cells, synapses and ion channels contributes to the generation of accurate and reproducible movements. Some models like the frog embryo and the lamprey have been very useful in this context (Grillner, 2000; McLean *et al.*, 2000) and others, generating walking (mudpuppy, turtle, neonatal rodents) promise to yield important information (Jovanovic *et al.*, 1998; Nishimaru and Kudo, 2000; Stein *et al.*, 1998; Tresch and Kiehn, 2000). The organisation of these neural control systems in the brainstem/spinal cord is similar in all vertebrates (Grillner, 1985). On spinal cats it has been shown, that the motor output for rhythmic movements underlying locomotion is generated and controlled by the brain stem/spinal cord (e. g. Grillner and Zangger, 1984; Forssberg *et al.*, 1980; Barbeau and Rossignol, 1987). Within the brain stem/spinal cord, specialized neuronal circuits underlying the generation of rhythmic motor patterns („neural oscillators“ or „central pattern generators“ (CPGs)) are responsible for locomotion patterns (Delcomyn, 1980; Pearson, 2000; Marder, 2001). CPGs *in vivo* do not have a fixed output but can produce a wide variety of motor patterns according to sensory (Getting and Dekin, 1985; Bekoff *et al.*, 1987; Katz and Harris-Warrick, 1991) and central modulatory inputs (Harris-Warrick *et al.*, 1992). CPGs are located not only in the brain stem, as in cases of breathing, chewing and swallowing (Jordan *et al.*, 1992; Marder and Calabrese, 1996) but can also be, in case of locomotion patterns, located in the spinal cord itself (Grillner, 1975). Evidences for CPGs are not only given in vertebrates like cat (Grillner, 1975), neonatal rat (Smith and Feldman, 1987; Cazalets *et al.*, 1992; Magnuson and Trinder, 1997),

chicken (Bekoff *et al.*, 1989), turtle (Currie and Stein, 1988; Mortin and Stein, 1989), *Xenopus* tadpole (Roberts and Clarke, 1982; Kahn and Roberts, 1982; Roberts, 2000; Soffe, 1993) or lamprey (Grillner *et al.*, 1981), but also in invertebrates like in lobster the stomatogastric nervous system (STG) (Maynard and Dando, 1974; Harris-Warrick *et al.*, 1992), in *Clione* the locomotor system (Arshavsky *et al.*, 1985a, 1985b, 1985c), *Tritonia* (Getting, 1981; Getting and Dikin, 1985), in insects (Bässler, 1983) and in crayfish the swimmeret system (Paul and Mulloney, 1986). It has been assumed that the general functional organization of CPGs, responsible for locomotion, appears to be quite similar in all the studied species (Pearson, 1993).

Studies with both the intact and the deafferented animals show that the central pattern generating networks do not always operate as structurally and functionally independent units; in fact, they have to interact in order to produce complex different patterns of motor output characteristic of different behaviours. For example in *Tritonia*, different combinations of interacting neurons result in swimming or a defensive withdrawal response (Getting and Dikin, 1985), while in lamprey's spinal cord, changes in coordination of segmental rhythm generating circuits can produce undulatory movements appropriate for forward or backward swimming (Grillner, 1991).

One important question of the locomotion analysis concerns the neural and cellular basis of the intra- and the intersegmental control of coordination of different population sets of muscles. It is relatively easy to examine the cellular, synaptic and neural network properties of walking of the invertebrates: these organisms, as compared to the vertebrates, have a simpler organisation of the nervous system and a lower number of neurons. Thus a significant amount of information is available on the control and organization of locomotion and coordination of different sets of muscles involved in walking of invertebrates (Bässler, 1983; Delcomyn, 1985; Gewecke and Wendler, 1985; Cruse, 1990; Bässler and Büschges, 1998).

One well-studied object is the stick insect walking system (Bässler and Büschges, 1998). In the stick insect each segmental ganglion contains separate CPGs for each leg joint in every hemisegment, driving the three different muscle sets (protractor/retractor, levator/depressor and flexor/extensor) (Bässler and Wegner, 1983; Büschges *et al.*, 1995). Unfortunately, these results cannot easily be

extrapolated to the mammals, inasmuch as the organization of the nervous system of these two groups of organisms is too different. Also the organization of the neural systems of higher vertebrates is so complex (there are hundreds of different muscles which in order to produce locomotion have to act in a highly concerted action (Grillner and Orlovsky, 1991)), that in spite of all the deduced studies on these systems, it has not been possible to extract detailed information about the cellular and neural basis properties of these systems. Therefore, for examining more closely the cellular and network basis of motor behaviour and coordination of different muscle groups, other more simple vertebrate models have to be used.

Lamprey (Grillner *et al.*, 2002) and tadpole (Roberts *et al.*, 1997) are two well-established lower-vertebrate model systems which in comparison with higher vertebrates have a similar overall organization of the nervous system (Grillner *et al.*, 1997). In both systems, the CPGs for organizing the coordination of the alternating muscle contractions are well investigated (Butt *et al.*, 2002; Grillner, 2003). Both, tadpole and lamprey are capable of producing several fixed behaviour pattern (e. g. swimming- and struggling pattern in tadpole (Soffe, 1993), upward-, down-, forward- and backward swimming in lamprey (Grillner and Wallén, 2002)), controlled by locomotor circuits located in the spinal cord. Due to the lack of a second motoneuron population which would differ from the tadpole myotomal motoneurons, the tadpole model system is not usable for the study of systems which control different sets of motoneurons. In contrast, the lamprey is an ideal model system for investigation of coordination of two different motoneuron populations, because of its two different muscle sets, the fin muscles and the myotomal muscles, each set controlled by different motoneurons.

1.1 The spinal motor system organization in lamprey

As many other fish and amphibians the intact lamprey swims by producing a mechanical wave propagated from head to tail pushing the animal forward. This propulsion wave is produced by successive activation of myotomal muscles located in the body wall, coordinated by neurons located within the segments of the spinal cord. The activity of the different neurons in the lamprey spinal cord can be induced *in vitro* by continuous perfusing the spinal cord with an exogenous glutamate

receptor agonist (e. g. NMDA) and recorded via ventral roots (Cohen and Wallén, 1980; Poon, 1980). The recorded burst patterns are similar to those recorded electromyographically in the intact swimming animal and are therefore called „fictive swimming“ (Wallén and Williams, 1984). The motor pattern of lamprey swimming consists of lateral undulations of the body which propagate from the head towards the tail. In the spinal cord/notochord preparation, the corresponding pattern consists of rhythmic bursts of action potentials in ventral roots which alternate between the two sides of the spinal cord, and the burst onset of each ventral root leading to the burst onset in the next caudal ventral root of the same side. Both the durations of the action potential bursts and the delays of the burst onsets along the cord are scaled to cycle period so that for a wide range of cycle periods, the burst durations remain constant at about 35-40% of the cycle period, and the onset delays remain constant at about 1% of the cycle period per segment (Grillner, 1974, 1985; Wallén and Williams, 1984). The lamprey CPG controlling the myotomal motoneurons and therefore the rhythmical muscle contractions during swimming is well understood (Grillner and Wallén, 2002; Grillner, 2003).

The present findings suggest that the CPG, located in each segment of the spinal cord of the lamprey, is built of two half centres each inhibiting the other when active. Each of the half centres of the

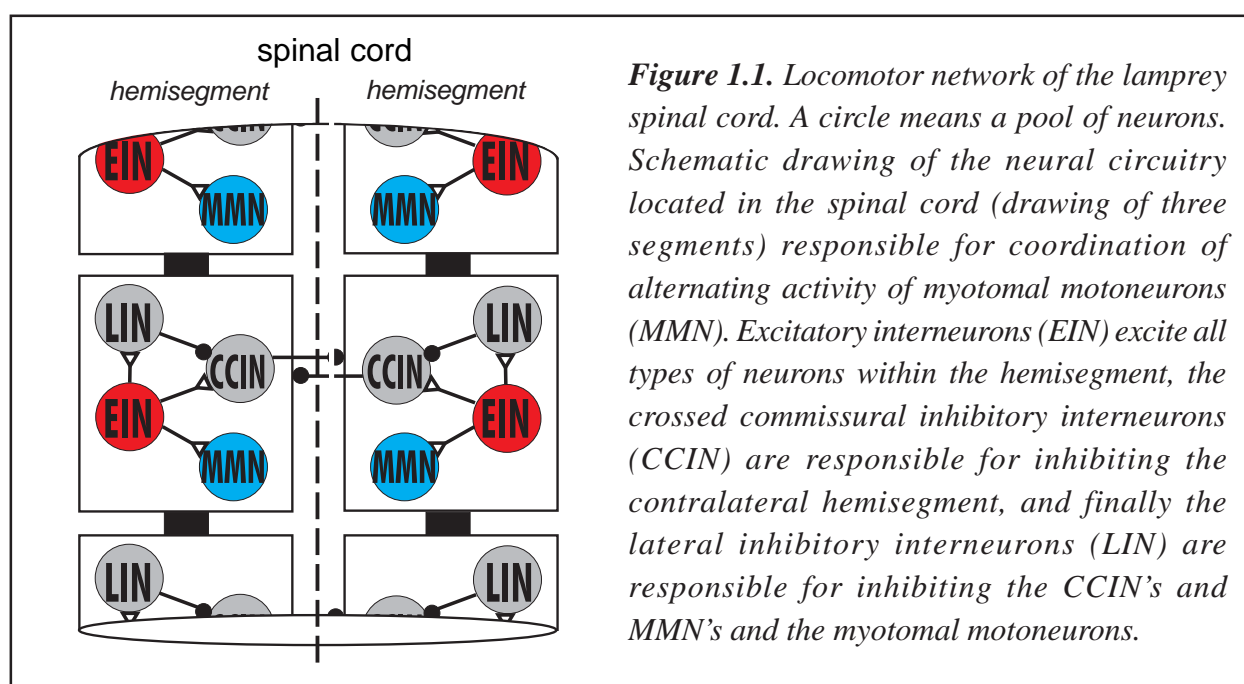


Figure 1.1. Locomotor network of the lamprey spinal cord. A circle means a pool of neurons. Schematic drawing of the neural circuitry located in the spinal cord (drawing of three segments) responsible for coordination of alternating activity of myotomal motoneurons (MMN). Excitatory interneurons (EIN) excite all types of neurons within the hemisegment, the crossed commissural inhibitory interneurons (CCIN) are responsible for inhibiting the contralateral hemisegment, and finally the lateral inhibitory interneurons (LIN) are responsible for inhibiting the CCIN's and MMN's and the myotomal motoneurons.

spinal network (Fig 1.1) contains different classes of well-described neurons. Excitatory glutamatergic interneurons (EIN) are able to generate excitatory bursting activity projecting them to all types of ipsilateral interneurons and myotomal motoneurons (MMN) (Buchanan, 1982; Buchanan and Grillner, 1987). Some of their axons can project as far as nine segments (Dale, 1986), but mostly they are much shorter (Buchanan *et al.*, 1989).

Crossed commissural inhibitory glycinergic interneurons (iCCIN) are members of propriospinal commissural neurons and inhibit all types of cells in the contralateral half oscillator producing the alternating left-right activity (Buchanan, 1982; Buchanan and Grillner, 1987). Axons of iCCINs are extended directly towards the midline from the soma or from a dendrite and cross in the ventral commissure. There, the axon turns caudalward as single axon or ramify into rostral- and caudalward going branches (Buchanan, 1982). In most cases the typical axon length does not exceed more than five segments (Ohta *et al.*, 1991). It is only the rostral part of the spinal cord which contains glycinergic lateral inhibitory interneurons (LIN) localized with long ipsilateral axons projecting as far as the tail region of the spinal cord (Rovainen, 1974), mostly inhibiting the ipsilateral iCCINs but in several cases also the motoneurons (Buchanan, 1982).

Lateral interneurons also receive polysynaptic excitatory and inhibitory inputs from dorsal cells (DC), which are mechanosensory neurons located in the dorsomedial region of the spinal cord (Rovainen, 1974) and correspond to the Rohon-Beard cells of larval teleosts and amphibians (Clarke *et al.*, 1984; Nakao and Ishizawa, 1987). They are bipolar, processing rostrally and caudally. The peripheral process of each DC innervates the skin and enters the spinal cord via a dorsal root (Rovainen 1967; Selzer, 1979).

Additionally, there are other sensory neurons located laterally in the spinal cord. Excitatory and inhibitory stretch receptor neurons (SRE, SRI), called edge cells measure the lateral bending of the animal/spinal cord and affect directly on the CPG neurons (Grillner *et al.*, 1984; Di Prisco *et al.*, 1990). The axons of the SRI project contralateral, whereas SRE axons remain ipsilateral. The length of the axons of both types does not exceed more than a few segments (Rovainen, 1974; Tang and Selzer, 1979).

1.2 Two different types of motoneurons in the lamprey spinal cord

There are two groups of motoneurons in lamprey spinal cord. Myotomal motoneurons, responsible for the alternate contraction of the body wall and therefore the propulsion of the animal and fin motoneurons, innervating the dorsal fin and responsible for stabilizing the body of the animal (Tretjakoff, 1909; Birnberger and Rovainen, 1971; Rovainen and Birnberger, 1971; Teräväinen, 1971; Deliagina *et al.*, 1993; Ullén *et al.*, 1995). During „fictive swimming“, fin motoneurons are activated in antiphase with the ipsilateral located myotomal motoneurons of the trunk locomotor system (Buchanan and Cohen, 1982; Shupliakov *et al.*, 1992).

Although the network and cellular properties of the myotomal motoneurons are well understood (Buchanan, 1999; Buchanan, 2001; Grillner *et al.*, 2000; Grillner, 2003; Wadden *et al.*, 1997; Wallén *et al.*, 1992), little is known about the organization of fin motoneurons, its activation in antiphase to the myotomal motoneurons and their integration in the myotomal locomotor network.

Myotomal motoneurons have wide dendritic ramifications, but unlike fin motoneurons, they do not project into the dorsal column (Wallén *et al.*, 1985; Shupliakov *et al.*, 1992) Cell bodies of fin motoneurons are generally located in the lateral cell column. The size of somata in fin MN does not exceed 35x55 μm , which is considerably smaller than myotomal motoneurons, which reach up to 100 μm in dimension (Shupliakov *et al.*, 1992; Buchanan, 2001). Along the spinal cord, the fin motoneurons are distributed both rostrally and caudally with respect to their origin ventral root. The axons of fin motoneurons are mixed with the fibres of the myotomal motoneurons, not forming a separate tract. Fin motoneuron somata can lie separately or in pairs, whereas myotomal motoneurons form a column of cells laying close to each other (Shupliakov *et al.*, 1992).

Shupliakov *et al.* (1992) distinguished two different types of fin motoneurons, differing in anatomical shape and ramification of dendrites. The first group, called type I, is characterized by elongated triangular or oval shaped somata with three to four stem dendrites and a wide dendritic tree extending in the rostro-caudal direction; it is normally restricted to the ipsilateral side, but it could cross the midline in few cases (approx. 4%) though never above the central canal. In contrast, the second group, called type II, has always dendritic ramifications toward the midline below and above the central canal making close appositions with large axons both ipsi- and contralaterally. Dendrites of

type I fin motoneurons project to the ipsilateral dorsal column but not to the contralateral side, whereas dendrites of type II fin motoneurons always have dendrites crossing the midline projecting to the contralateral hemisegment (el Manira *et al.*, 1996). Similar to myotomal motoneurons, which have monosynaptic connections with sensory edge cells (Grillner *et al.*, 1981, 1984; Viana Di Prisco *et al.*, 1990), fin motoneurons have monosynaptic connections with dorsal cells (Shupliakov *et al.*, 1992; el Manira *et al.*, 1996) from which at least four of them project to one fin motoneuron (el Manira *et al.*, 1996).

1.3 Questions and aims of thesis

The main purpose of this thesis was to investigate the mechanisms responsible for controlling the antiphase activation of fin motoneurons in comparison with the myotomal motoneurons during „fictive swimming“. Therefore the main focus of the research was aimed at fin motoneurons and their possible input from other neurons located in the spinal cord. For answering the main question of controlling fin motoneurons three questions were posed: (i) Are there morphologically or electrophysiologically different types of fin motoneurons involved in coordination of fin muscle activation during „fictive swimming“? (ii) Do fin motoneurons get inhibitory or excitatory phasic or tonic input during fictive swimming? (iii) Do different lesions of the spinal cord influence the rhythmic pattern of fin motoneuron membrane potential modulation during „fictive swimming“?

2. Material and Methods

All experiments were performed on adult lampreys (*Lampetra fluviatilis*) of both sex. The animals for the study were obtained from Sweden (Karolinska Institute, Stockholm).

The lampreys were kept in aerated water tanks cooled down to 4° C, with a circadian day/night rhythm of 12 hours. The room temperature during both the preparation of the animals and the experiments was 20° C. During the whole dissection, which was performed on ice, the animal was additionally cooled with oxygenated lamprey Ringer solution (Brodin and Grillner, 1985) (8° C), which was exchanged several times. After dissection, the preparation was transferred to an experimental chamber, perfused with cooled fresh oxygenated lamprey Ringer solution and the temperature was maintained at 10-12° C. If the experiment was not performed at the same day, the dissected spinal cord could be stored for several days at 4-8° C.

In most cases the experiments were carried out under the same conditions. The spinal cord of the lamprey contains approx. 100 segments (Buchanan, 2001). The caudal part i.e. the posterior 60 segments, which is covered by the dorsal fin in the intact animal (Rovainen, 1979) was used for the experiments. It was used in pieces of 10-15 segments of length. The isolated spinal cord or spinal-cord/notochord was superfused with oxygenated lamprey Ringer solution. After letting the spinal cord acclimate for 10-15 minutes to the new conditions, the lamprey Ringer solution was changed to fresh oxygenated lamprey Ringer solution containing 150 µM N-Methyle-D-Aspartate (NMDA; Tocris) to activate the spinal pattern generator for swimming located in the lamprey spinal cord inducing rhythmic activity of spinal motoneurons (Cohen and Wallén, 1980; Grillner *et al.*, 1981b; Brodin *et al.*, 1985).

2.1 Preparations

2.1.1 Intracellular retrograde staining of fin motoneurons

Fluoresceine-coupled-dextrane-amine (FDA, 3000MW, anionic, lysine fixable; Molecular Probes) was used for labelling fin-motoneurons for optical recognition under a fluorescence microscope (Wild M3 with fluorescence-filter and mercury lamp (150 W) from Leitz). 10-14 days prior to an experiment, two lampreys were anesthetized with alpha, alpha, alpha-Trichloride-tert.-butanol Hy-

drate (100 mg/l water; Aldrich) for staining. 10 mg of the FDA was solved in 700 µl of lamprey Ringer solution (Brodin and Grillner, 1985). The solved dye was taken up with a 1-ml-syringe (Henke Sass Wolf (HSW)) and 350 µl was then injected via an injection needle (0.40 x 0.40; Sterican) in each basal fin lacuna of the anesthetized lampreys. For damaging as many axons of fin motoneurons as possible, the injection needle was taken in and out of the lacuna several times before starting the injection (Shupliakov *et al.*, 1992). After injection, the animals were kept under the same conditions as before the treatment, but were separated from the other lampreys in a different water tank until the start of experiments.

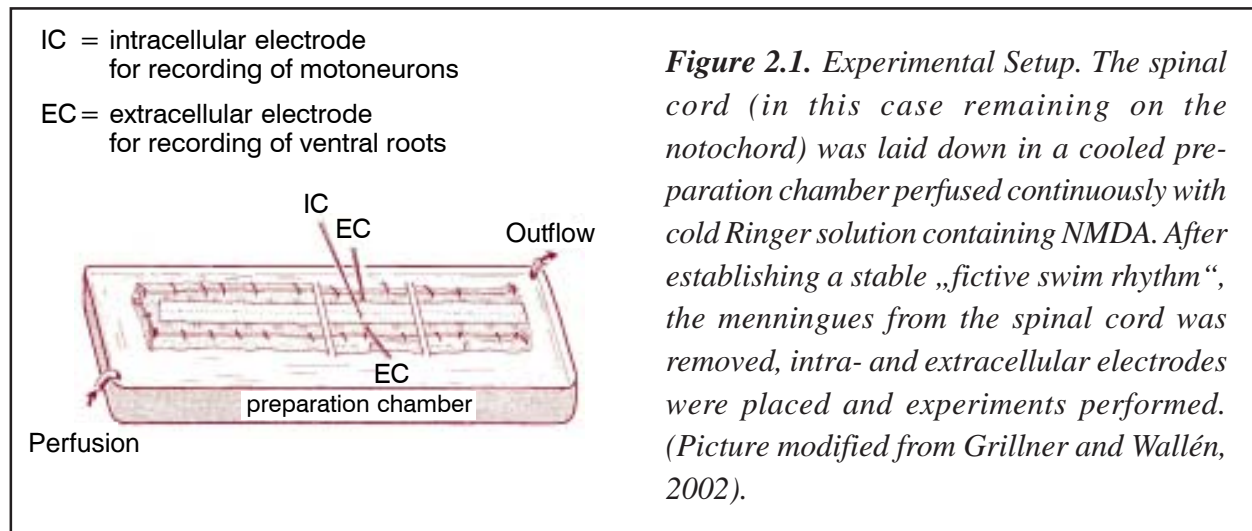
2.1.2 Spinal cord/notochord preparation

The lamprey was anesthetized with alpha, alpha, alpha-Trichloride-tert.-butanol Hydrate (100 mg/l water; Aldrich), until the agitation of the tail did not initiate any reflex reactions of the animal. It was then placed in a preparation tray (containing Sylgard gel; Dow Corning), kept on ice, and filled with fresh oxygenated cooled (8° C) lamprey Ringer solution (Brodin and Grillner, 1985). The animal was decapitated with a scalpel (Fine Science Tools, FST) caudal of the gills, also the tail was removed caudal from the genital pores. After this, the ventral myotomal muscles and the inner organs were removed with scissors (Fine Science Tools, FST) close to the notochord. Afterwards the spinal-cord/notochord preparation was moved to a different sylgard-lined preparation tray with fresh lamprey Ringer solution. There it was pinned down, the lateral muscles were cut away, before the dorsal muscles were removed down to the orange-red coloured fatty tissue. Next, the lamprey Ringer solution was changed again and the further dissection was performed under a dissection microscope (Zeiss, 60-fold-magnification).

With microscissors (Fine Science Tools, FST) the ectomeninges were removed and the spinal cord was accessible. After cutting a piece of 10-15 segments, the rest of the preparation was stored in a refrigerator at 4-8° C.

The short piece of the spinal cord/notochord preparation was positioned on the lateral side and pinned down in a sylgard-lined tray with fresh oxygenated lamprey Ringer solution, before the notochord was divided horizontally with a scalpel. After this the preparation was pinned down, dorsal side up, and the fatty tissue was removed from the spinal cord with a fine tweezers (Fine

Science Tools, FST). Finally, the spinal cord/notochord preparation was transferred into a cooled experimental chamber (modified after Wallén *et al.* (1985) (Fig. 2.1), and perfused with cooled fresh oxygenated lamprey Ringer solution.



2.1.3 Isolated spinal cord preparation

After removal of the fatty tissue (see also 2.1.2), which covers the spinal cord, the ventral roots were optically identified under a dissection microscope (Zeiss; 120-fold magnification) and cut out with an injection needle (0.55x0.25; Brillant) at their entrance to the muscle tissue. The spinal cord was carefully lifted at the rostral end with fine tweezers (Fine Science Tools, FST) and the remaining intact ventral roots with fatty tissue at the ventral side of the spinal cord were cut with the sharp end of an injection needle (0.55x0.25; Brillant). After removing the spinal cord from the notochord the cord was transferred, ventral side up, into the sylgard lined cooled experimental chamber perfused with cooled fresh oxygenated lamprey Ringer solution. There it was pinned down at the most rostral and caudal part with small insect needles (0.2 mm diameter).

2.1.4 Lesions of the spinal cord

Lesion-experiments were performed on the spinal cord/notochord as well as on the isolated spinal cord preparations. In both cases different lesions were made. The spinal cord was always pinned down in the cooled experimental chamber and a stable fictive locomotion rhythm induced by NMDA

(150 μ M) was established before the lesion was performed. For lesioning the spinal cord, the perfusion was stopped and all electrodes were removed from the spinal cord. The lesions were performed with a splinter of a razor blade, fixed in a razor-blade-holder (Fine Science Tools, FST). The sagittal cut was made over a length of two to six segments along the midline, whereas transversal cuts reached from the midline close to the lateral side of the spinal cord. After finishing the lesions, the perfusion was restarted and the electrodes were replaced. Stable rhythm re-established generally within 30-60 minutes after cutting the spinal cord.

2.2 Electrophysiology

The spinal cord/notochord was pinned down dorsal side up (see also 2.1.2) in the cooled experimental chamber perfused with cooled oxygenated lamprey Ringer solution. It was laterally fixed with insect needles (0.2 mm diameter) in the way that the ventral roots were visible by using a dissection microscope (Wild M3).

The isolated spinal cord was pinned down ventral side up (see also 2.1.2 and 2.1.3) in the cooled experimental chamber perfused with cooled oxygenated lamprey Ringer solution. It was fixed with two insect needles (0.2 mm diameter) on each side laterally rostral and caudal, and the fatty tissue was removed from the ventral side using fine tweezers.

2.2.1 Extracellular recordings

The motor activity of the motoneuron axons projecting through the ventral roots was monitored by extracellular recordings with suction electrodes made of borosilicate glass (tip diameter approx. 100 μ m). The suction electrode holders were made at the workshop of the Zoological Institute of the University of Cologne.

In the case of the spinal cord/notochord preparation, the suction electrode was positioned close to the ventral root for recording and suction was established with a syringe (20 ml, Henke Sass Wolf (HSW)) in order to move the ventral root close to the tip of the suction electrode. In general, the

recordings were made from two ventral roots at opposite sides of the spinal cord. In some experiments, up to three different ventral roots were recorded simultaneously.

In case of the isolated spinal cord preparation, the suction electrode was positioned close to the cut and opened end of the ventral root for recording, before suction was established with a syringe (20 ml, Henke Sass Wolf (HSW)) and the ventral root was sucked inside the suction electrode. In general, two ventral roots at opposite sides of the spinal cord were recorded.

The signals were amplified (1000-fold; AM-Systems, Differential AC Amplifier, Model 1700) and bandpass-filtered at lower and upper corner frequencies of 300 Hz and 5000 Hz, respectively.

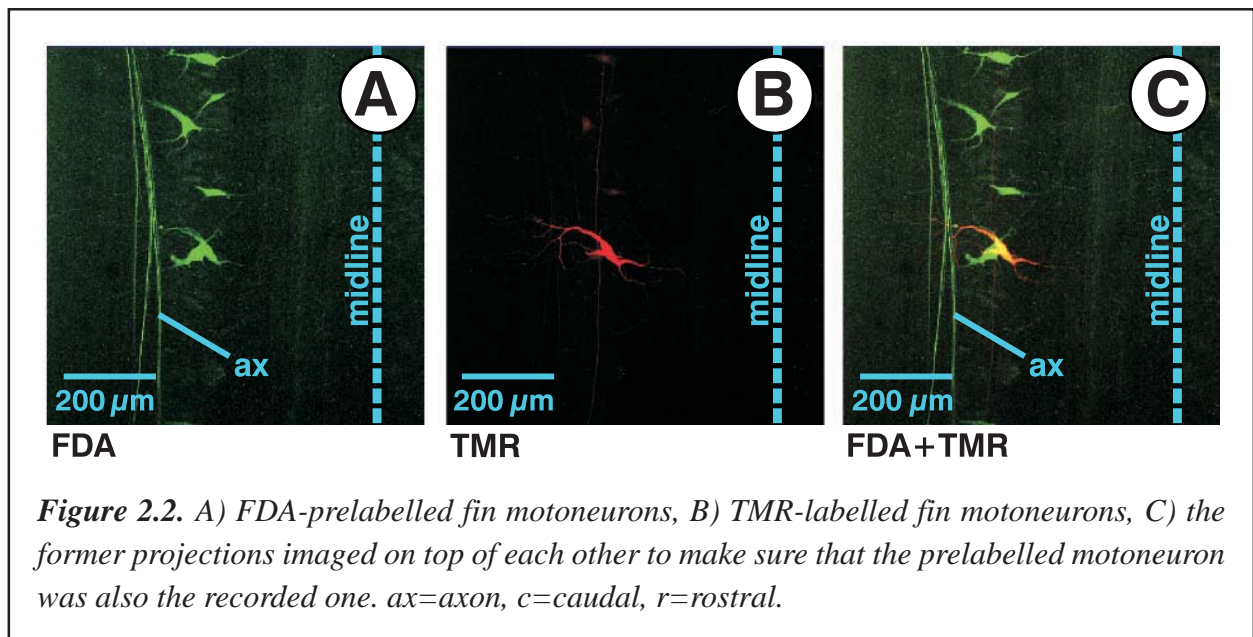
2.2.2 Intracellular recordings

Intracellular recordings from fin motoneurons were performed from the isolated spinal cord. The spinal cord was fixed with insect needles and the meningeal sheath (Rovainen, 1979) was removed. In addition to the insect needles at both ends of the spinal cord, it was fixed in the cooled sylgard experimental chamber by gently pressing it downwards with bent insect needles. The prelabelled fin motoneurons and dorsal cells (see 2.1.1) were visualized under a fluorescence microscope (Wild M3 with fluorescence filter from Zeiss) with UV light source (Zeiss). The excitation wave length was 450-490 nm, the emission wave length 520 nm.

Intracellular recordings were made with thin-walled sharp microelectrodes (GC100TF-10; Clark Electromedical Instruments) in the bridge mode by using an intracellular amplifier (SEC-10L; NPI). The electrodes had a resistance of 15-32 M Ω when filled with 0.1M KCl/3M KAc. The neurons were identified as fin motoneurons by at least two of the following criteria with exclusive d) or e): a) the recorded motoneurons were in antiphase active with the corresponding myotomal burst activity recorded *via* the ipsilateral ventral roots; b) the labelled fin motoneurons could be identified optically; c) an action potential could be recorded in a corresponding ventral root (Russel and Wallén; 1985); d) an action potential could be recorded in an adjacent ventral root during intracellular stimulation of the penetrated neuron; or e) an antidromic spike could be recorded during stimulation of a corresponding ventral root.

In several cases fin motoneurons were labelled with dextran tetramethylrhodamine (TMR, 3000MW, anionic, lysine fixable; Molecular Probes). The tip of the electrode was first filled with 5% dextran

in 0.1 M KCl/3M KAc, then the shaft of the electrode was filled with 0.1M KCl/3M KAc solution. After the experiment, the fin motoneuron was filled with dye by injecting 1 nA depolarizing current for 25-60 minutes. After labelling the fin motoneuron with the dye, the spinal cord was transferred to 4% paraformaldehyde in a 0.1 M phosphate buffer (pH 7.4) for two hours. The preparation was dehydrated using an alcohol series by replacing the paraformaldehyde solution for 20 minutes by 30%, 50%, 70%, 90% and two times 100% ethanol. Finally, the spinal cord was transferred to a microscope slide with methylsalicylate to clear the tissue. After adding the cover, the fin motoneuron was viewed with a Zeiss 510 confocal laser scanning microscope equipped with Axiovert 100M objective, HeNe Laser (543nm), and LP 560 filter (Fig. 2.2). For further use, the images were stored on a connected computer (Siemens Scenic 860).



2.3 Data analysis

For digitizing data a constant sampling rate of 13.3 kHz was used for the extracellular recordings, and a rate of 5.3 kHz for the intracellular ones, using an analogue-to-digital converter CED 1401 plus (Cambridge Electronics). The data were stored on a computer (Pentium-II, 350 MHz) using CED Spike 2 software (ver. 4.16). The program was also used together with Microcal Origin (ver. 7.0) and Microsoft Excel (ver. 2000) for analyzing data and plotting graphs. Statistical evaluation was carried out with Microcal Origin (ver. 7.0), SPSS for Windows (ver. 11.5) and Microsoft Excel

(ver. 2000). In some cases it was necessary to remove action potentials from the intracellular recordings, e.g. for plotting the mean of the membrane potential oscillation. This was done by a Spike 2 script, which removed the unwanted action potentials by exchanging the data of each action potential with a linear interpolation of its duration.

The start and termination of an intracellular period (cycle, phase) was referred to the middle of an extracellular recorded ipsilateral burst (Fig. 2.3; A1). For distributing the phase of an intracellular recording a Spike 2 script was used, classifying the area between each burst into 1000 classes and calculating the mean of all cycles (Fig. 2.3; A2). The data were normalized for comparing all different types of cells and the mean was pooled with the data from other fin motoneurons of the same type. The middle of a burst was also used as marker for analyzing the membrane potential distribution in a time area from +/-200 ms around the middle of the burst (Fig. 2.3; B1). The area around each burst was separated into 2000 classes and the mean of all classes was calculated (Fig. 2.3; B2). The data were normalized and the mean was pooled with the data from other fin motoneurons of the same type (Fig. 2.3).

„N“ means the number of experiments, whereas „n“ is the number of samples within one experiment. For calculating the mean of the maximum and minimum amplitude during one phase, circular statistical analysis was used. Therefore one period was classified from 0 to 360 degree to use a rectangular coordinate system with x (cos n) and y (sin n) axes (n=single sample value). Then the mean of the two components were calculated as followed.

$$\text{For the x component: } \bar{x} = \frac{(\cos n_1 + \cos n_2 + \dots + \cos n_m)}{m}$$

$$\text{For the y component: } \bar{y} = \frac{(\sin n_1 + \sin n_2 + \dots + \sin n_m)}{m}$$

The mean angle of the sample ($\bar{\phi}$) was then calculated as followed:

$$\bar{\phi} = \arctan(\bar{y}/\bar{x}) \text{ if } \bar{x} > 0$$

$$\bar{\phi} = 180^\circ + \arctan(\bar{y}/\bar{x}) \text{ if } \bar{x} < 0$$

$$\bar{\phi} = 90^\circ \text{ if } \bar{x} = 0 \text{ and } \bar{y} > 0$$

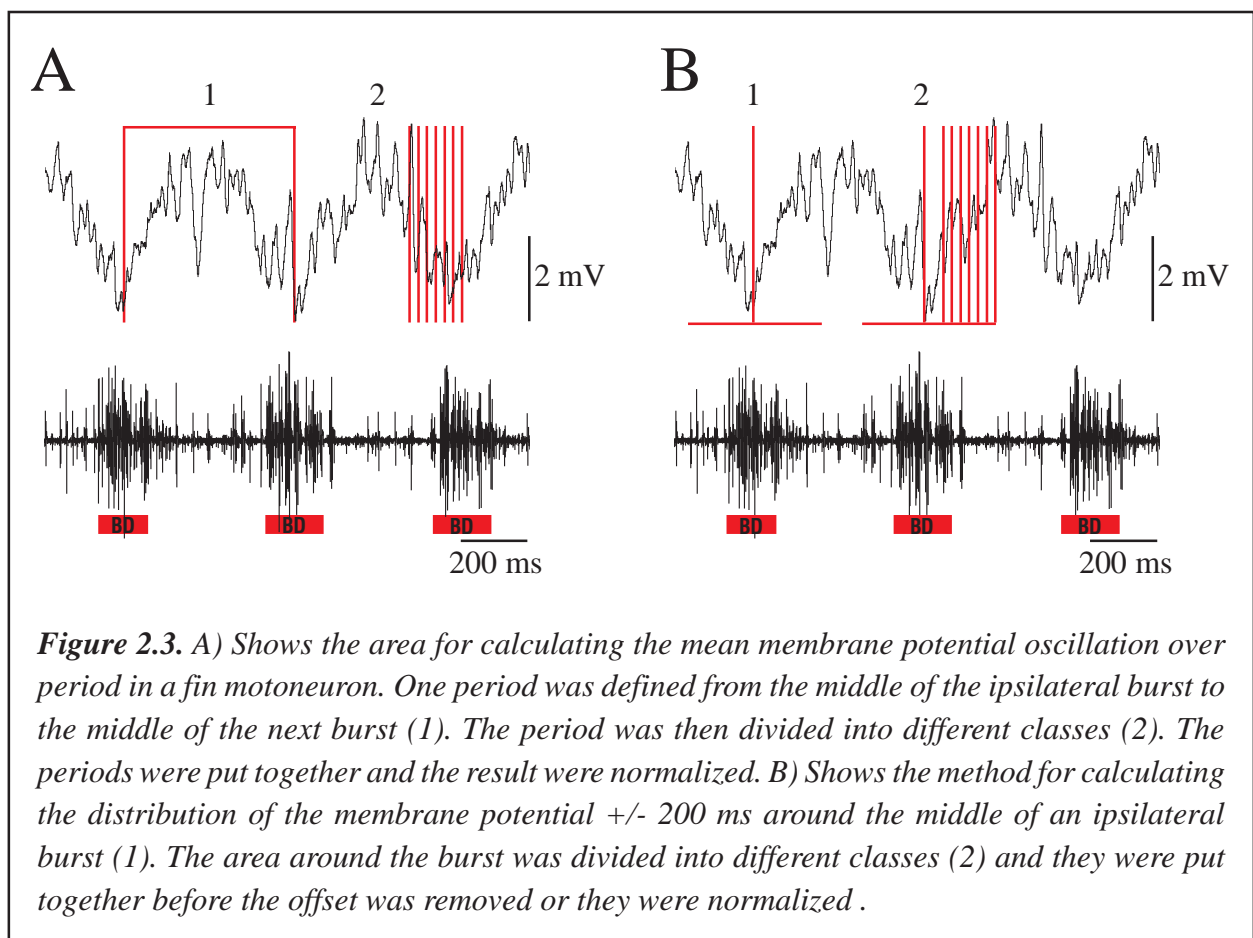
$$\bar{\phi} = 270^\circ \text{ if } \bar{x} = 0 \text{ and } \bar{y} < 0$$

For calculating the scatter of the mean, the length of the resultant mean vector (R) with the components \bar{x} and \bar{y} was used and calculated as followed:

$$R = \sqrt{(\bar{x}^2 + \bar{y}^2)}$$

At the end one gets therefore the mean phase of the min/max amplitude ($\bar{\phi}$) and the scatter of the mean ($0 \leq R \leq 1$). The larger is R , the smaller is the scatter (Batschelet, 1981; Zar, 1999; Mann *et al.*, 2003).

For finding different classes of cells distinguishing in their shape of membrane potential distribution over mean period, grouping of cells by visual inspection of membrane potential oscillation was complemented with a multivariant statistical technique, the hierarchical cluster analysis (Pennartz *et al.*, 1998; Ederer *et al.*, 2003). In the clustering method, the technique of distant neighbouring was used, and the interval was determined by means of squared Euclidean distances. The procedure of hierarchical clustering attempts to identify relatively homogeneous groups of cases based on selected characteristics. In this method, an algorithm is used that starts with each case in a separate



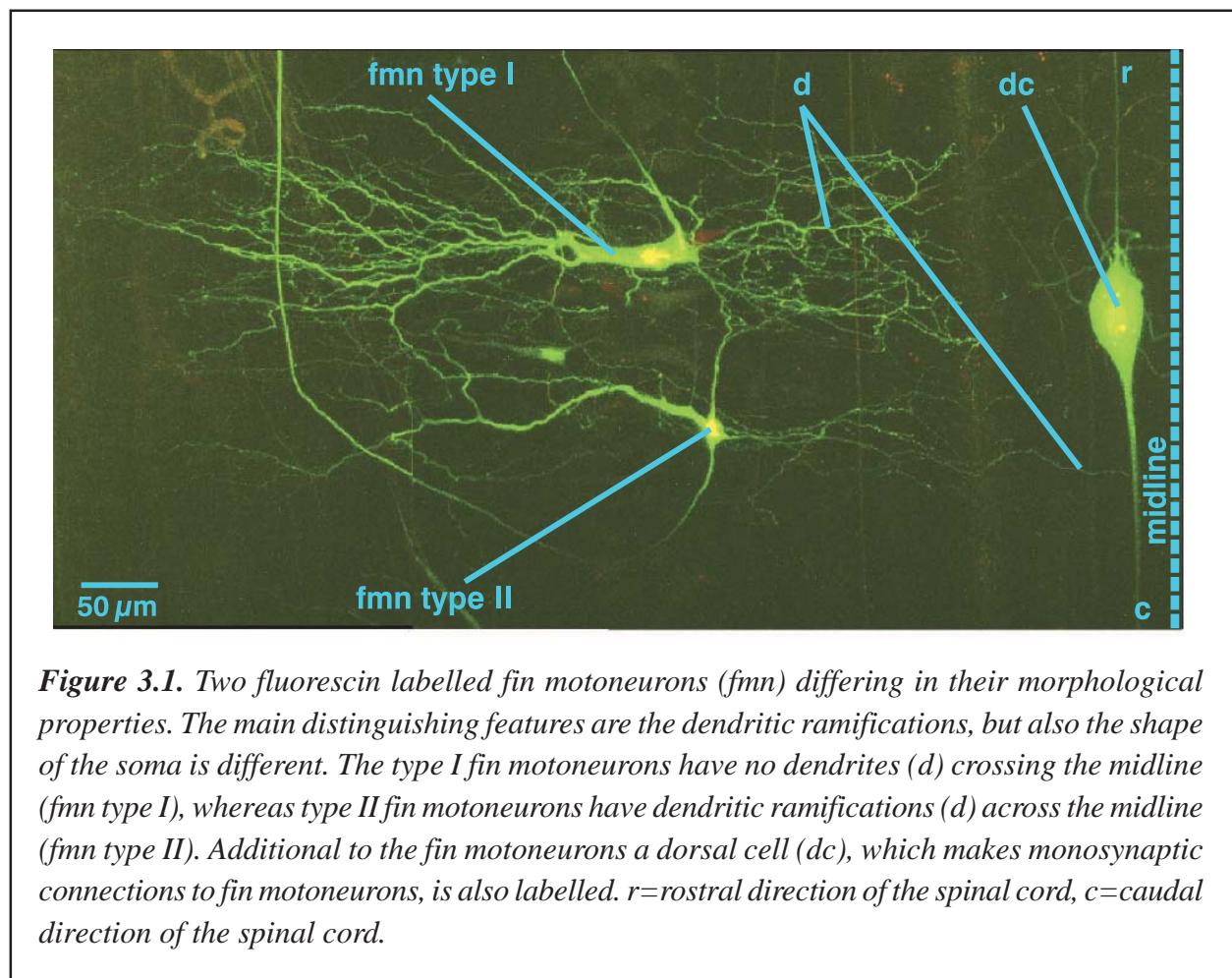
cluster and combines clusters until only one is left. This method can aid in uncovering structure in data sets and can suggest a scheme for classification. However, it does not permit rigorous conclusions about groupings of objects, nor does it produce any measure of statistical significance for property differences between suggested groups. Thus, it should be regarded primarily as objective tool to corroborate groupings produced by visual inspection.

For calculating the location of phase for the peak and trough potential for the three different types of motoneurons, 40 cycles were analyzed for each different recorded cell and the mean was calculated. The overall mean was calculated by pooling all different data of minima respectively maxima together.

3. Results

3.1 Two different types of fin motoneurons

There are two different morphological types of fin motoneurons located in the lamprey spinal cord that can be distinguished by their dendritic ramifications (Shupliakov *et al.*, 1992; el Manira *et al.*, 1996). One type has dendrites crossing the midline whereas the other type does not. According to Shupliakov (Shupliakov *et al.*, 1992) the latter one is called type I fin motoneuron whereas the former type is named type II (Fig 3.1).

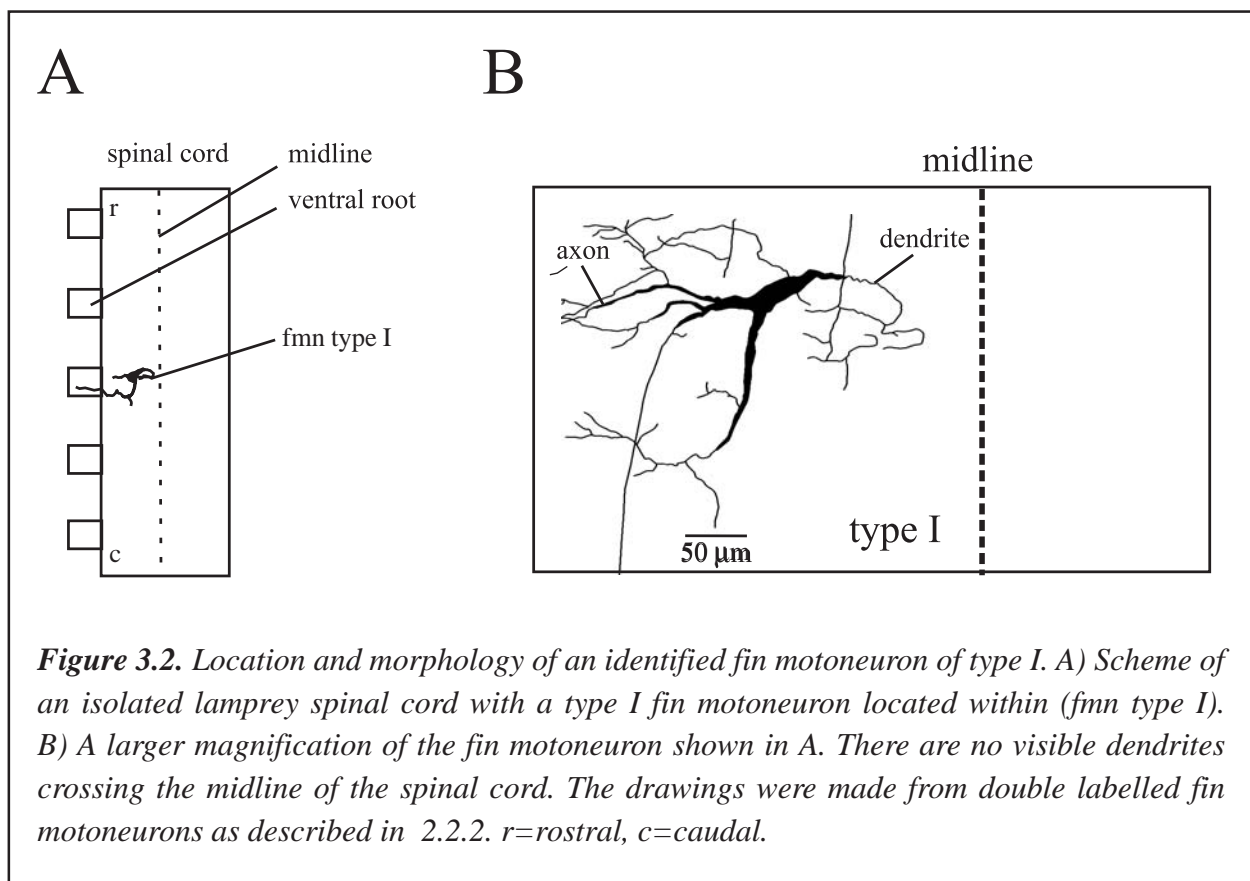


In most experiments the investigated fin motoneurons of both types showed only subthreshold activity after establishing a stable fictive swimming rhythm. Only three out of 38 investigated fin motoneurons (approx. 7%) showed superthreshold activity.

3.1.1 Type I fin motoneurons

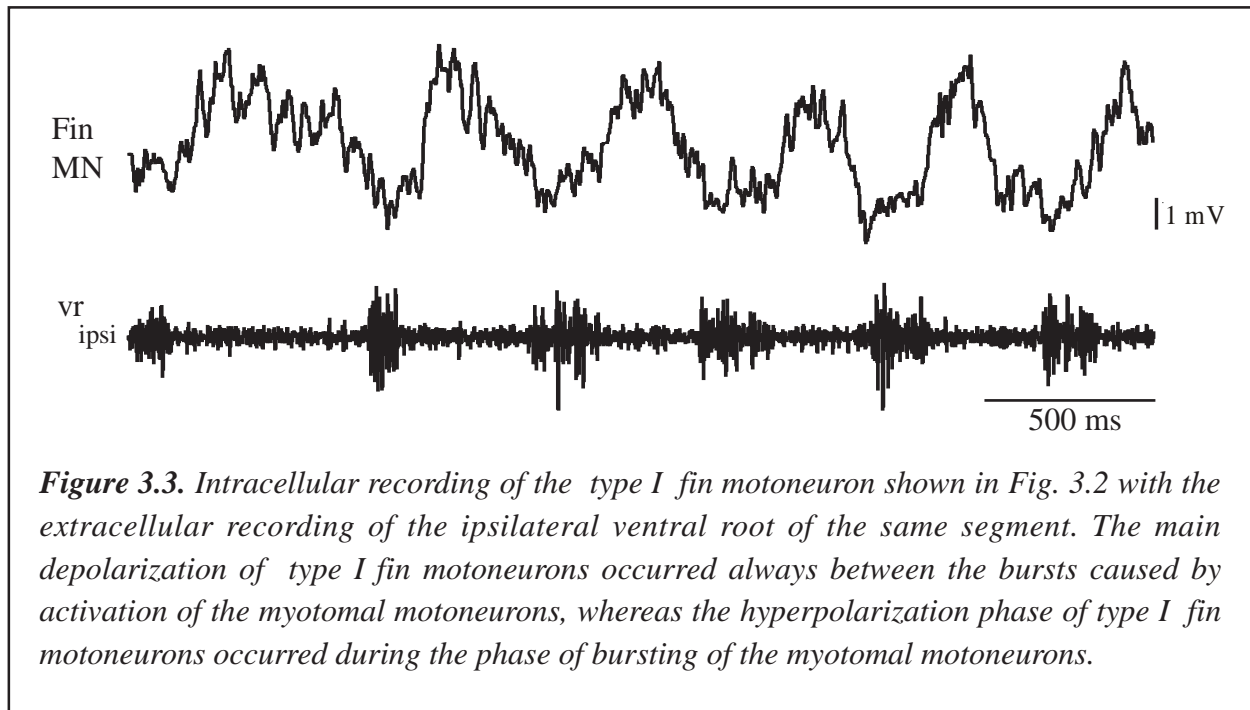
3.1.1.1 Morphological and electrophysiological description

All morphologically investigated motoneurons (N=14) were labelled with FDA through the lacuna of the dorsal fin, whereas five motoneurons were additionally stained with TMR through the microelectrode during electrophysiological recordings. Fin motoneurons of type I showed soma size of up to 30x85 μm (width of the spinal cord 600-1000 μm) with broad lateral and sagittal dendritic trees. The elongated triangular or oval shaped somata had in general two large dendritic extensions to the lateral side, and one to the sagittal as well (Fig. 3.2). The cells were located in the lateral cell column and within the spinal cord the fin motoneurons were arranged rostrally and caudally related to their parental ventral root.



Electrophysiological investigations of five double-labelled fin motoneurons of type I during „fictive swimming“ induced with 150 μM NMDA showed a measured trough potential ranging from -59.8

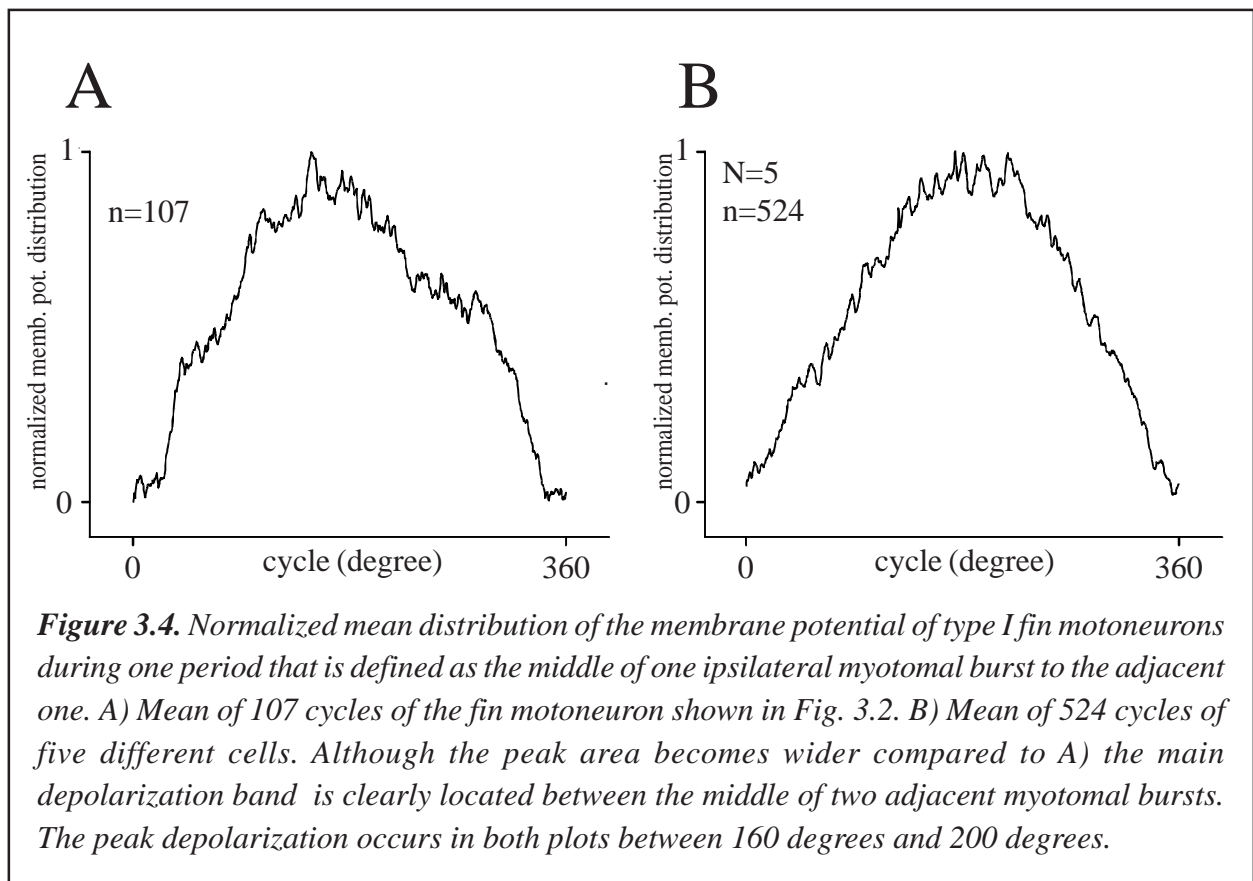
mV (n=45) to -47.3 mV (n=45) (mean -54.51 mV \pm 5.09 mV; N=5, n=225). The peak-to-peak-amplitude varied from 5.6 mV (n=45) up to 7.2 mV (n=45) (mean 6.42 mV \pm 0.69 mV; N=5, n=225). During the myotomal burst of the ipsilateral recorded ventral root, the membrane potential of type I fin motoneurons was the most hyperpolarized and reached its most depolarized membrane potential in between the myotomal burst cycle (Fig. 3.3).



The peak depolarization occurred at phase values between 157.49 deg to 181.42 deg (mean 169.92 deg, $R = 0.96$), whereas the peak hyperpolarization occurred at a phase value from 341.19 deg to 357.83 deg (mean 347.91 deg, $R = 0.88$) in relation to the middle of the ipsilateral myotomal burst cycle recorded from the ventral root located in the same segment. An overview of individual data is given in Tab. 3.1. Although only the individual cell peak depolarization was measured, there were different depolarization peaks very similar in values to the measured one in one cycle, so that the largest depolarization was not a single peak, but more like an area, reaching a band from 160-200 deg (Fig. 3.4). All five type I fin motoneurons showed only subthreshold activity. This means that no action potentials occurred during the observed time (50-60 min in general).

3.1.1.2 Phase dependency of membrane potential oscillations

In order to investigate if the shape of the intracellular recorded membrane potential between two myotomal bursts was similar in all electrophysiologically investigated cells of type I fin motoneurons, the mean distribution of the intracellular membrane potential over one burst cycle was calculated. The mean of the phasic membrane potential distribution of the intracellular recording was calculated for each experiment ($N=5$, $n=97$ to $n=126$), divided into 2000 classes and normalized. The data of the different classes were pooled together and the mean for all experiments was calculated and plotted (Fig. 3.4).

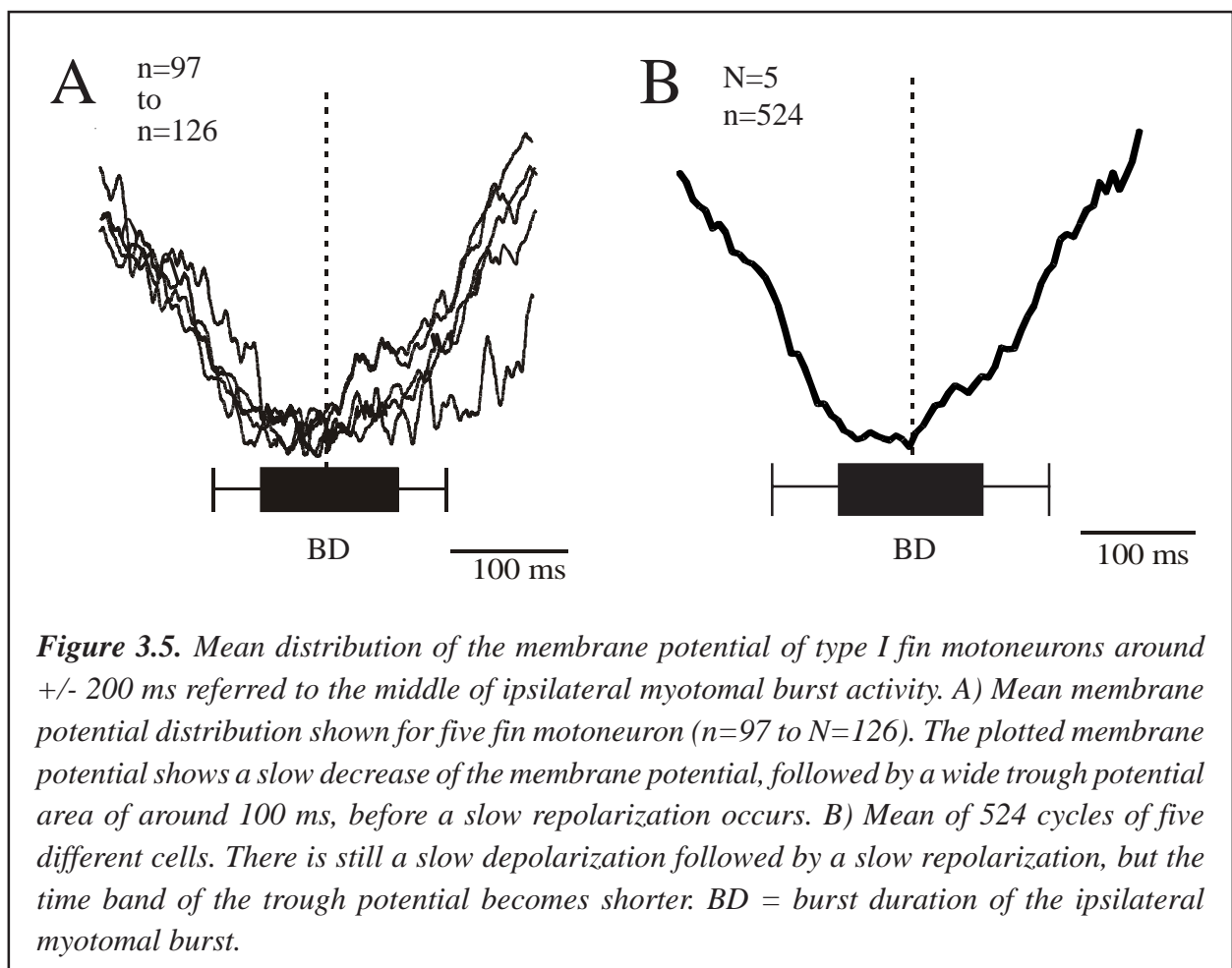


The result shows that in different cells the basic shape of the mean membrane potential distribution over one period is virtually the same. Measurements on five different fin motoneurons in altogether 524 cycles show that peak depolarizations occurred at a phase of approx. 180 deg. In other words, the shape of the membrane potential distribution of type I fin motoneurons was the same in all

investigated cells. So, if type I fin motoneurons had a unique membrane potential pattern, it should be possible to identify these motoneurons based on their membrane potential modulation only.

3.1.1.3 Temporal dependency of membrane potential oscillations

In order to show the mean shape of membrane potential distribution of type I fin motoneurons over a defined time period, and to find out whether there are similarities between the investigated cells of the same type, the mean membrane potential distribution over a time of ± 200 ms referred to the middle of the myotomal burst was calculated for each experiment ($N = 5$, $n = 97$ to $n = 126$). The time of the measured membrane potential distribution was separated into 2000 classes and the mean data of the membrane potential distribution of one and of all experiments ($N=5$) were plotted by removing the offset (Fig. 3.5). The measured peak-to-peak amplitude within this time band of 400 ms of all five motoneurons was between 1.4 mV and 2.9 mV (mean 2.12 mV \pm 0.57 mV).



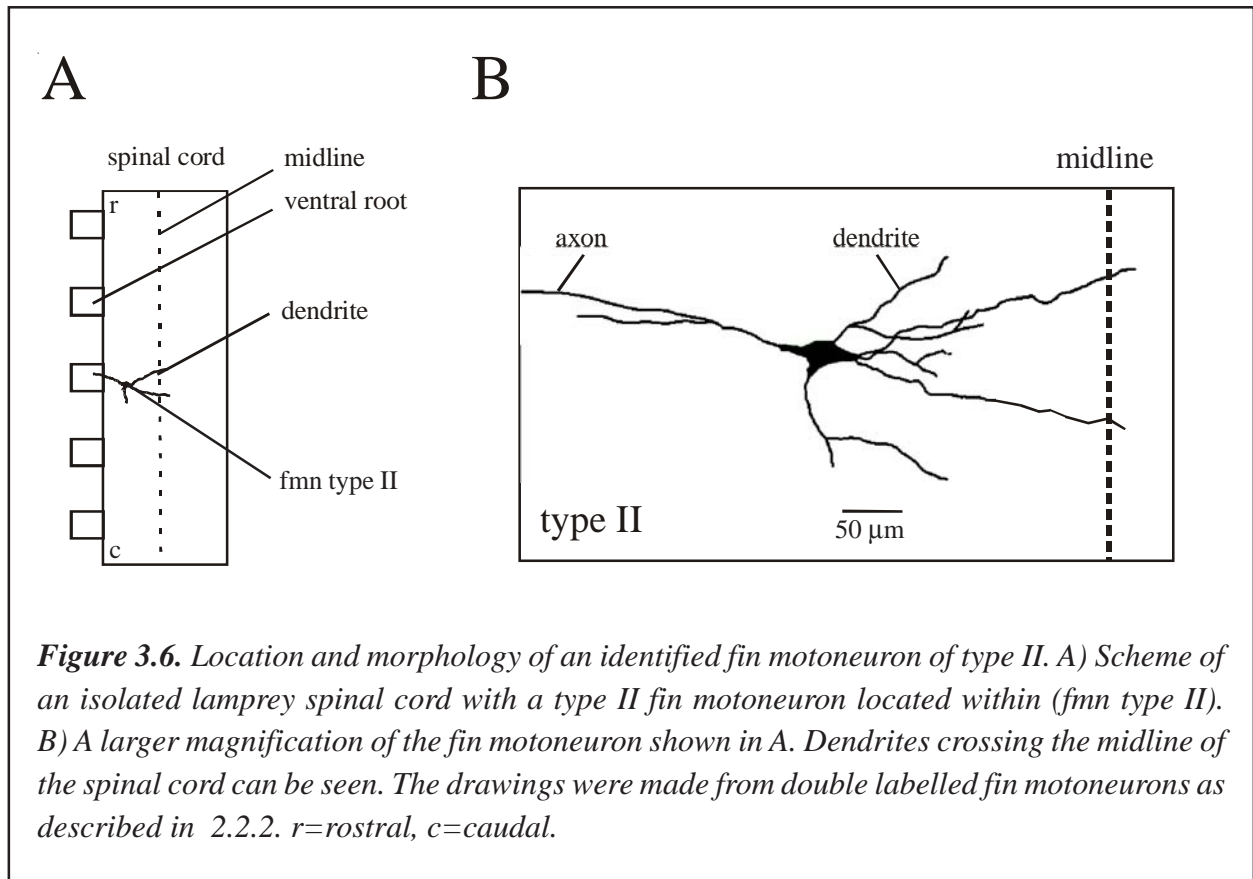
The result shows that despite the fact that the shape of the membrane potential distribution varies because of the strong synaptic noise at the area of the trough potential, the general shape of the peak is well defined. In all five different cells, the membrane potential decreases slowly at an angle of approx. 45 deg until the trough potential is reached. At this point the depolarizing phase lasts approx. 50-80% of the burst duration of the ipsilateral myotomal burst, and is eventually interrupted by depolarizing synaptic noise. Due to this noise, the summary of the membrane potential distribution for all investigated cells together shows only a small depolarized phase of approx. 15-20% of the ipsilateral myotomal burst duration. Both, the decrease and the increase of the membrane potential still occur at an angle of approx. 45 deg. This indicates that the membrane potential in fin motoneurons of type I approaches its most hyperpolarized state after a uniform decrease at approx. 45 deg, followed by a similar slow repolarization. Due to the steadily decrease and increase of the membrane potential it could be assumed that they get constant phasic input from other neurons during the whole measured depolarizing and repolarizing time of 400 milliseconds.

3.1.2 Type II fin motoneurons

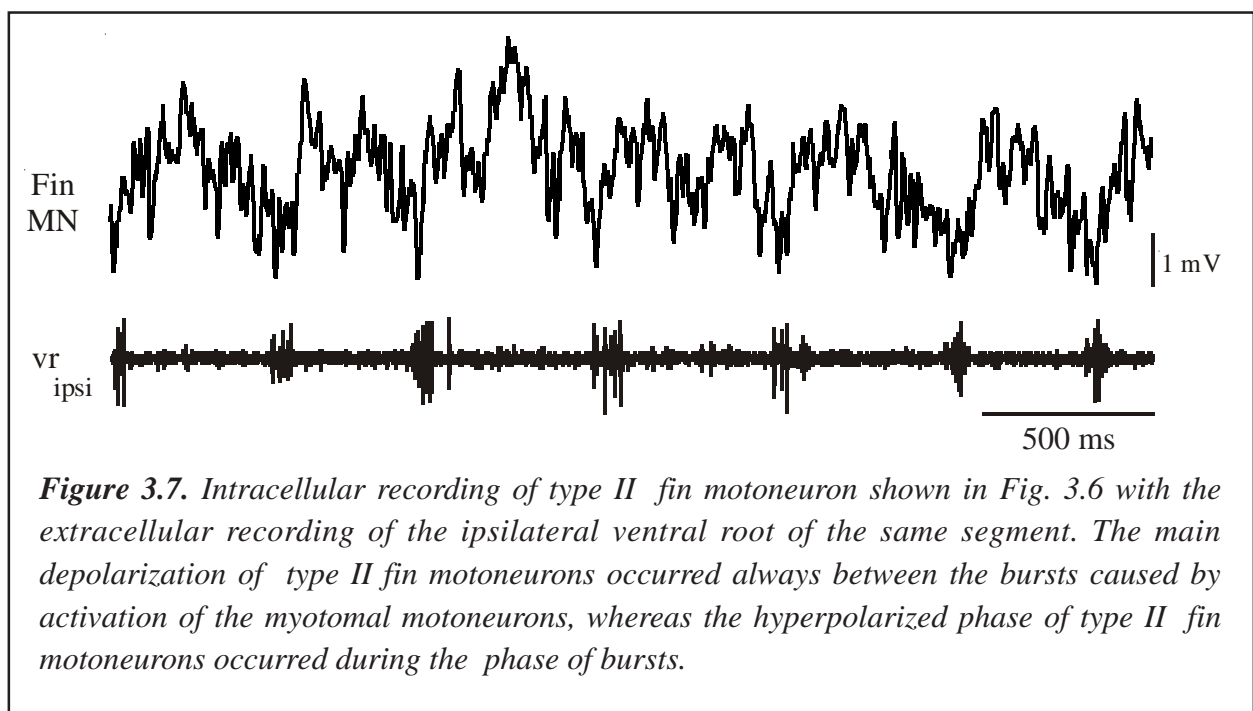
3.1.2.1 Morphological and electrophysiological description

The morphologically investigated fin motoneurons of type II (N=8) showed a soma size of up to 30x75 μm , and broad lateral and sagittal dendritic trees. The elongated star-shaped somata had in general several dendritic extensions to the lateral and to the sagittal side, whereas the sagittally directed dendrites could cross the midline of the spinal cord (Fig. 3.6). The cells were located in the lateral cell column. Within the spinal cord, the type II fin motoneurons were arranged rostrally and caudally related to the parental ventral root. On one occasion, more than one cell was labelled intracellularly, perhaps an indication of electrical synapses between fin motoneurons of type II and interneurons located in the same segmental half of the spinal cord.

Four fin motoneurons were investigated electrophysiologically. One was identified by staining with TMR during intracellular recording, whereas the remaining three were marked for later morphological analysis by injuring the spinal cord with a needle in the surrounding area of the recorded motoneurons. This technique was applicable because of the small amount of fin motoneurons located and labelled



in the spinal cord. All four fin motoneurons of type II showed a trough potential range from -53.9 mV (n=45) to -38.9 mV (n=45) (mean -46.78 mV \pm 6.15 mV; N=4, n=180). The peak-to-

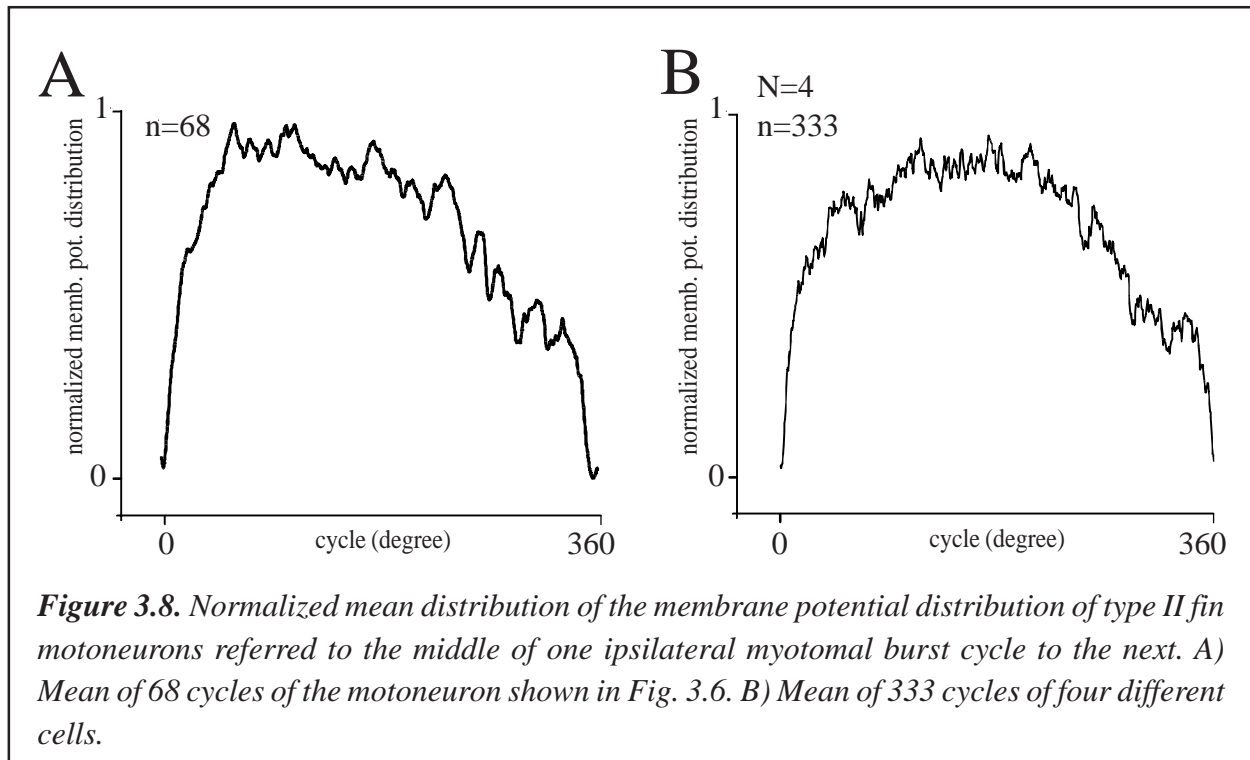


peak amplitude varied between 5.1 mV (n=45) and 6.8 mV (n=45) (mean 5.7 mV +/- 0.75 mV; N=4, n=180). The membrane potential of type II fin motoneurons was most hyperpolarized during the myotomal burst of the ipsilateral recorded ventral root (Fig. 3.7), and reached its most depolarized membrane potential during the middle of the contralateral myotomal burst. The peak depolarization occurred at phase values of 162.28 deg to 168.46 deg (mean 163.85 deg, R = 0.85), whereas the peak hyperpolarization occurred at phase values of 340.87 deg to 358.39 deg (mean 353.41 deg, R = 0.98) in relation to the middle of the ipsilateral myotomal burst cycle recorded from the ventral root located in the same segment (for individual data see Tab. 3.1). Although only the peak depolarization was measured, there were different depolarization peaks very similar in value to those measured in each cycle, so that the peak depolarization was not a single peak, but rather an area reaching a band of approx. 45-300 deg (Fig. 3.8). One of the four measured type II fin motoneurons showed suprathreshold activity, while the other three always displayed subthreshold activity. In order to calculate the mean of the membrane potential distributions and to determine the peak-to-peak amplitude, action potentials were removed from the recordings using a Spike 2 script as described in section 2.3.

3.1.2.2 Phase dependency of membrane potential oscillations

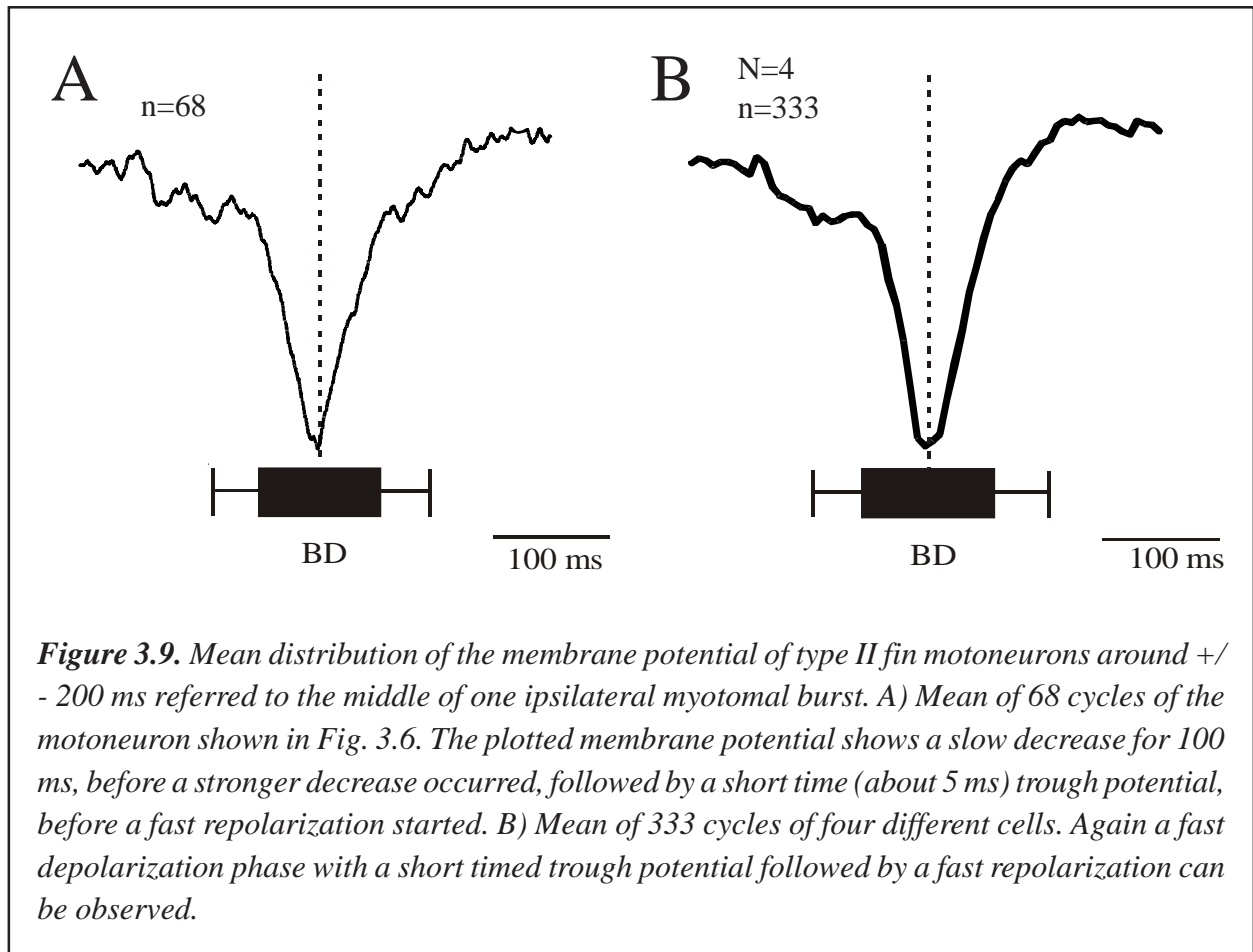
In order to find whether the mean distribution of the intracellular membrane potential over a burst cycle of one type II fin motoneuron was similar in all of the investigated type II cells, the mean of the intracellular membrane potential distribution per each cycle was calculated for every experiment (n=68 to n=102), divided into 2000 classes and then the normalized mean data of the membrane potential distribution for one and for all experiments (N=4) were plotted (Fig. 3.8). The results show that the shape of the membrane potential distribution in all tested cells were similar to each other. At the beginning it starts with a rapid strong depolarization phase around the middle of the myotomal burst (approx. 0-1 deg) at which the depolarization reaches approx. 50% of its maximum, followed by a slow increase of depolarization. The peak depolarization is at approx. 180 deg, after which a slow repolarization takes over, bringing the membrane potential back to approx. 50% of its peak depolarization. At approx. 360 deg a very strong repolarization begins, similar to that at the beginning of the cycle which brings the membrane potential back to its ground level. These results

suggest that type II fin motoneurons may have a unique membrane potential distribution pattern over one cycle. Provided that there are no other fin motoneurons with a similar membrane potential pattern, this characteristic could be used for identification of type II fin motoneurons.



3.1.2.3 Temporal dependency of membrane potential oscillations

In order to show the mean of the intracellular membrane potential distribution of type II fin motoneurons over a defined period of time, and to find out whether there are similarities between the cells investigated, the mean membrane potential distribution over a time of ± 200 ms around the middle of the myotomal burst was calculated for each experiment ($n=68$ to $n=102$). Therefore, the investigated time around the middle of the myotomal burst was separated into 2000 classes and after removing the offset, the mean data of the membrane potential distribution of one and of all experiments ($N=4$) were plotted (Fig. 3.9). The measured peak-to-peak amplitude within this time band of 400 ms of all four motoneurons was between 1.8 mV and 4.1 mV (mean 2.83 mV ± 0.97 mV).

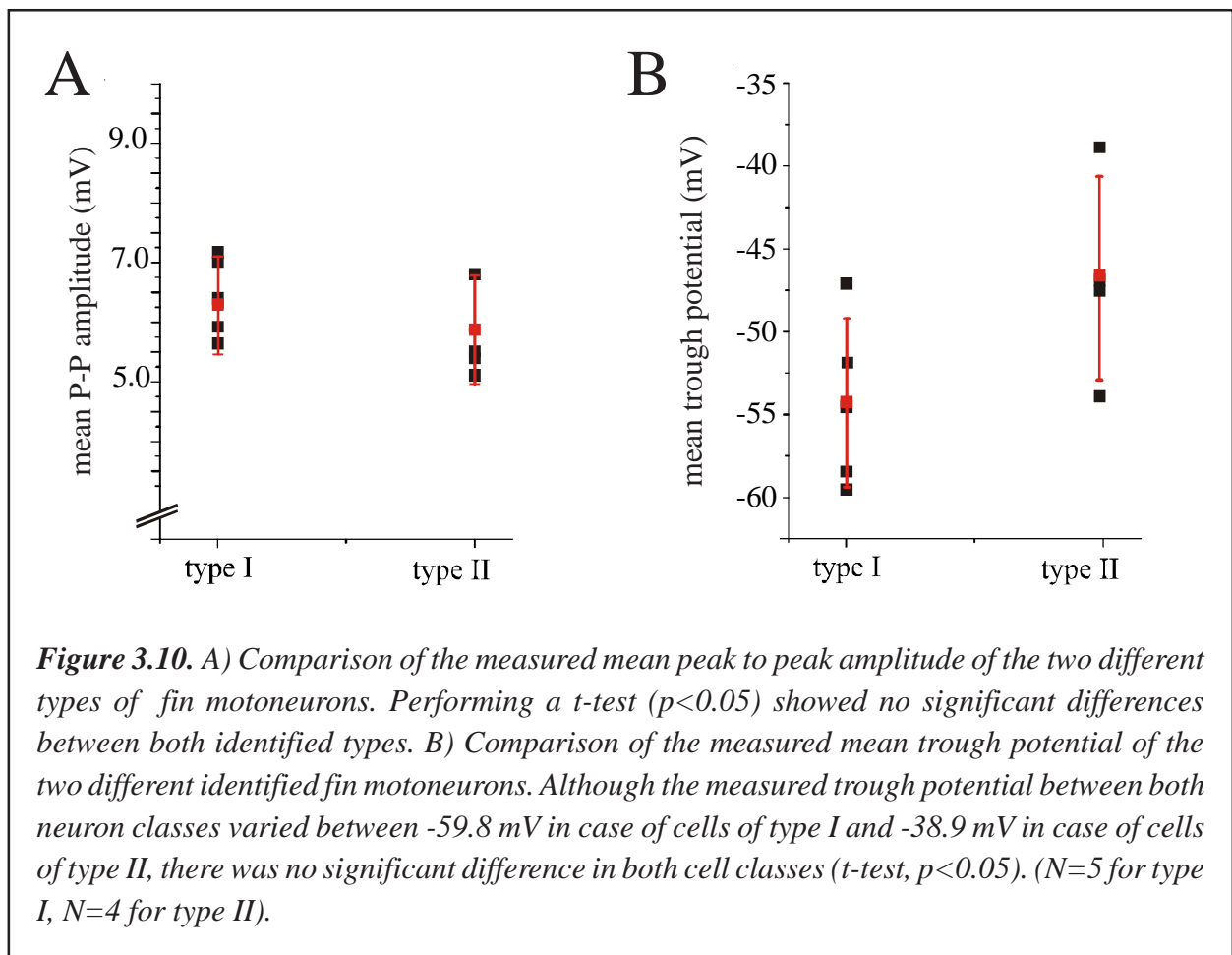


The results show that the shape of the membrane potential distribution is similar in all recorded cells. In all four individual motoneurons, the membrane potential slowly decreased during the first 160-170 ms to approx. 70-80% of its peak depolarization. After this, a strong membrane hyperpolarization occurred lasting for 35-40 ms that brought the membrane potential down to its trough potential. After this, a similar strong rapid depolarization occurred for 35-40 ms that brought the membrane potential back to 70-80% of its peak depolarization followed by a slow depolarization for the next 160 to 170 ms that brought the membrane potential back to its peak potential within the overall measuring period of 400 ms. It seems that there are two different states during hyperpolarization/depolarization meaning that one could hypothesize that fin motoneurons of type II could receive different phasic inputs from other neurons. At the beginning, slow influences of other interneurons could cause a slow membrane hyperpolarization until the membrane potential reaches approx. the center of the ipsilateral myotomal burst; after this, a second pool of interneurons activated during the middle of the ipsilateral myotomal burst could cause the rapid hyperpolarization.

3.1.3 Comparison of both types of fin motoneurons

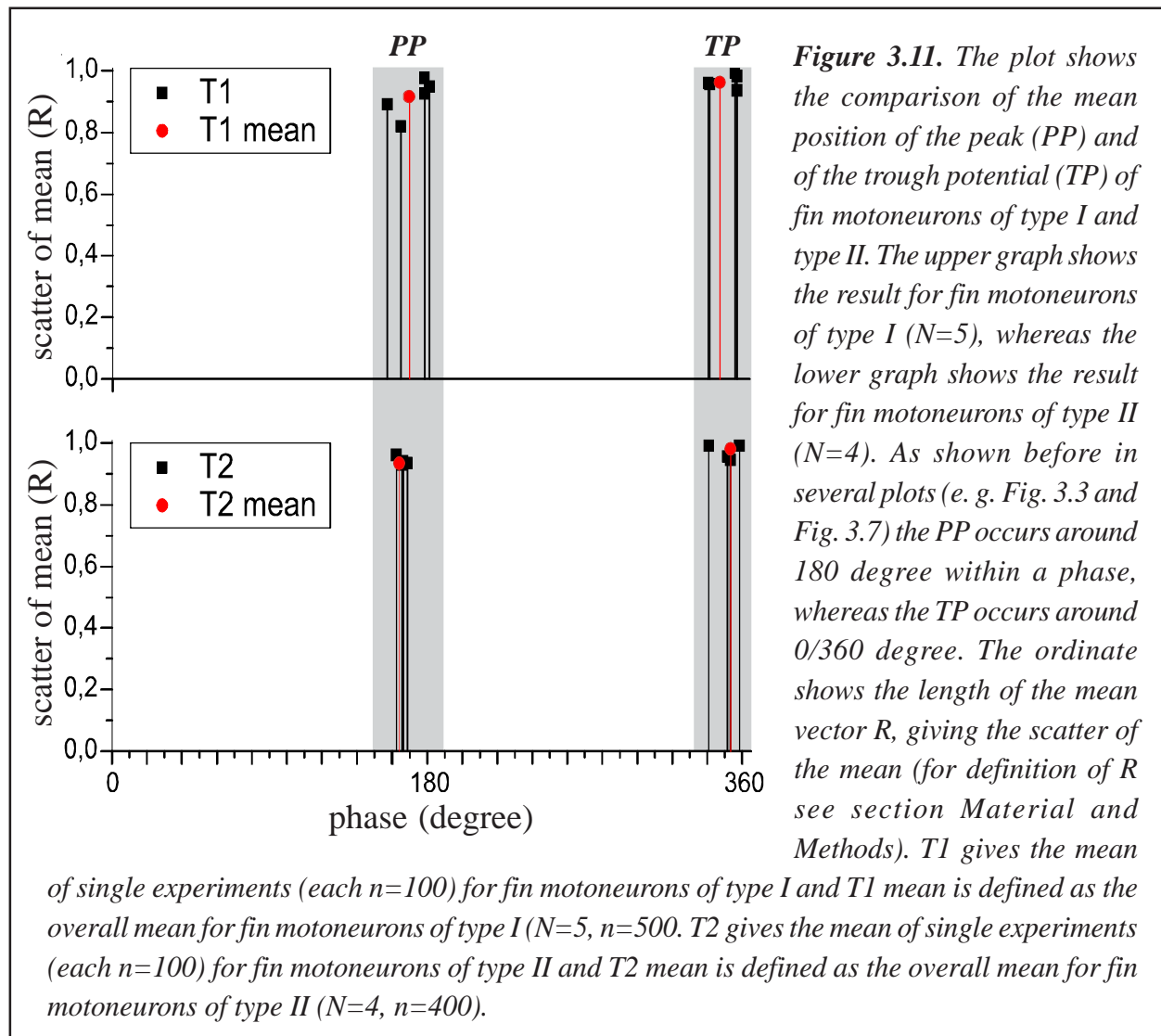
3.1.3.1 Membrane potential oscillation

For the comparison of the measured peak-to-peak amplitudes and the resting trough potential of both of the morphologically identified fin motoneurons of type I and type II, the data were subjected to an independent two samples t-test ($p < 0.05$). The results show that significant differences are neither between the resting membrane potentials nor between the peak-to-peak amplitudes (Fig. 3.10). Tests were also performed to find out whether there are differences in the position of the peak



and trough potential within one phase. To achieve this the mean of the minima and maxima, respectively, of the phase locations of the membrane potential were calculated using trigonometric functions (see material and methods part) by adding the single values of 100 cycles per each experiment. Additionally, all data of the different experiments for each type of motoneuron were

taken together to calculate the overall mean for the two different types of fin motoneurons. The results were then plotted (Fig. 3.11). Statistical evaluation using an independent two sample t-test ($p < 0.05$) did not show any significant difference between the data of the two different types of motoneurons. The single values of the measured peak-to-peak amplitudes are shown in Table 3.1.

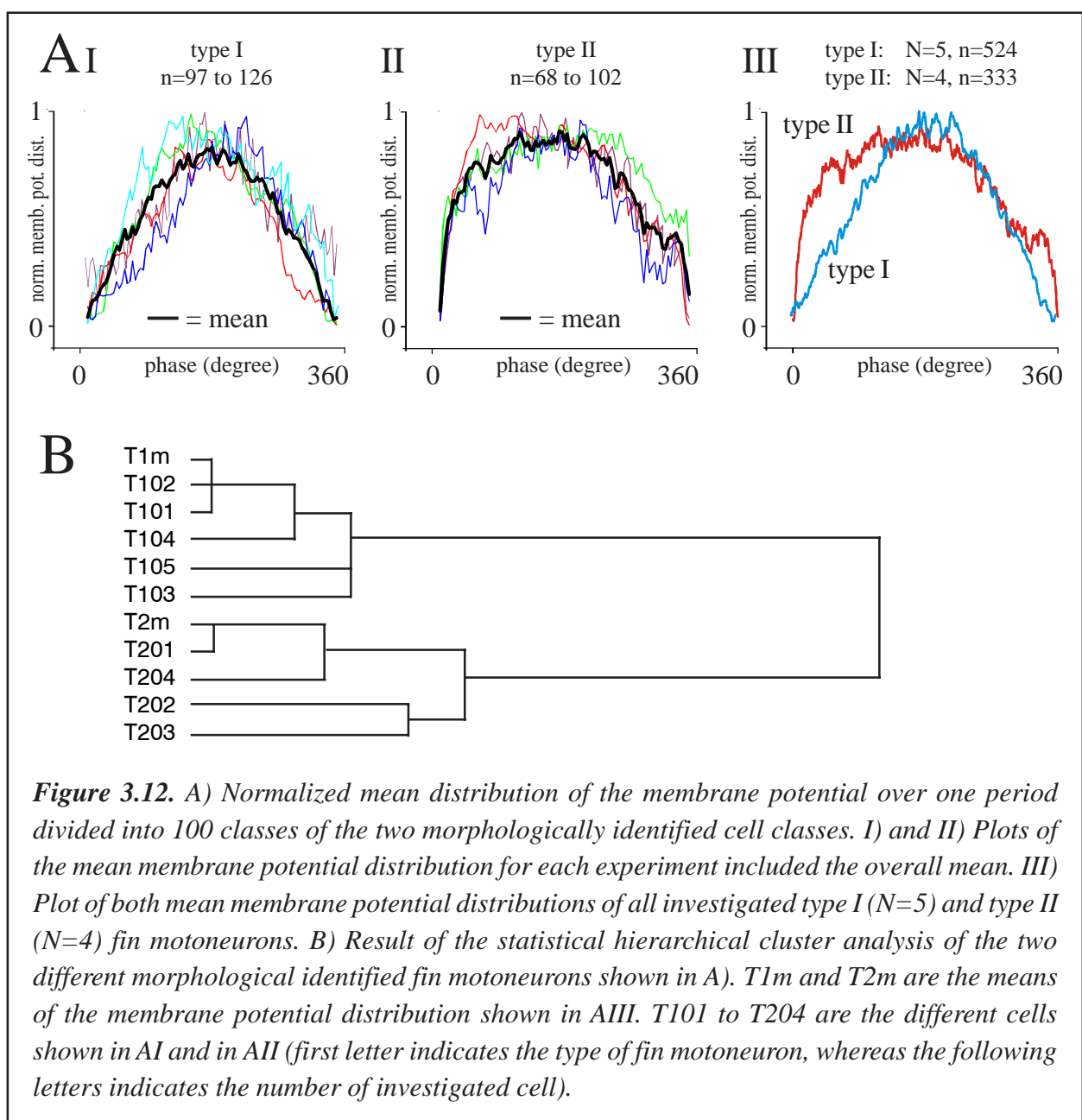


The results show that the peak and the trough potentials of the two different types of fin motoneurons occur approx. at the same phase (180 deg and/or 360 deg). Also the mean values for the trough potential (-54.51 mV \pm 5.09 mV, type I; -46.78 mV \pm 6.15 mV, type II) and for the peak-to-peak amplitude (6.42 mV \pm 0.69 mV, type I; 5.7 mV \pm 0.75 mV, type II) are similar and not significantly different in both types of fin motoneurons. Therefore, it is not possible to uniquely characterize and

determine fin motoneurons using these factors only. Hence it was necessary to find another way to distinguish between the different morphological types of fin motoneurons found in the lamprey.

3.1.3.2 Phase dependency

In order to perform the statistical analysis and the comparison of the normalized mean distributions of the membrane potential oscillation during one period within reasonable time, the number of classes was reduced from the original 2000 down to 100. The two morphological different fin



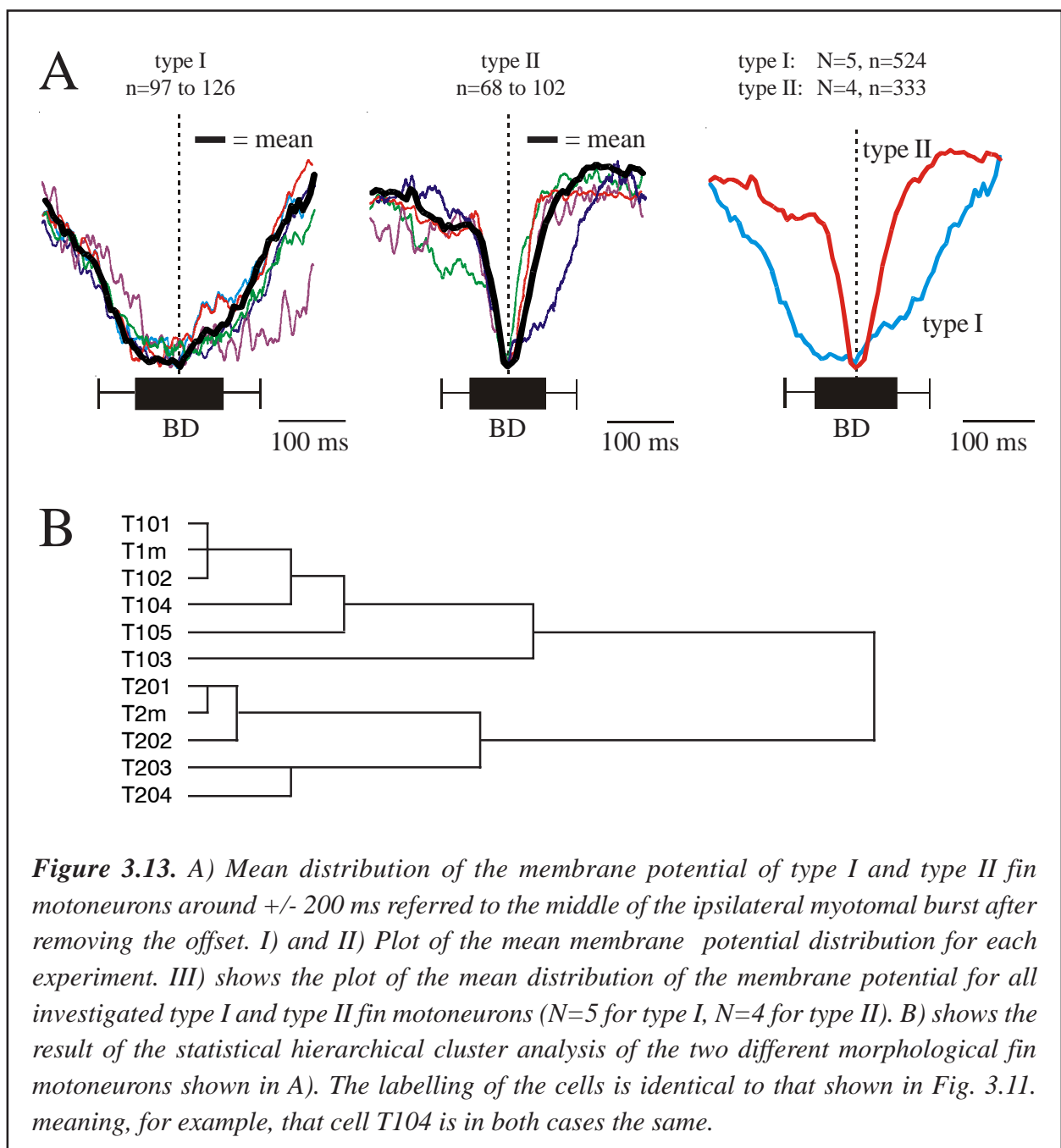
motoneuron classes were tested both optically and by hierarchical clustering for finding differences in the distribution of the membrane potential oscillation over one cycle (Fig. 3.12). The aim of the test was to find out whether there are clear-distinguishable differences between the classes which would allow their classification and characterization by their different shapes of cyclic membrane potential distribution. The results show, that fin motoneurons of type I display a smaller overall depolarization plateau than these of type II. The latter group has a rapid increase in depolarization and hold it over up to approx. 90% of the phase until the repolarization starts (see also 3.1.1.2 and 3.1.2.2). Cluster analysis revealed two large classes; the first class contains all cells of type I (T101 to T105, T1m), while the second one all cells of type II (T201 to T204, T2m). These results suggest that it should be possible to distinguish between the two different morphological types of fin motoneurons by a simple comparison of the shape of the cyclic membrane potential oscillation.

fMN	P-P amplitude	Phase min	Phase max
Type I	7.2 mV +/-1.53 mV	342.2 (R=0.956)	157.5 (R=0.891)
Type I	7.0 mV +/-0.92 mV	341.2 (R=0.962)	164.9 (R=0.821)
Type I	5.9 mV +/-0.85 mV	357.8 (R=0.982)	181.4 (R=0.949)
Type I	5.6 mV +/-0.94 mV	356.7 (R=0.994)	178.5 (R=0.977)
Type I	6.4 mV +/-0.56 mV	357.8 (R=0.936)	178,6 (R=0.926)
Type II	5.5 mV +/-0.73 mV	358.4 (R=0.991)	162.3 (R=0.961)
Type II	5.1 mV +/-0.55 mV	340.9 (R=0.991)	165.7 (R=0.930)
Type II	5.4 mV +/-1.02 mV	351.6 (R=0.957)	168.5 (R=0.935)
Type II	6.8 mV +/-1.34 mV	353.3 (R=0.946)	166.2(R=0.941)

Table 3.1. Mean of the peak-to-peak amplitude (P-P amplitude), occurrence of the mean trough potential within one cycle (phase min) and occurrence of the mean peak depolarization over one cycle (phase max) for the morphologically different fin motoneurons of type I and type II (n=45).

3.1.3.3 Temporal dependency

The two morphological different fin motoneuron classes were examined both optically and statistically, using hierarchical clustering to find differences between their membrane potential distribution within ± 200 ms referred to the middle of one ipsilateral myotomal burst (Fig. 3.13). The results suggest that it is possible to classify the two morphological types of fin motoneurons only by their mean membrane potential distribution within a time band of ± 200 ms around the

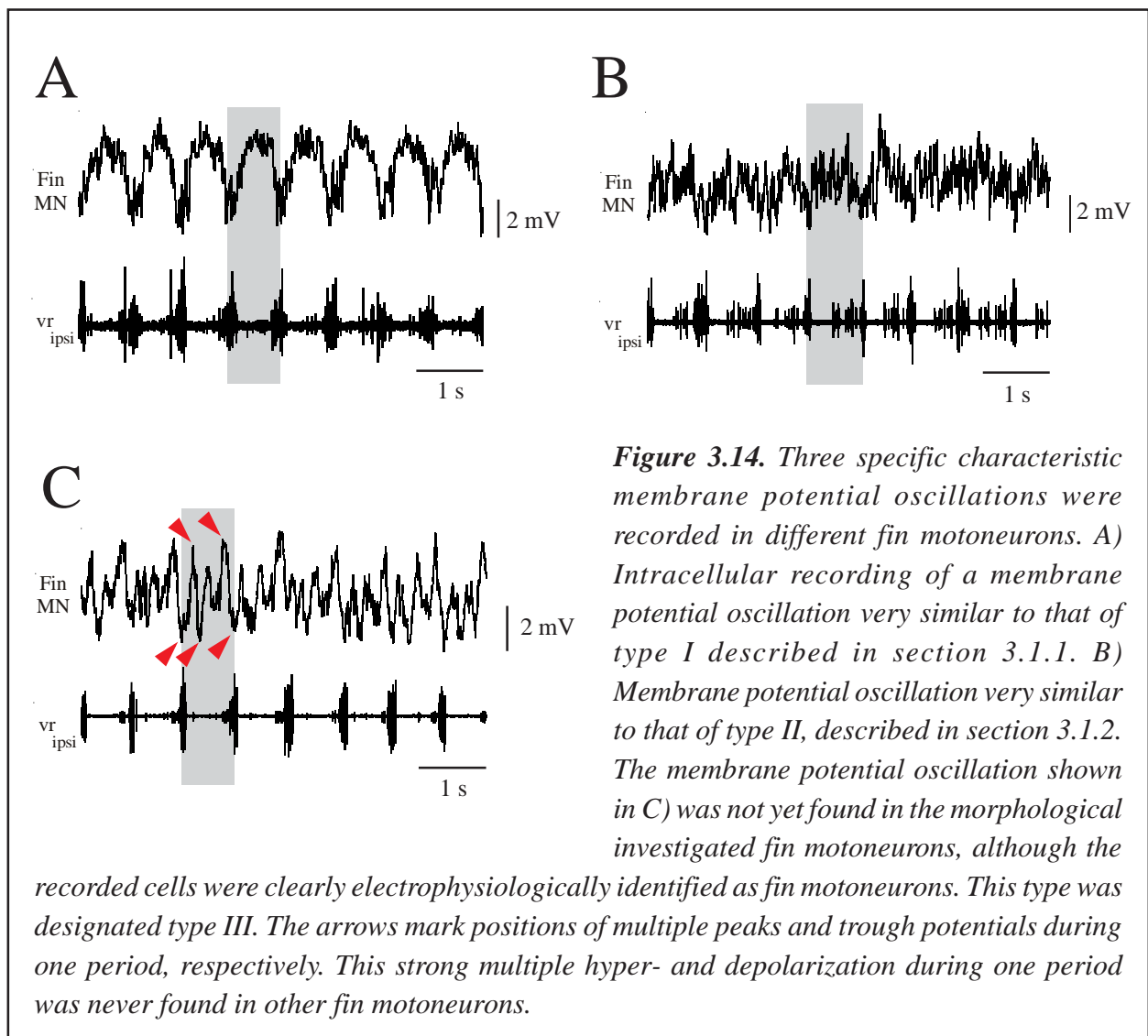


middle of the ipsilateral myotomal burst. These results indicate that the different input to fin motoneurons of type I and type II described in section 3.1.1.2 and 3.1.2.2 could be used in distinguishing between them just by the shape of their membrane potential distribution \pm 200 ms around the middle of the ipsilateral myotomal burst.

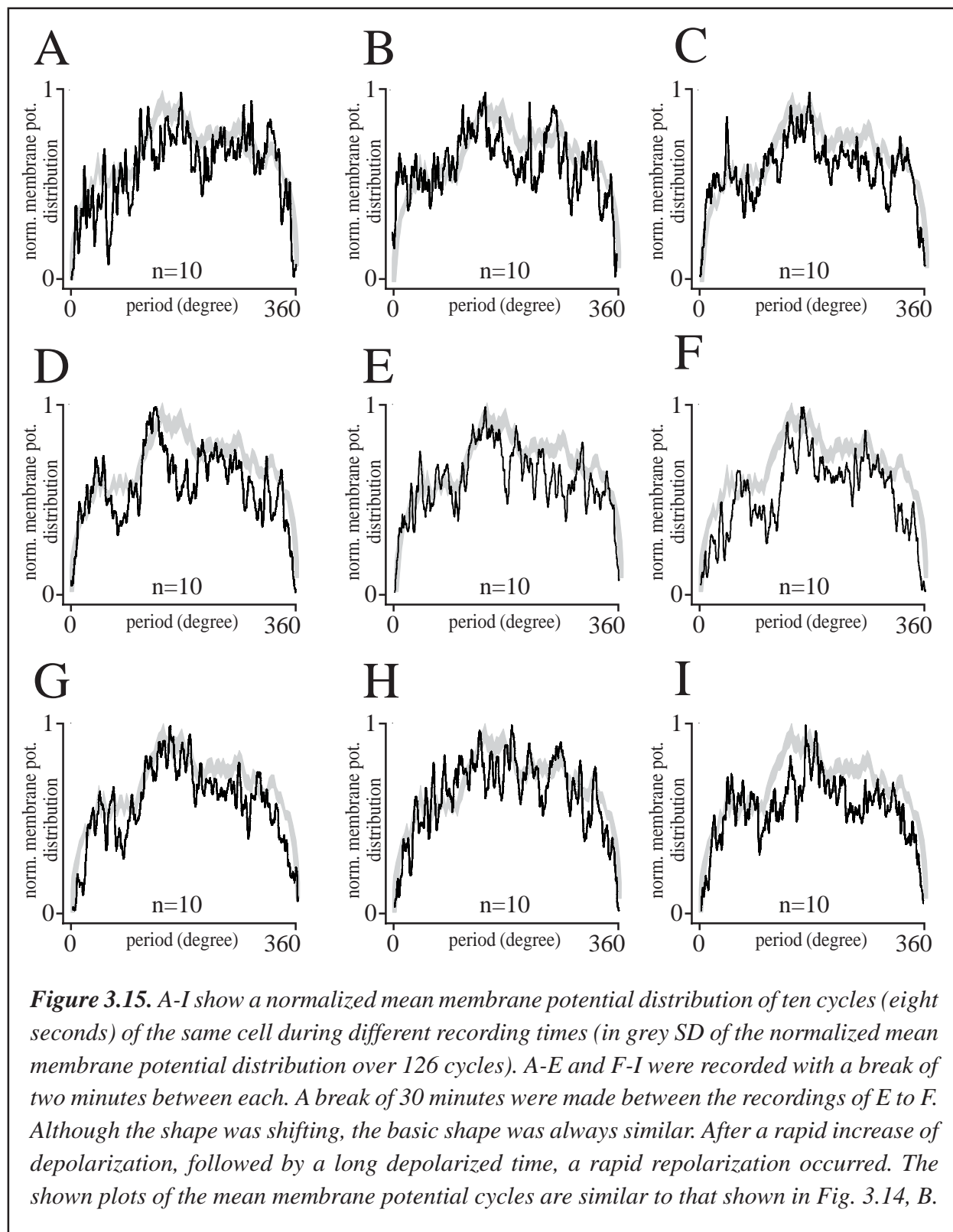
3.2 Different types of membrane potential oscillations in fin motoneurons

3.2.1 Different membrane potential oscillations within one period

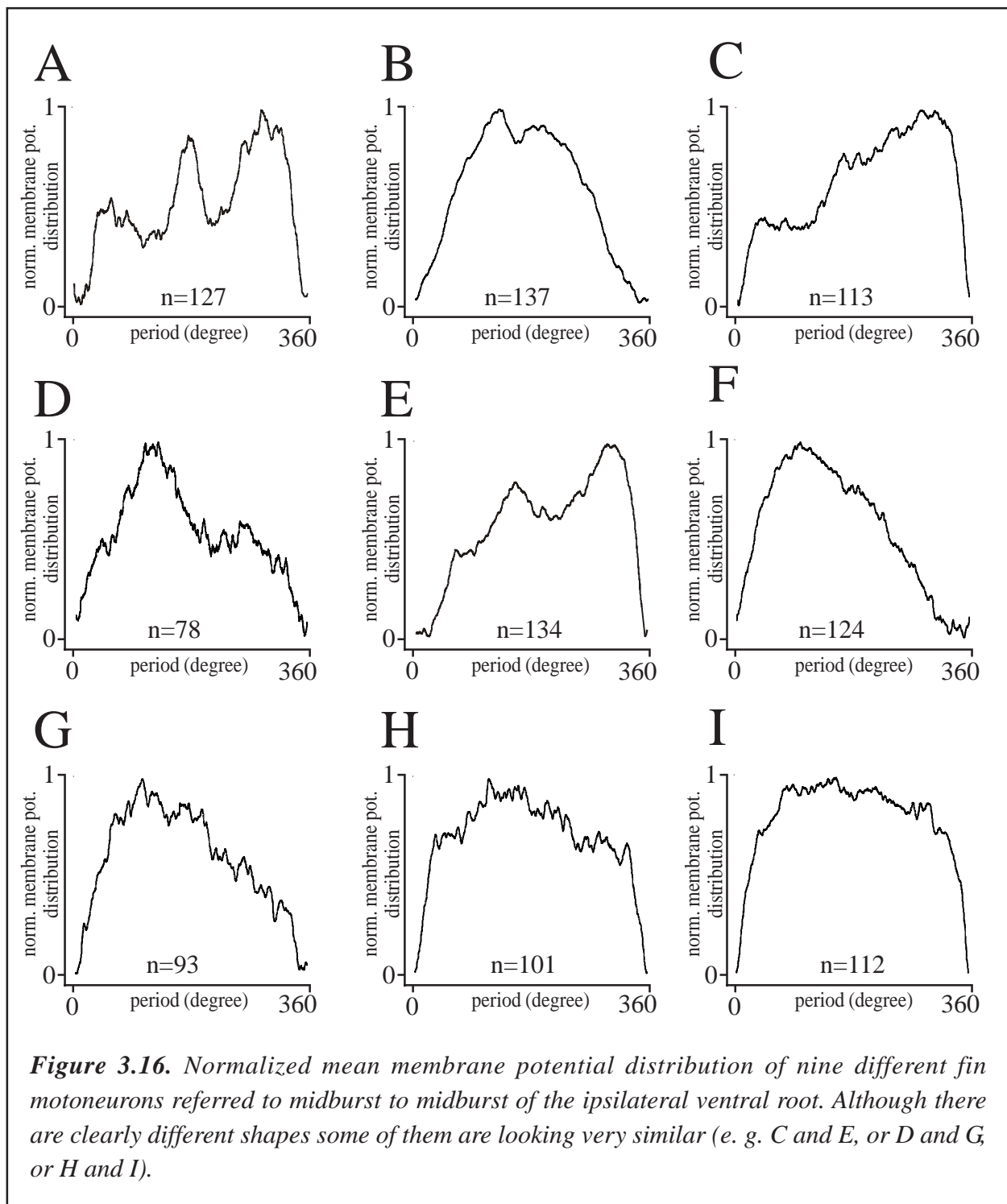
In many cases fin motoneurons were only identified electrophysiologically but not morphologically. The question arose whether differences in membrane potential oscillation are robust enough to



justify a physiologically based classification (Fig. 3.14). The cells were measured for 50 to 180 minutes (the neurons were recorded every five to ten minutes for 60 to 120 seconds to reduce the



amount of data). To ensure that there were no significant changes of the shape of the membrane potential oscillation during recording, the recording periods were separated into eight seconds each and the membrane potential distribution over a period of ten cycles were summed, averaged, normalized and plotted (Fig. 3.15). Despite the fact that the membrane potential distributions were



not the same in all cycles, their shape for one neuron was always similar. There were no large changes in the membrane potential oscillation seen within one fin motoneuron. This means that the different types of fin motoneurons could be classified according to the cyclic mean of the membrane potential oscillations. Due to the similarities of the shape of the membrane potential over a period within one fin motoneuron it is most probable that a significant different shape of a membrane potential distribution recorded over a measured cycle was specific for a given cell recorded, and thus could be partially used as class criterion between them. Fig. 3.16 shows the mean periodical membrane potential oscillation of nine different fin motoneurons referred to midburst to midburst of the ipsilateral ventral root analyzed over 78 up to 137 cycles. In some cases the different cells showed a very similar pattern of the membrane potential distribution. Some fin motoneurons had a slow constant depolarization with a similar slope almost until the end of the period (around 320 deg) before a fast repolarization occurred (e. g. C and E). Others fin motoneurons had a very fast depolarization at one constant level, followed by a very light membrane potential fluctuation almost to the end of the period and followed by a fast repolarization (e. g. H and I, similar to that of type II fin motoneurons). A third case showed a slow steadily depolarization, but after reaching its peak depolarization (around 120 deg to 240 deg) a similar slow repolarization occurred (e. g. B, D and G similar to type I fin motoneurons). Yet another type showed at the beginning a rapid depolarization followed by a slow and long lasting phase of repolarization (F).

3.2.1.1 Statistical classification of cells with different shape of membrane potential distribution within one period

According to the observed similarities and dissimilarities of the different shapes of the membrane potential distribution shown in Fig. 3.16, it was important to classify these cells to put similar types of fin motoneurons together and probably to find new classes of cell types. Grouping of cells by visual inspection of membrane potential oscillation was complemented by a multivariant statistical technique, the hierarchical cluster analysis. After performing this classification on all different fin motoneurons (N=38), including the morphological described and identified ones (see chapter 3.1) as well as two others recorded by Tim Mentel. The results (Fig. 3.17) distinguished five different main classes (A-E), meaning that there could be five different types of fin motoneurons existing in

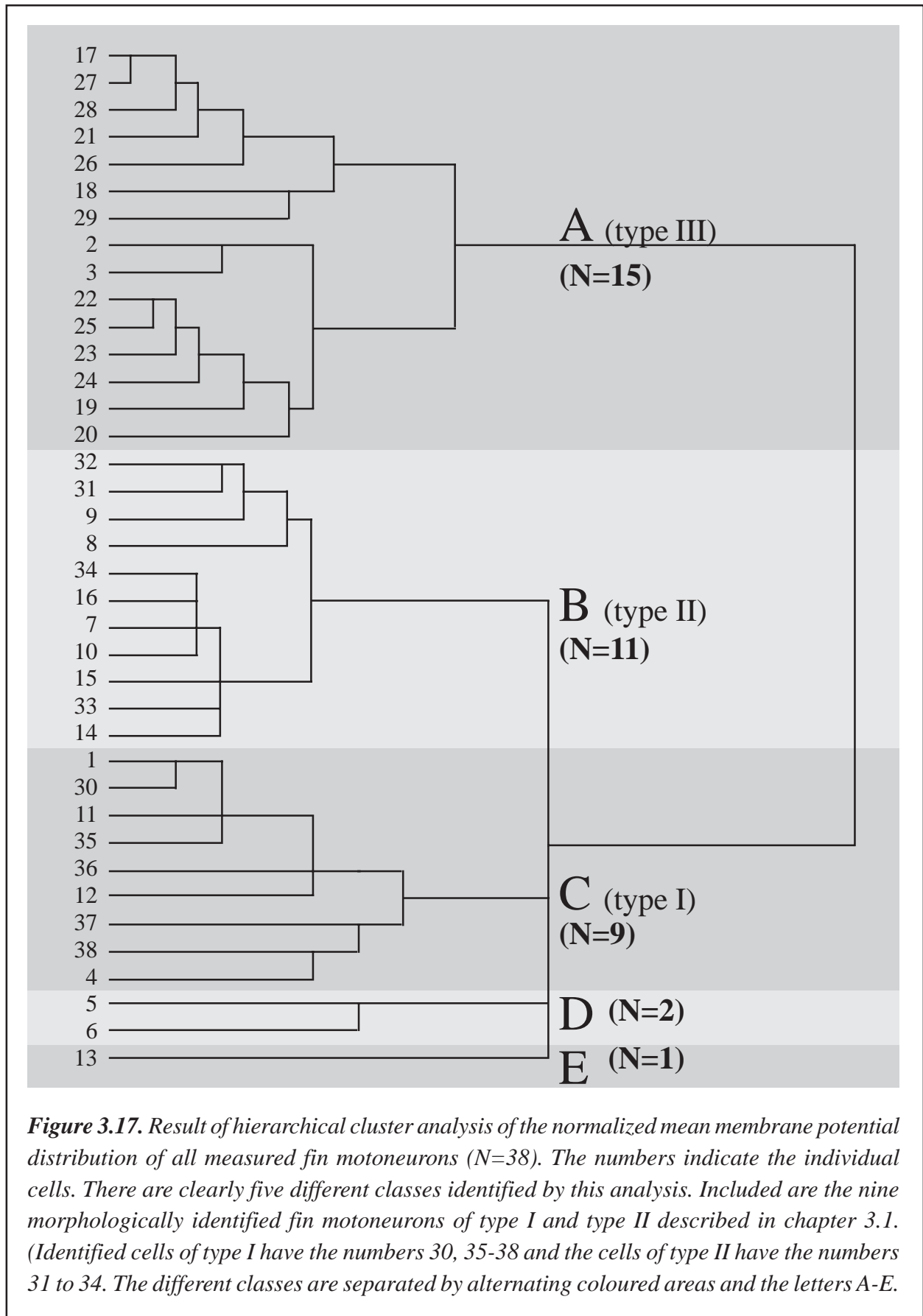
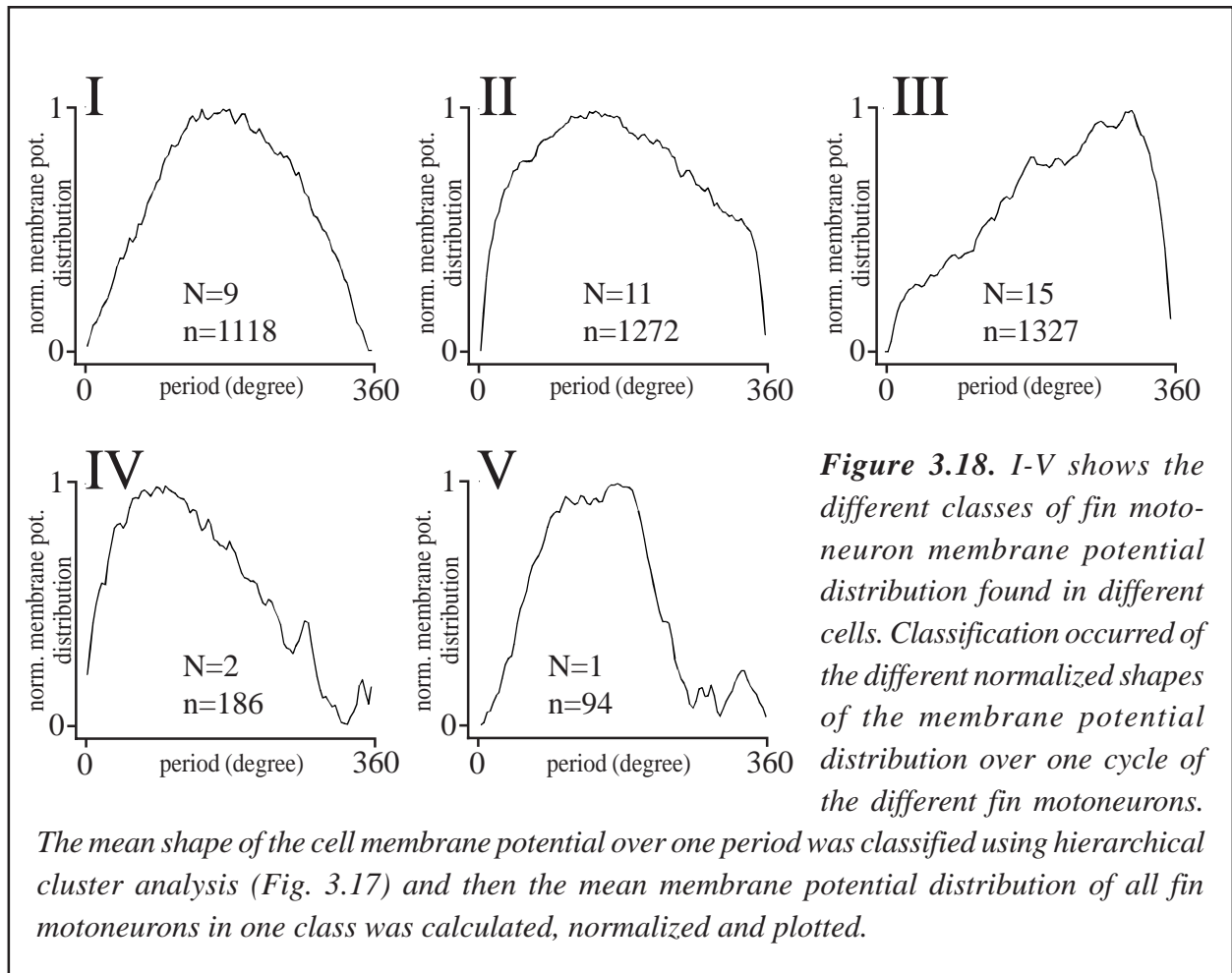


Figure 3.17. Result of hierarchical cluster analysis of the normalized mean membrane potential distribution of all measured fin motoneurons ($N=38$). The numbers indicate the individual cells. There are clearly five different classes identified by this analysis. Included are the nine morphologically identified fin motoneurons of type I and type II described in chapter 3.1. (Identified cells of type I have the numbers 30, 35-38 and the cells of type II have the numbers 31 to 34. The different classes are separated by alternating coloured areas and the letters A-E.

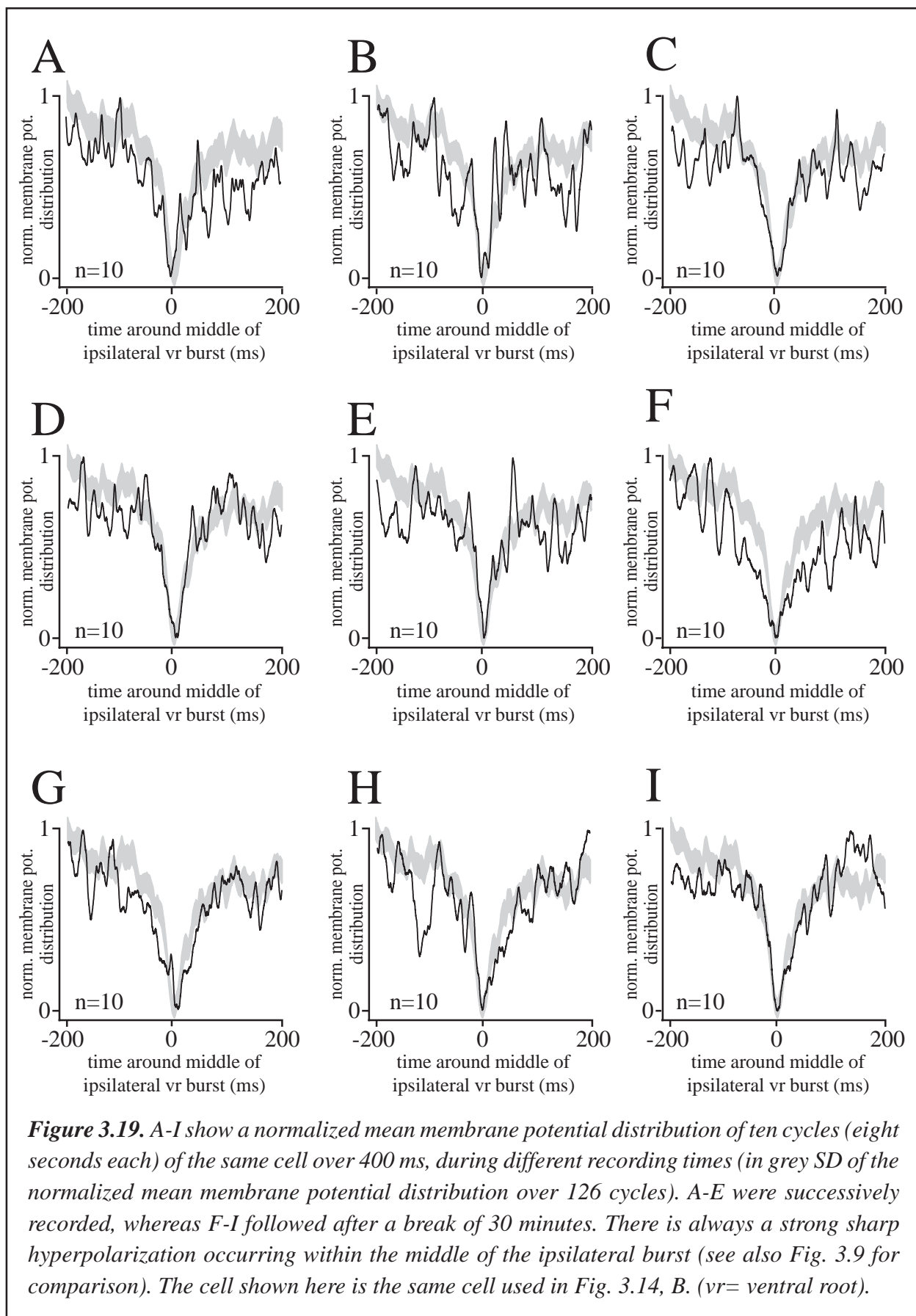


lamprey. Although class A was subdivided into two smaller classes, these could be taken together due to their close similarity. For analyzing these different classes and calculating the mean membrane potential oscillation of all investigated fin motoneurons, the number of classes within the period of one neuron was reduced from 2000 down to 100 and the mean membrane potential distribution was plotted (Fig. 3.18). The number of cycles for calculating the mean of the membrane potential oscillation varied between $n=63$ up to $n=137$. The different classes were renamed from I to V due to the included morphological identified fin motoneurons of type I and type II. Therefore the classes including these neurons were labelled with I (class C) and II (class B) and the next larger one with III (class A). The last two classes were then labeled with IV and V. From these different five classes of fin motoneurons the two last ones were ignored for later analysis, because of their low number of samples ($N=2$ for class IV, $N=1$ for class V). Class number IV had similarities in membrane potential distribution to class number II (fast increase of depolarization) whereas class number V had

similarities in membrane potential oscillation with class number I (maximum depolarization at a phase of 140 deg to 190 deg within one mean period). The other three classes were interpreted as different and independent fin motoneurons. After hierarchical clustering 9 cells of type I (class C in Fig. 3.17) were found. This means that additional to the five morphologically identified types four more cells fitted to the criteria of the mean shape of membrane potential distribution for fin motoneurons of type I. At the same way seven more fin motoneurons were found (N=11), which had a similar mean membrane potential distribution compared to type II fin motoneurons (class B in Fig. 3.17). The third class of fin motoneurons (type III, class A in Fig. 3.17) was not identified morphologically in this work, although it seems after our results that there has to be a large number of type III fin motoneurons located in the lamprey spinal cord. This means that at least three different types of fin motoneurons in the lamprey were found identifiable on the basis of their different membrane potential oscillation over one period, meaning that there could be three different morphological types of fin motoneurons in the lamprey spinal cord.

3.2.2 Different membrane potential oscillations over time

Fin motoneurons (N=29) which were electrophysiologically, but not morphologically identified, showed different membrane potential oscillations (Fig. 3.14). The cells were measured for 50 to 180 minutes (the neurons were recorded every five to ten minutes for 60 to 120 seconds to reduce the amount of data). To be sure that there were no significant changes of the shape of the membrane potential oscillation during „fictive swimming“, the same method was used described in paragraph 3.2.1. Although the membrane potential fluctuation was not the same in all cycles, the shape in all cases was very similar within the recorded neuron. These results showed no large changes in the membrane potential oscillation of a recorded fin motoneuron during „fictive swimming“. This means that the mean membrane potential oscillations over a time of 200 ms around the middle of the ipsilateral burst activity might represent another suitable way of classifying the different types of fin motoneurons. Due to the similarities of the membrane potential distribution within one fin motoneuron over time it is most probably that a certain characteristic shape of a membrane potential distribution over a measured time around the ipsilateral burst is specific for a given type of fin



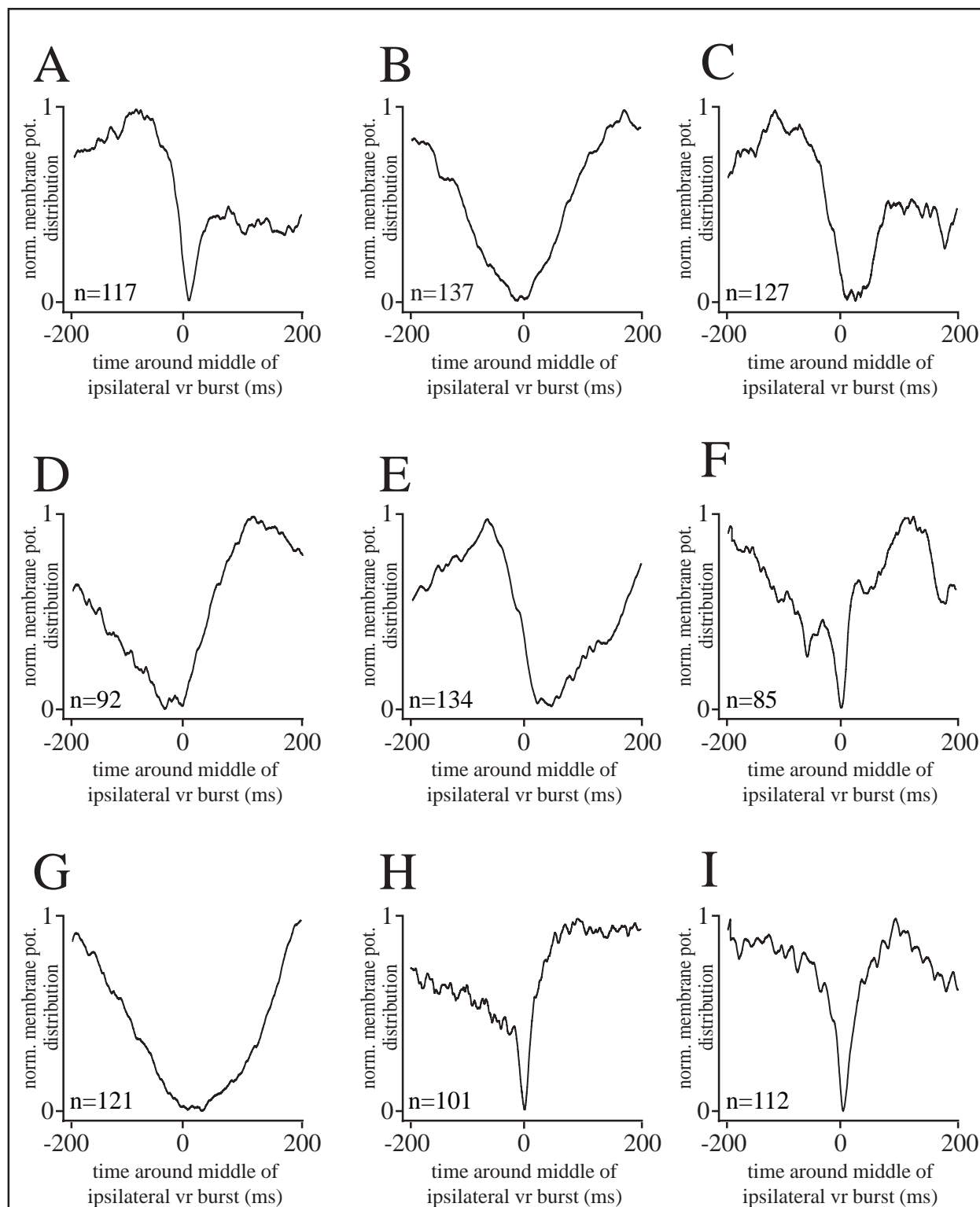


Figure 3.20. Normalized mean of the membrane potential distribution of nine different fin motoneurons over a time of 400 ms referred to the middle of the ipsilateral ventral root (-200 ms to +200 ms). Some shapes of the mean membrane potential distribution show a very fast hyper- and depolarization around the middle of the ipsilateral ventral root (vr) burst caused by activity of myotomal motoneurons.

motoneuron. Fig. 3.20 shows the mean membrane potential distribution of nine different fin motoneurons around ± 200 ms referred to the middle of one burst caused by ipsilateral ventral root activity. 78 up to 137 cycles were analyzed. In some cases the different cells showed a similar shape of the membrane potential distribution. Some of the fin motoneurons had a slow constant depolarization with a similar wide slope to the middle of the burst (time zero) of the ipsilateral recorded ventral root followed by a similar slow depolarization (B and G), whereas others had a very fast hyperpolarization at the middle of the burst that was followed by a similar fast depolarization (A, F, I and H). In a third case cells had a slow steadily hyperpolarization, but after reaching its trough potential (at around zero) a faster depolarization occurred (C and D), whereas another type revealed the opposite membrane potential distribution, i.e., after a faster hyperpolarization a slower depolarization occurred (E).

3.2.2.1 Statistical classification of cells with different shape of membrane potential distribution over time

According to the observed similarities and dissimilarities of the different shapes of the membrane potential distribution (shown in Fig. 3.20) it was important to classify these cells for clustering similar fin motoneurons together and probably to find new classes of cell types and to find out if the classification of the membrane potential distribution over a time of 400 ms around the middle of the myotomal burst would show the same result in clustering as seen in Fig. 3.17 for the shape of the mean membrane potential over one cycle. Therefore, as described earlier (chapter 3.2.1.1), grouping of cells by visual inspection of membrane potential oscillation was complemented with a multi-variant statistical technique, the hierarchical cluster analysis. After performing this classification on all different fin motoneurons (N=38), included the morphologically described and identified ones, the result (Fig. 3.21) distinguished three different main classes (A-C), meaning that there could be three different types of fin motoneurons existing in lamprey. For analyzing these different classes and calculating the mean membrane potential distributions over a time of 400 ms of all investigated fin motoneurons, the number of classes within the period of one neuron was reduced from 2000 down to 100 and the mean membrane potential distribution was plotted (Fig. 3.22). The number of cycles for calculating the mean of the membrane potential oscillation varied between

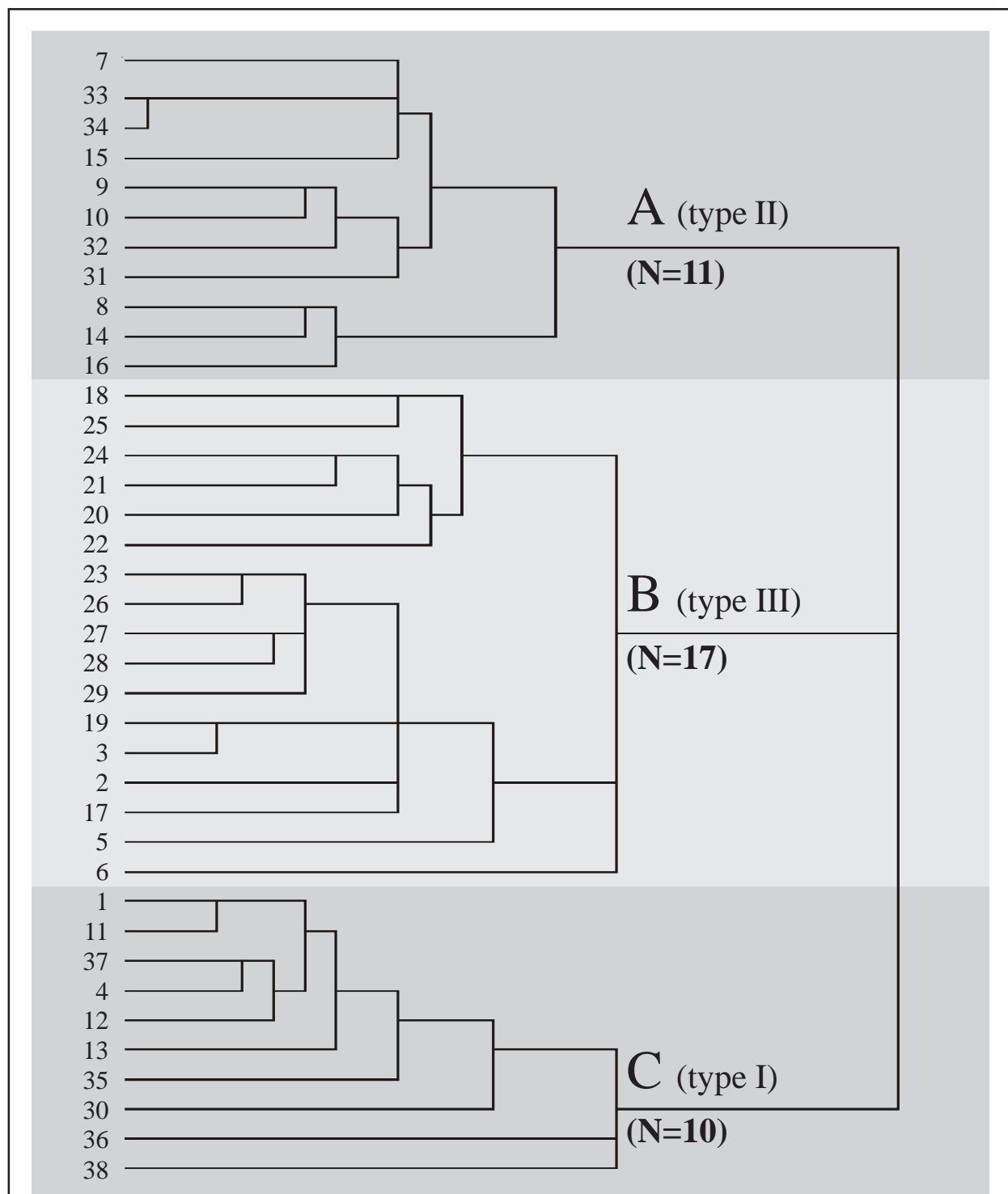
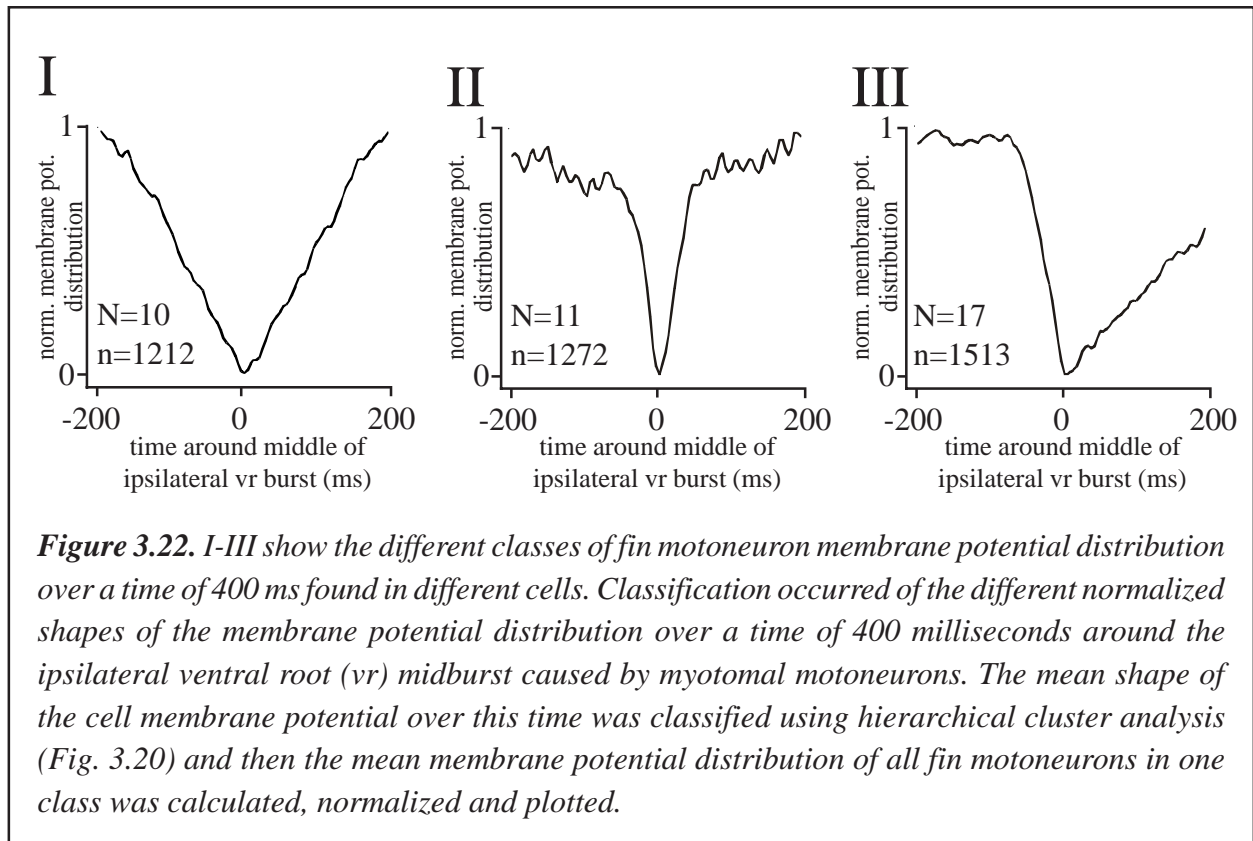


Figure 3.21. Result of hierarchical cluster analysis of the normalized mean membrane potential distribution of all measured fin motoneurons over time ($N=38$). The numbers indicate the individual cells (same as in Fig. 3.17). There are clearly three different classes identified by this analysis. Included are the nine morphologically identified fin motoneurons of type I and type II described in chapter 3.1. (cells of type I have the numbers 30, 35-38 and cells of type II have the numbers 31 to 34). The different classes are separated by alternating coloured areas and the letters A-C.

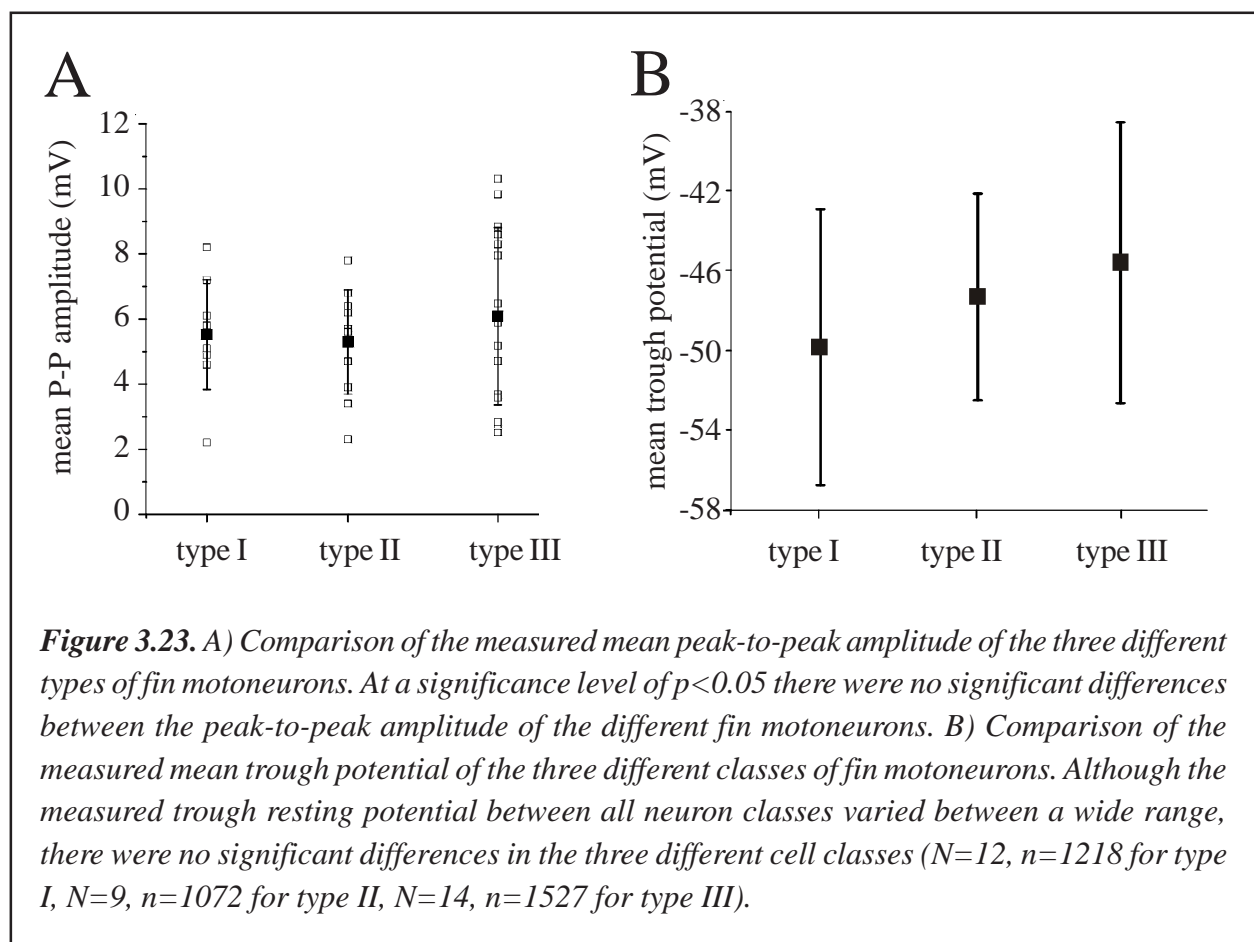


n=63 up to n=137. The different classes were renamed from I to III. Classes including the morphologically and electrophysiologically identified fin motoneurons of type I and type II were labelled with I (class C) and II (class A) respectively, whereas the last one was named with III. The three classes found were taken as different and independent types of fin motoneurons, meaning that at least three different fin motoneurons in lamprey could exist identifiable due to their different membrane potential distribution over a time of 400 milliseconds around the ipsilateral midburst activity caused by myotomal motoneurons.

3.2.3 Electrophysiological comparison of the newly classified groups of fin motoneurons

Analysing the three different cell classes of fin motoneurons with hierarchical cluster analysis showed in both cases a similar result. The three different classes in Fig. 3.21 include the same cells as in Fig. 3.17 but also the two additional classes (D and E) from Fig. 3.17 were calculated into class C (class E) and into class B (class D) respectively. Class A of Fig. 3.21 included the same cells as in class B

of Fig. 3.17. 88% to 90% of cells of type I and type III were classified the same via the mean membrane potential distribution over period, or over a time of 400 ms around the midburst activity of the ipsilateral ventral root, whereas in both cases all cells of type II were classified the same. Classifying by membrane potential shape over period resulted in five different classes, whereas classifying over time did not. Furthermore, in the latter case the two additional classes were solved and included in cells of type I and type III, whereas the other cells were the same in both analyzing methods. Therefore it seemed that classifying fin motoneurons by their membrane potential distribution over mean period was a more exact way than to classify them over a time of 400 ms. The result showed that hierarchical cluster analysis should be a good method for distinguishing and grouping of different electrophysiological and/or morphological types of motoneurons and that probably there are three different classes of fin motoneurons located in the spinal cord of lamprey. Although two morphological different types were described earlier in this thesis (see chapter 3.1), the summary of properties of the three different classes of cells were not described yet. For the

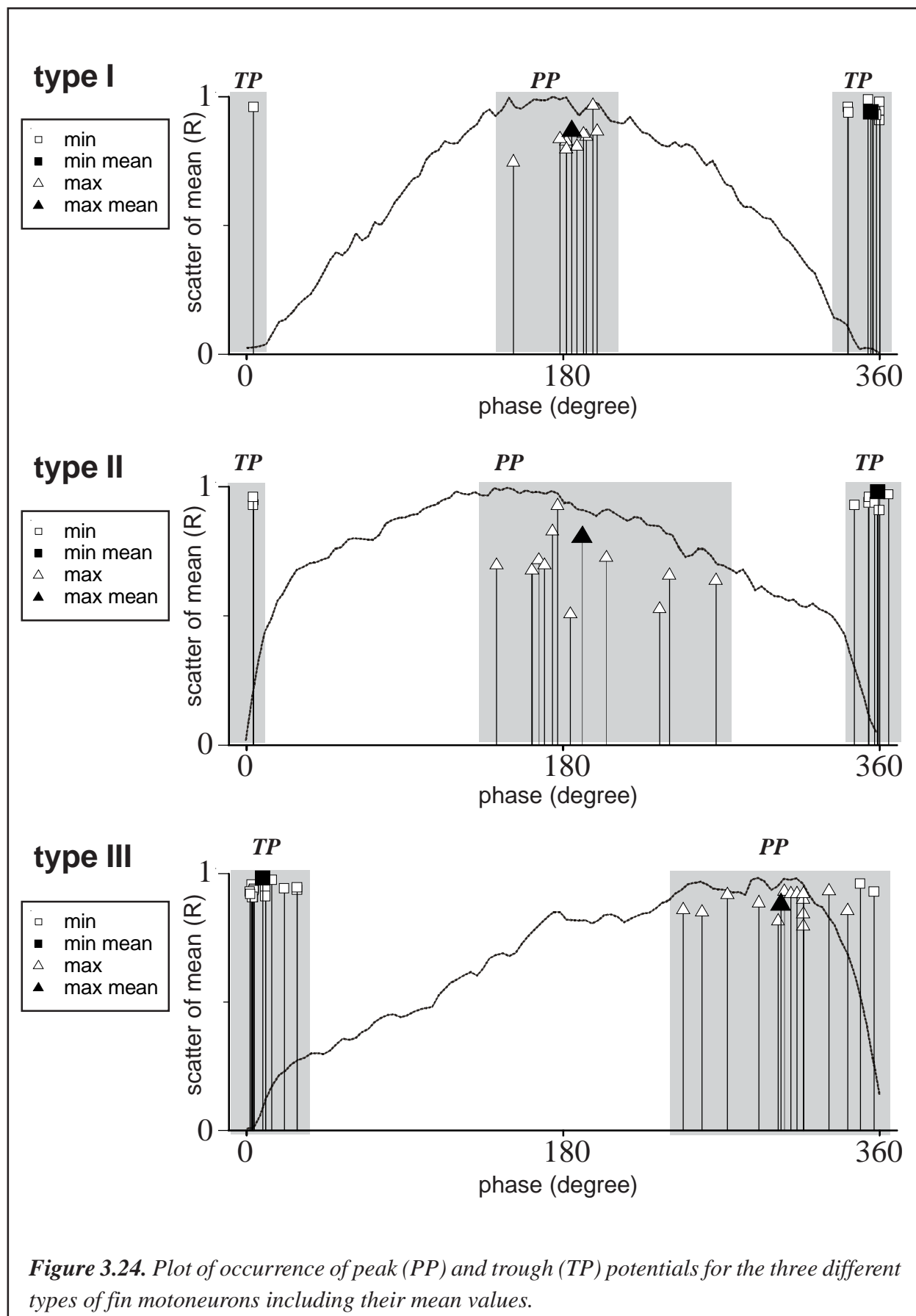


electrophysiological description of the different types of fin motoneurons all cells of one class were taken together and the mean of the properties were calculated. The three different types of fin motoneurons now included all the different, statistically determined cells of the different classes. Only those cells were taken, which were found in the same class in both different used methods for classification (see Fig. 3.17 and 3.21). Therefore 9 fin motoneurons of type I, 11 of type II and 15 different cells of type III were investigated. The electrophysiological properties of these three different types of fin motoneurons are shown in Fig. 3.23. Fin motoneurons of type I showed a measured trough potential ranged from -59.8 mV to -40.8 mV (mean -49.8 mV \pm 6.9 mV). The peak-to-peak amplitude varied from 2.2 mV up to 8.2 mV (mean 5.5 mV \pm 1.7 mV). Type II fin motoneurons showed a measured trough potential ranged from -53.8 mV to -38.9 mV (mean -47.3 mV \pm 5.2 mV). The peak-to-peak amplitude varied from 2.3 mV up to 7.8 mV (mean 5.3 mV \pm 1.6 mV). Finally the third class of fin motoneurons (type III) showed a trough potential from -36.7 up to -55.3 (mean -45.6 mV \pm 7.1 mV) and a peak-to-peak amplitude from 2.5 mV up to 10.3 mV (mean 6.1 mV \pm 2.7 mV). For comparison of the measured values of the peak-to-peak amplitude and the resting trough potential of all three different types of fin motoneurons an one sample ANOVA-test was performed on the data at significance level of $p < 0.05$. It was found that no significant differences were recorded in the trough potential, nor a significant difference was found in the peak-to-peak amplitude.

In comparison of the different calculated mean shapes for the membrane potential distribution (Fig. 3.18, I-III) showed between type I and type II fin motoneurons no significant shift in the position of peak amplitude, but type III fin motoneurons had a significant shifted peak amplitude. In type I the mean minimum of the membrane potential was reached at a phase of - 4.9 deg ($R=0.942$) and the mean maximum at 184.9 deg ($R=0.872$). Type II fin motoneurons showed their mean minima and maxima at - 0.9 deg ($R=0.982$) and 190.9 deg ($R=0.812$) respectively. Finally cells of type III reached their mean minimum at 9.2 deg ($R=0.983$) and their mean maximum at 303.9 deg ($R=0.885$) (Fig. 3.24, Tab. 3.2).

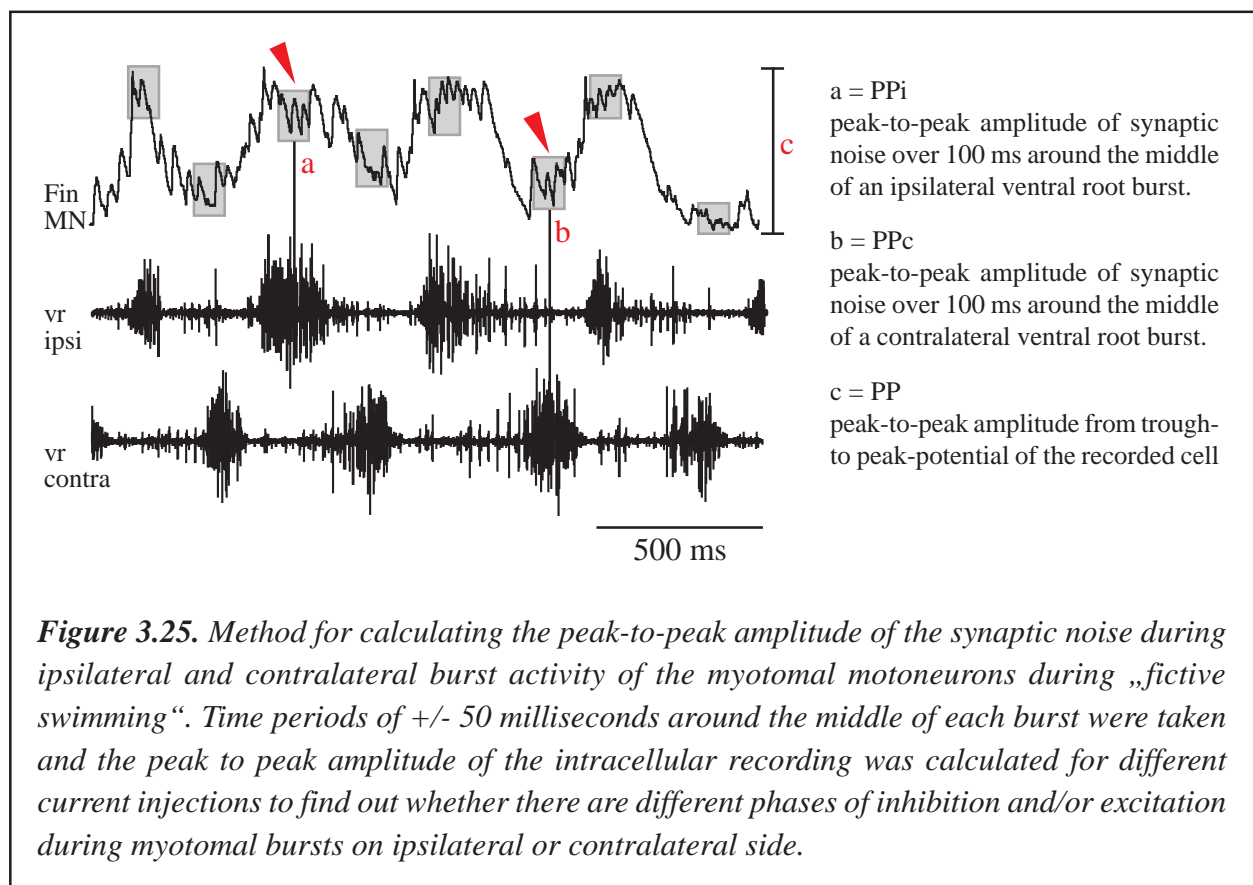
<u>type I fin motoneuron</u>	minimum	minimum	- 35.8 degree
		maximum	3.8 degree
		mean	- 4.9 degree, R=0.942
	maximum	minimum	151.6 degree
		maximum	197.2 degree
		mean	184.9 degree, R=0.872
<u>type II fin motoneuron</u>	minimum	minimum	- 14.2 degree
		maximum	3.9 degree
		mean	- 0.9 degree, R=0.982
	maximum	minimum	142.2 degree
		maximum	267.2 degree
		mean	190.9 degree, R=0.812
<u>type III fin motoneuron</u>	minimum	minimum	-10.8 degree
		maximum	28.8 degree
		mean	9.2 degree, R=0.983
	maximum	minimum	248.4 degree
		maximum	342.0 degree
		mean	303.9 degree, R=0.885

Table 3.2. Location of minimum-, maximum- and mean trough (minimum)- and peak (maximum)-potentials during each phase of the three different types of fin motoneurons.



3.3 Excitatory and inhibitory influences from other neurons to fin motoneurons

Knowing that myotomal motoneurons in lamprey are getting different phasic inputs for causing fluctuation of membrane potential (Wallén *et al.*, 1993) does not answer the question how the mechanisms of this modulation in fin motoneurons are organized and controlled by different interneurons. It could be that there is only excitatory synaptic drive, only inhibitory synaptic drive or maybe a combination of both for causing the antiphase peak depolarization of the fin motoneurons membrane potential during burst activity of the ipsilateral ventral root caused by myotomal motoneuron activity. Therefore it was investigated how the different types of fin motoneurons react to strong hyperpolarized current injection (up to -4.0 nA). During this injection an only excitatory synaptic drive would have no influence to the shape of the membrane potential, but a larger peak-to-peak amplitude. In the opposite way only the phasic inhibition (caused by chloride ions) would result in a lower peak-to-peak amplitude and after reaching the reversal potential of chloride the phase would be fully reversed resulting in an increased amplitude. Finally an alternating combination of both different synaptic drives (inhibition and excitation) during negative current injection would



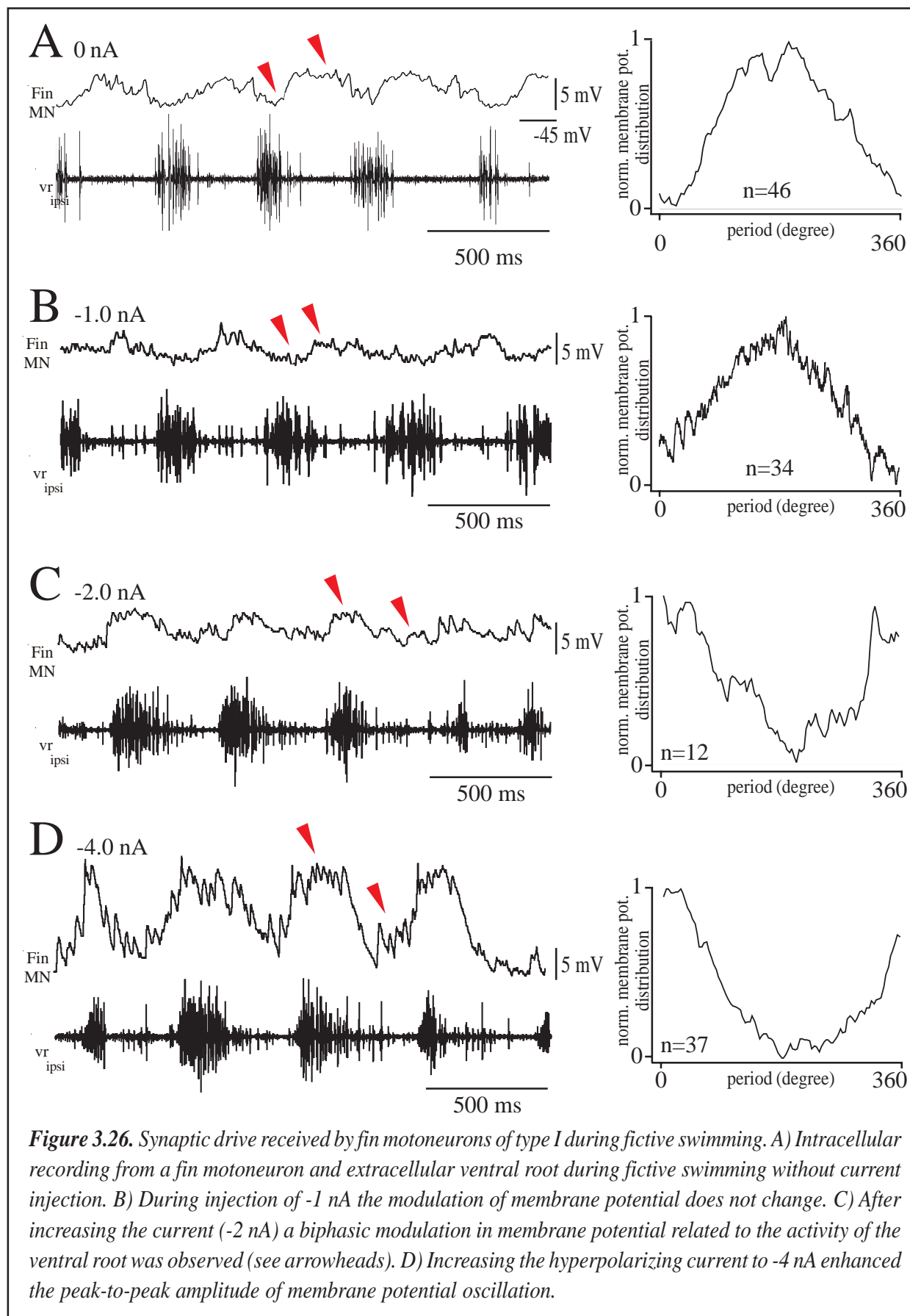
cause an increase of the peak-to-peak amplitude for the excitatory phase of the membrane potential distribution depending to the strength of the phasic inhibition whereas the peak-to-peak amplitude of the inhibitory phase would get lower and after reaching its reversal potential it would be reversed. This means it could be that there is a constant inhibition of fin motoneurons with periodical excitation in the midburst intervals of the ipsilateral ventral root. For analyzing the latter effect, the mean peak-to-peak amplitude of the different types of fin motoneurons were taken 100 milliseconds around the middle of the ipsilateral ventral root burst activity (PPi) and also 100 milliseconds around the middle of the contralateral burst activity (PPc) to investigate if there were significant changes during the analyzed time in the amplitude between trough- and peak potential of the synaptic noise during current injection (see also Fig. 3.25).

3.3.1 Synaptic input to fin motoneurons of type I

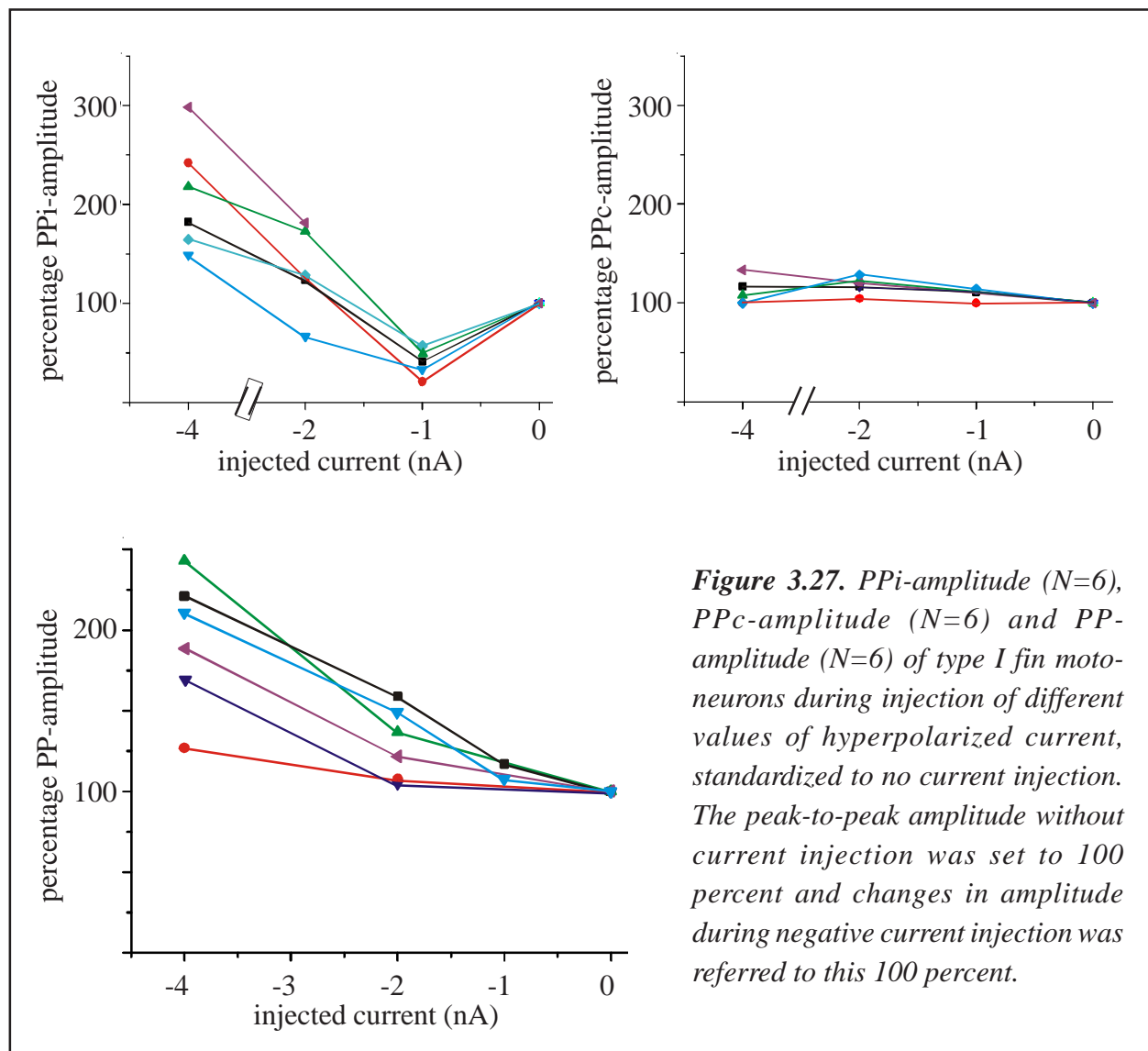
During injection of hyperpolarizing current into fin motoneurons of type I a biphasic modulation of the membrane potential oscillation was visible (Fig. 3.26). This means that the phasic membrane

injected current (nA):	0	-1	-2	-4
N:	6	5	6	6
n:	545	448	545	545
PPi min (mV):	1.1	0.4	1.8	2.3
PPi max (mV):	3.3	0.8	3.1	5.1
PPi mean (mV):	1.86 +/- 0.76	0.61 +/- 0.21	2.25 +/- 0.47	3.71 +/- 0.91
PPc min (mV):	0.8	1.8	1.6	1.4
PPc max (mV):	2.9	2.1	3.4	3.1
PPc mean (mV):	1.64 +/- 0.74	1.97 +/- 0.25	2.11 +/- 0.68	2.18 +/- 0.75
PP min (mV):	2.9	3.4	4.6	6.1
PP max (mV):	6.2	6.5	5.2	8.5
PP mean (mV):	4.35 +/- 1.31	4.95 +/- 2.19	4.87 +/- 0.31	7.13 +/- 1.47

Table 3.3. Minima, maxima and mean values of ipsilateral peak to peak amplitude (PPi), contralateral peak-to-peak amplitude (PPc) and overall peak-to-peak amplitude (PP) during different negative current injections to fin motoneurons of type I. N=number of measured cells, n=number of measured cycles.



potential oscillation over one cycle measured from midburst to midburst of the ipsilateral ventral root, caused by myotomal motoneuron activity, is changed around 180 deg after injection of a current of at least -2.0 nA, meaning that the reversal potential was reached and crossed (Fig. 3.26, Tab. 3.3, 3.6, 3.7). After further increasing the hyperpolarizing current the peak-to-peak amplitude increased. This result indicates that there is an inhibition to fin motoneurons of type I, but it does not give evidence if this inhibition occurred during phasic time or during the whole cycle time. Therefore PPc and PPi amplitudes were analyzed. During negative current injection (-1 nA) there was at first a reduction of the PPi amplitude (Fig. 3.27), followed by an increase, showing that there is a phasic inhibition during ipsilateral myotomal burst activity. On the other hand, the PPc amplitude did not change significantly during current injection compared with the PPi amplitude, meaning



that there was no active inhibition during the activity of the contralateral myotomal burst. Also there had to be a slow conductance during the contralateral burst activity, because there was no significant increase of the PPc amplitude during negative current injection, meaning that the intrinsic properties of the fin motoneurons could also play an important role for membrane potential oscillation.

3.3.2 Synaptic input to fin motoneurons of type II

During injection of hyperpolarizing current into fin motoneurons of type II a biphasic modulation of the membrane potential oscillation was visible (Fig. 3.28). This means that the phasic membrane potential oscillation over one cycle measured from midburst to midburst of the ipsilateral ventral root, caused by myotomal motoneuron activity, was changed around 180 deg after injection of a current of around -3.0 to -4.0 nA, meaning that the reversal potential was reached and crossed (Fig. 3.28, Tab. 3.4, 3.6, 3.7). This result shows that there is, similar to type I fin motoneurons, an inhibition to fin motoneurons of type II. The result does not provide if this inhibition occurred during a specific phase or during the whole cycle. Therefore PPc and PPI amplitudes were analyzed. During negative

injected current (nA):	0	-1	-2	-4
N:	6	4	5	4
n:	567	431	478	431
PPi min (mV):	1.2	0.8	1.9	2.9
PPi max (mV):	1.6	2.7	3.4	4.1
PPi mean (mV):	1.43 +/- 0.36	1.81 +/- 0.75	2.35 +/- 0.26	3.53 +/- 0.6
PPc min (mV):	1.7	1.5	1.7	1.5
PPc max (mV):	2.7	2.1	2.0	2.1
PPc mean (mV):	2.16 +/- 0.39	1.89 +/- 0.26	1.95 +/- 0.26	1.84 +/- 0.24
PP min (mV):	3.0	3.1	3.3	5.96
PP max (mV):	5.2	5.8	4.4	7.86
PP mean (mV):	3.92 +/- 0.92	4.23 +/- 1.41	3.97 +/- 0.59	6.3 +/- 0.57

Table 3.4. Minima, maxima and mean values of ipsilateral peak-to-peak amplitude (PPi), contralateral peak-to-peak amplitude (PPc) and overall peak-to-peak amplitude (PP) during different negative current injections to fin motoneurons of type II. N=number of measured cells, n=number of measured cycles.

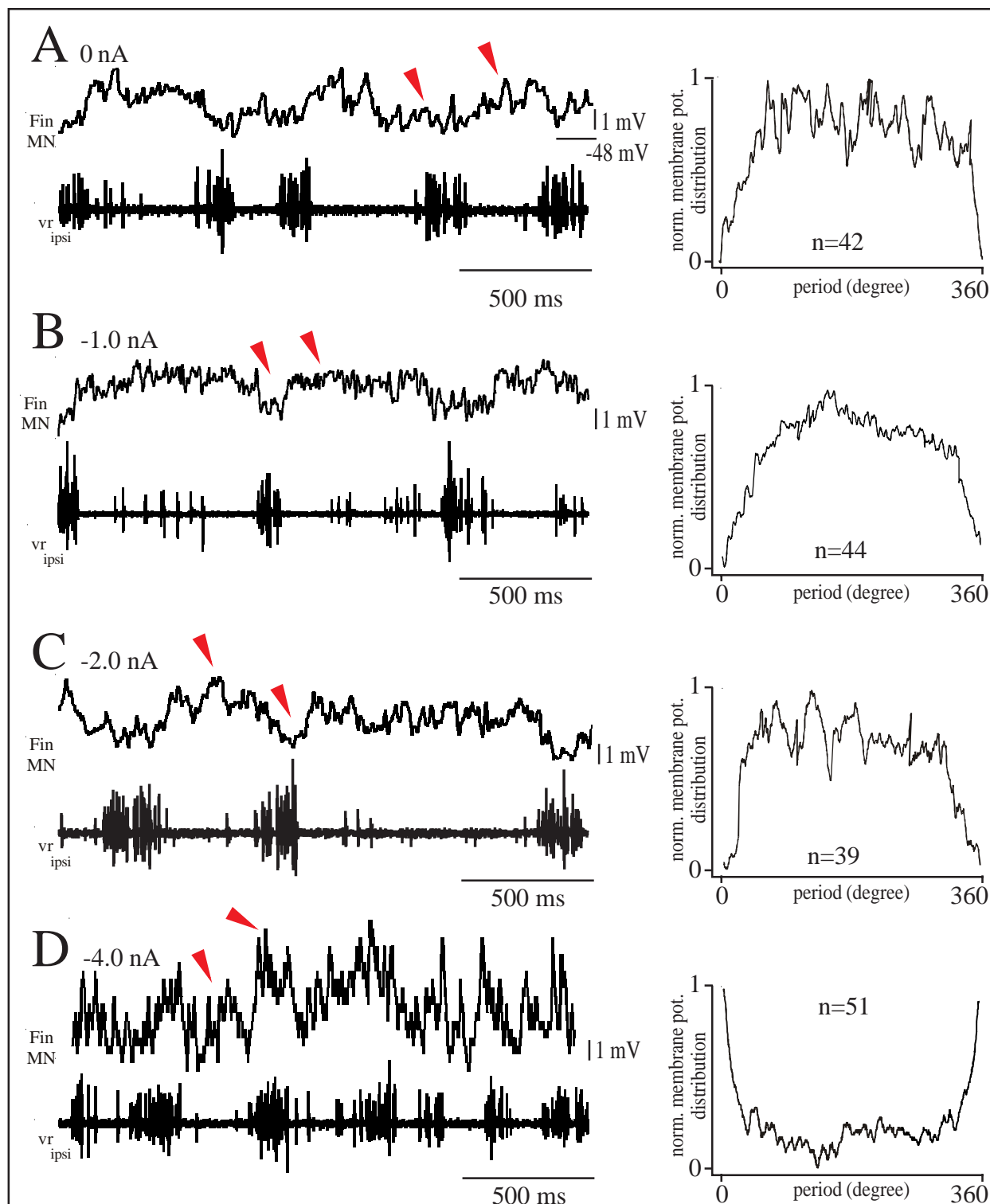
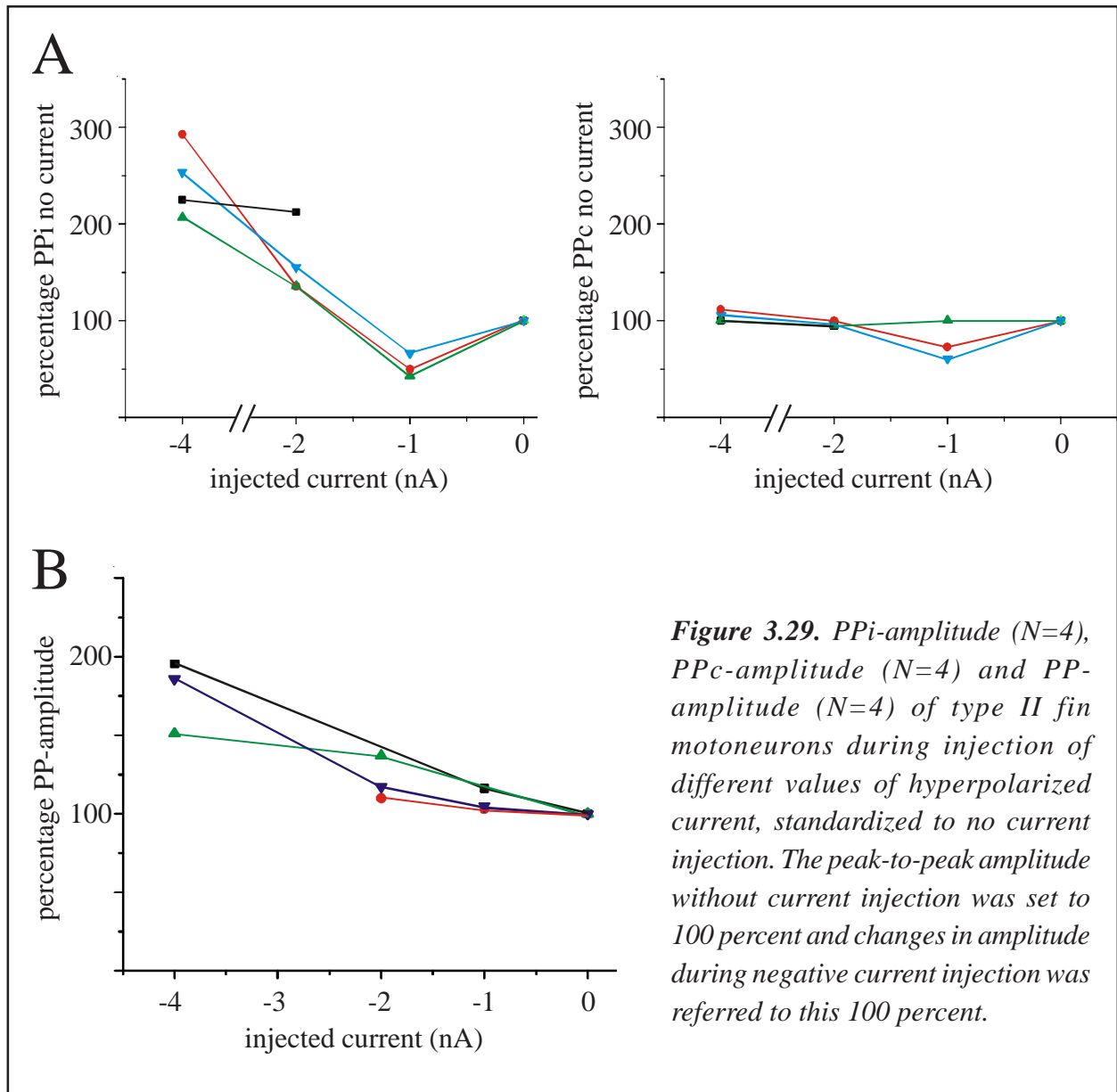
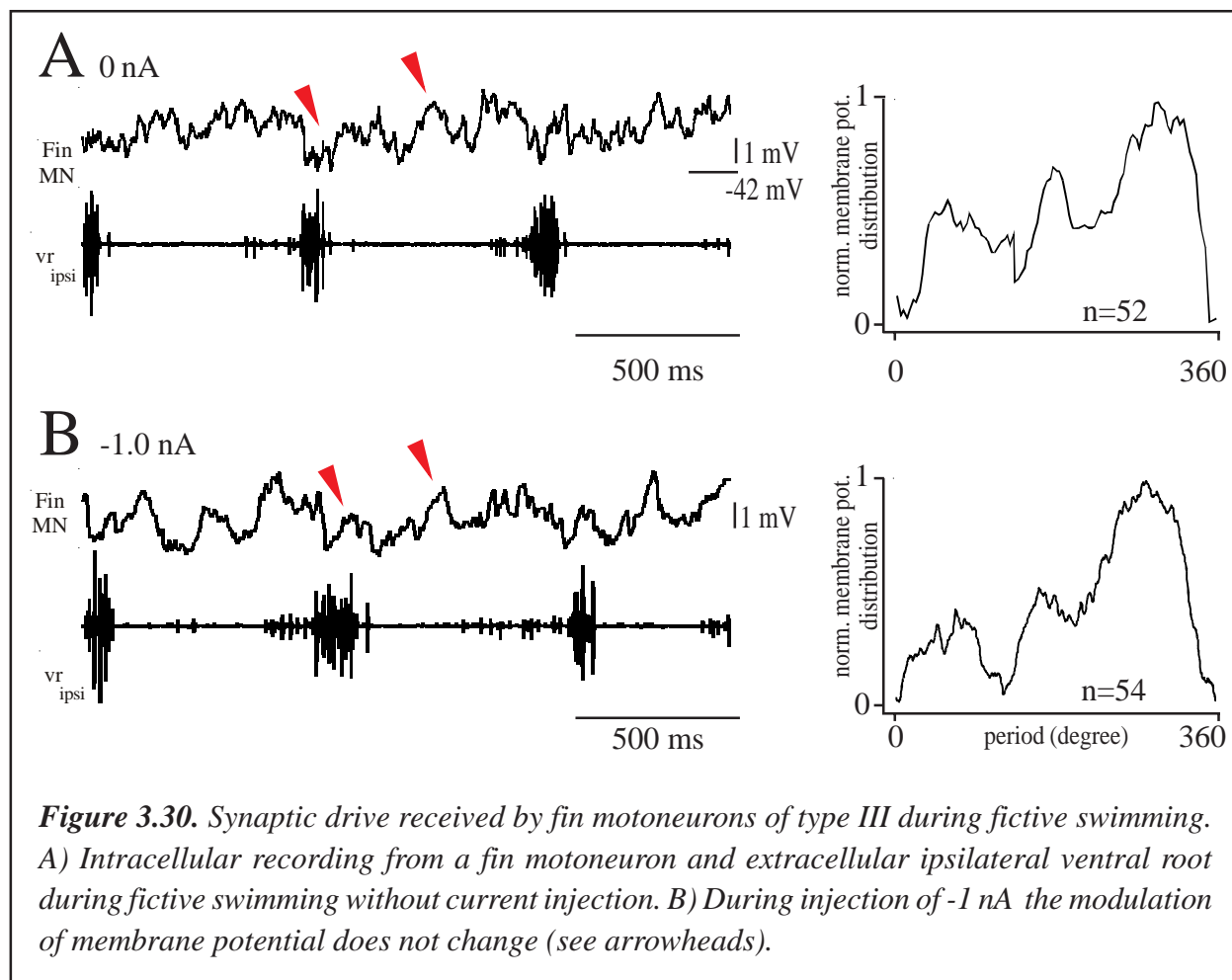


Figure 3.28. Synaptic drive received by fin motoneurons of type II during fictive swimming. *A)* Intracellular recording from a fin motoneuron and extracellular ventral root during fictive swimming without current injection. *B)* and *C)* During injection of -1 nA and -2 nA the modulation of membrane potential does not change. *D)* After increasing the current to -4 nA a biphasic modulation in membrane potential related to the activity of the ventral root was observed (see arrowheads).



current injection (-1 nA) there was at first a reduction of the PPI amplitude, followed by an increase, showing that there is a phasic inhibition during ipsilateral myotomal burst activity (Fig. 3.29). On the other hand, the PPc amplitude did not change significantly during current injection compared to that of the PPI amplitude, meaning that there was no active inhibition during activity of the contralateral myotomal burst. Also, there had to be a slow conductance during the contralateral burst activity, because there was no significant increase of the PPc amplitude during negative current injection.

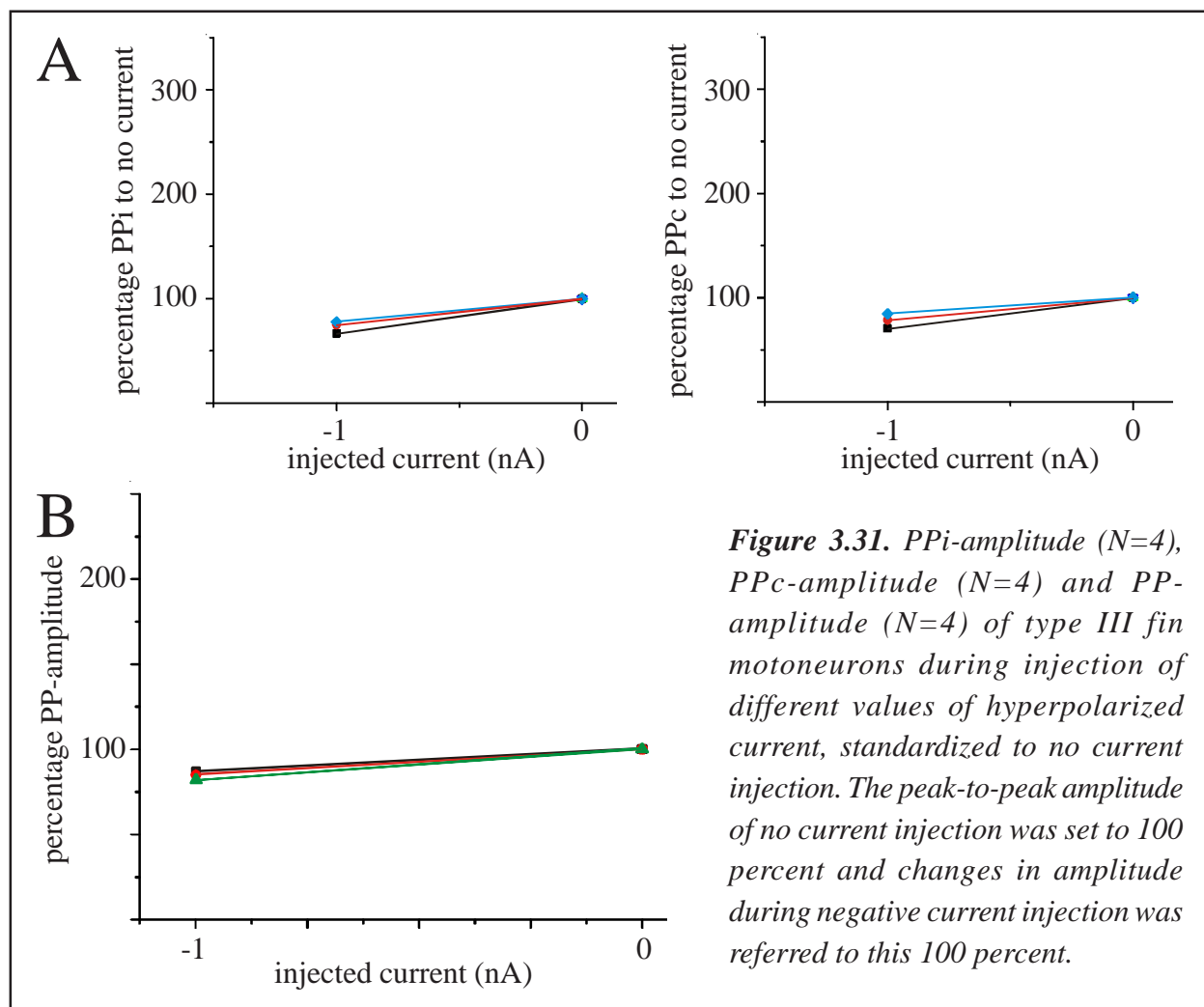


3.3.3 Synaptic input to fin motoneurons of type III

During injection of hyperpolarizing current to fin motoneurons of type III no biphasic modulation of the membrane potential oscillation was visible as seen in the other two types described in 3.3.1 and 3.3.2 with a low hyperpolarized current injection (Fig. 3.30, Tab. 3.5, 3.6, 3.7). This means that the phasic membrane potential oscillation over one cycle measured from midburst to midburst of the ipsilateral ventral root does not change after injection of a current of -1.0 nA. This result (Fig. 3.31) indicates that, similar to motoneurons of type I and II, after injection of a current of -1 nA the reversal potential was not reached. The result does not give evidence if the reversal potential is reached later by increasing the injected current. PPc and PPi amplitudes were analyzed and during negative current injection there was at first a reduction of the PPi amplitude, followed by an increase, that showed that there could be a phasic inhibition during ipsilateral myotomal burst activity (Fig.

injected current (nA):	0	-1
N:	5	5
n:	481	481
PPi min (mV):	0.7	0.6
PPi max (mV):	1.4	0.8
PPi mean (mV):	0.93 +/- 0.28	0.68 +/- 0.1
PPc min (mV):	1.1	0.7
PPc max (mV):	2.7	1.4
PPc mean (mV):	1.62 +/- 0.65	1.05 +/- 0.26
PP min (mV):	3.9	4.2
PP max (mV):	6.4	5.2
PP mean (mV):	5.1 +/- 1.12	4.8 +/- 0.78

Table 3.5. Minima, maxima and mean values of ipsilateral peak-to-peak amplitude (PPi), contralateral peak-to-peak amplitude (PPc) and overall peak-to-peak amplitude (PP) during different negative current injections to fin motoneurons of type III. N=number of measured cells, n=number of measured cycles.



3.31). The PPc amplitude did not change during current injection, meaning that there could be no active inhibition during the activity of the contralateral myotomal burst.

3.3.4 Statistical analysis and comparison of the results of current injection to the three different types of fin motoneurons

To investigate if there were significant changes in the membrane potential oscillation peak-to-peak amplitude before and after hyperpolarized current injection, an one sample ANOVA test was performed on the data at significance level of $p < 0.05$ for each of the different classes of fin motoneurons and for all different measured real peak-to-peak amplitudes (PP, PPI, PPc). After checking for significant differences via ANOVA-test, a t-test was performed ($p < 0.05$) between the first data point (without current injection) and the following data (for each current injection). The means of the original data sets of these single values (Tab. 3.6 and 3.7) were taken and a new graph was plotted including the mean data (Fig. 3.32). The stars are marking significant differences between the different data sets. Finally the mean data of the three different types of amplitudes (PP, PPI, PPc) for cells of type I and type II fin motoneurons were plotted in one diagram and the data compared for significant differences (Fig. 3.33). Type III fin motoneurons were not compared due to the fact, that there were no sufficient data collected.

injected current	type I	type II	type III
0 nA	4.35 mV +/- 1.31 mV	3.92 mV +/- 0.92 mV	5.10 mV +/- 1.12 mV
-1 nA	4.95 mV +/- 2.19 mV	4.23 mV +/- 1.41 mV	4.53 mV +/- 0.94 mV
-2 nA	4.87 mV +/- 0.31 mV	3.97 mV +/- 0.59 mV	--
-4 nA	7.13 mV +/- 1.47 mV	6.30 mV +/- 0.57 mV	--

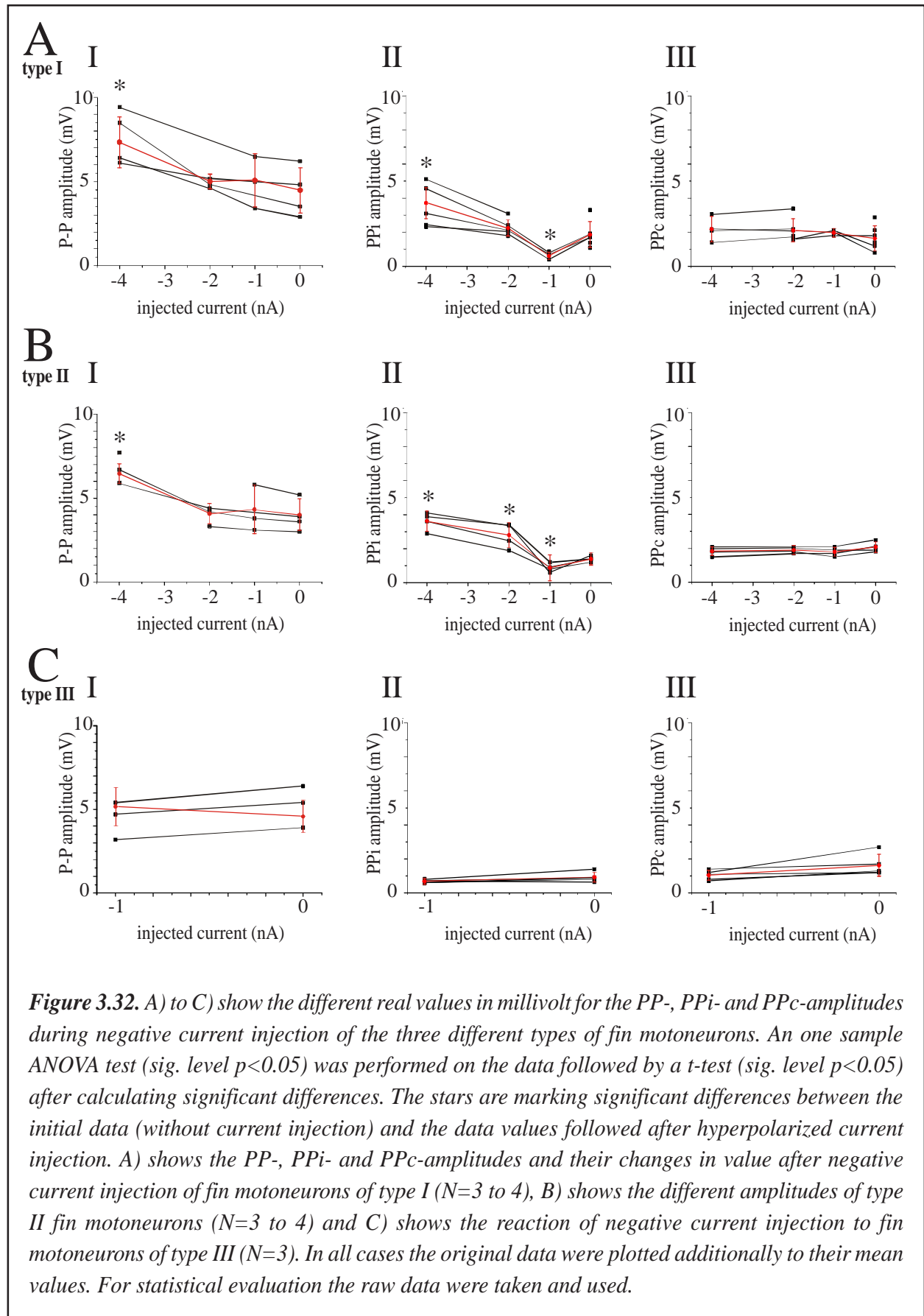
Table 3.6.

Mean overall peak-to-peak amplitude of the three different types of fin motoneurons during hyperpolarized current injection between 0 and -4 nA (N=6 for type I, N=5 for type II and type III. In case of type III motoneurons there were no sufficient data for measuring the mean peak-to-peak amplitude for -2nA and -4 nA).

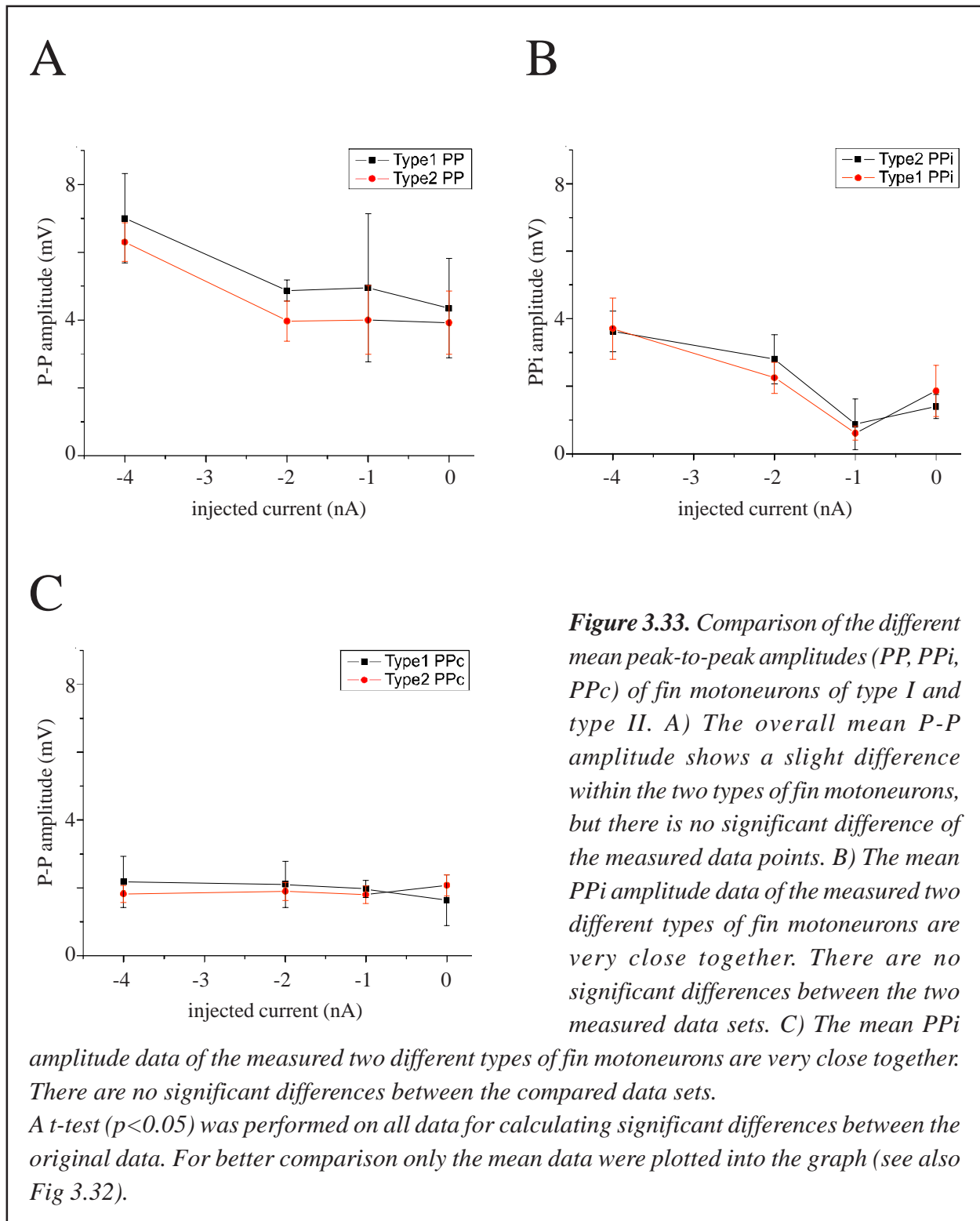
type/current	P-P ipsi	P-P contra
T1: 0 nA	1.86 mV +/- 0.76 mV	1.64 mV +/- 0.74 mV
T1: -1 nA	0.61 mV +/- 0.21 mV	1.97 mV +/- 0.25 mV
T1: -2 nA	2.25 mV +/- 0.47 mV	2.11 mV +/- 0.68 mV
T1: -4 nA	3.71 mV +/- 0.91 mV	2.18 mV +/- 0.75 mV
T2: 0 nA	1.43 mV +/- 0.36 mV	2.08 mV +/- 0.31 mV
T2: -1 nA	0.88 mV +/- 0.75 mV	1.89 mV +/- 0.26 mV
T2: -2 nA	2.85 mV +/- 0.73 mV	1.95 mV +/- 0.26 mV
T2: -4 nA	3.63 mV +/- 0.60 mV	1.84 mV +/- 0.25 mV
T3: 0 nA	0.93 mV +/- 0.28 mV	1.62 mV +/- 0.65 mV
T3: -1 nA	0.68 mV +/- 0.10 mV	1.05 mV +/- 0.26 mV

Table 3.7. Mean overall PPI- and PPc-amplitude of the three different types of fin motoneurons during hyperpolarized current injection between 0 and -4 nA (N=6 for type I, N=5 for type II and type III, current injection for type III 0 to -1 nA).

The statistical analysis of the results show that the different fin motoneurons behave similar during negative current injection. The peak-to-peak amplitude did not change significantly after injection of current up to -2 nA, but after increasing the current up to -4 nA a significant change in the amplitude, compared to the amplitude without current injection, was detectable (Fig. 3.32, I). This shows that a reversal potential was reached and crossed. Further current injection would even more increase the peak-to-peak amplitude (not shown). The effect of reaching a reversal potential was much better visible when analyzing the PPI-amplitudes. There was a significant decrease of the amplitude after injecting a current of -1 nA for fin motoneurons of type I and II, compared to its initial PPI-amplitude. After further increasing of the injected negative current, the PPI-amplitudes increased significantly (Fig. 3.32, II). Although the PPI-amplitude changed significantly after injection of negative current, the PPc-amplitude was unaffected (Fig. 3.32, III). So the injected current had no influence to the fin motoneurons during activity of the contralateral myotomal motoneurons.



This means, that there is a phasic inhibition to fin motoneurons in phase with activity of the ipsilateral myotomal fin motoneurons. Due to the similar reactions of fin motoneurons of type I and type II to negative current injection, the raw data of PP-, PPI- and PPc-amplitudes were taken and the mean



plotted together in one diagram to see their similarities (Fig. 3.33). Although there are light dissimilarities in the peak-to-peak amplitude (the mean amplitude of type I fin motoneurons is higher than that of fin motoneurons of type II), no significant difference is detectable. Observing the PPI- and PPc amplitudes of the two different fin motoneurons indicates that the results are even closer. The plots of the two motoneurons types are very similar to each other. This means that both different types of fin motoneurons may get phasic inhibition maybe from same sources during ipsilateral activity of myotomal motoneurons. At present it was not possible to show the reaction of fin motoneurons of type III to negative current higher than -1 nA.

3.4 Lesion experiments

It could be shown that for myotomal motoneurons the inhibitory and excitatory phase during fictive swimming was still present after a sagittal spinal cord lesion. Moreover a transversal lesion for checking the influence of ipsilateral descending inputs reduced significantly (about 70%) the outward current during the inhibitory phase as well as the inward, excitatory current in caudally located motoneurons (Wallén *et al.*, 1993). Furthermore it was shown that even after a full hemisection of the lamprey spinal cord a slow myotomal rhythm persisted (Cangiano and Grillner, 2003). At present, nothing is known about the influence of descending and contralateral input to fin motoneurons. Therefore, it was investigated in this work whether there is an influence of descending axons to fin motoneurons and also whether there are influences from the contralateral side for initiating and maintaining the antiphase activity of fin motoneurons compared to myotomal ones.

3.4.1 Extracellular recordings

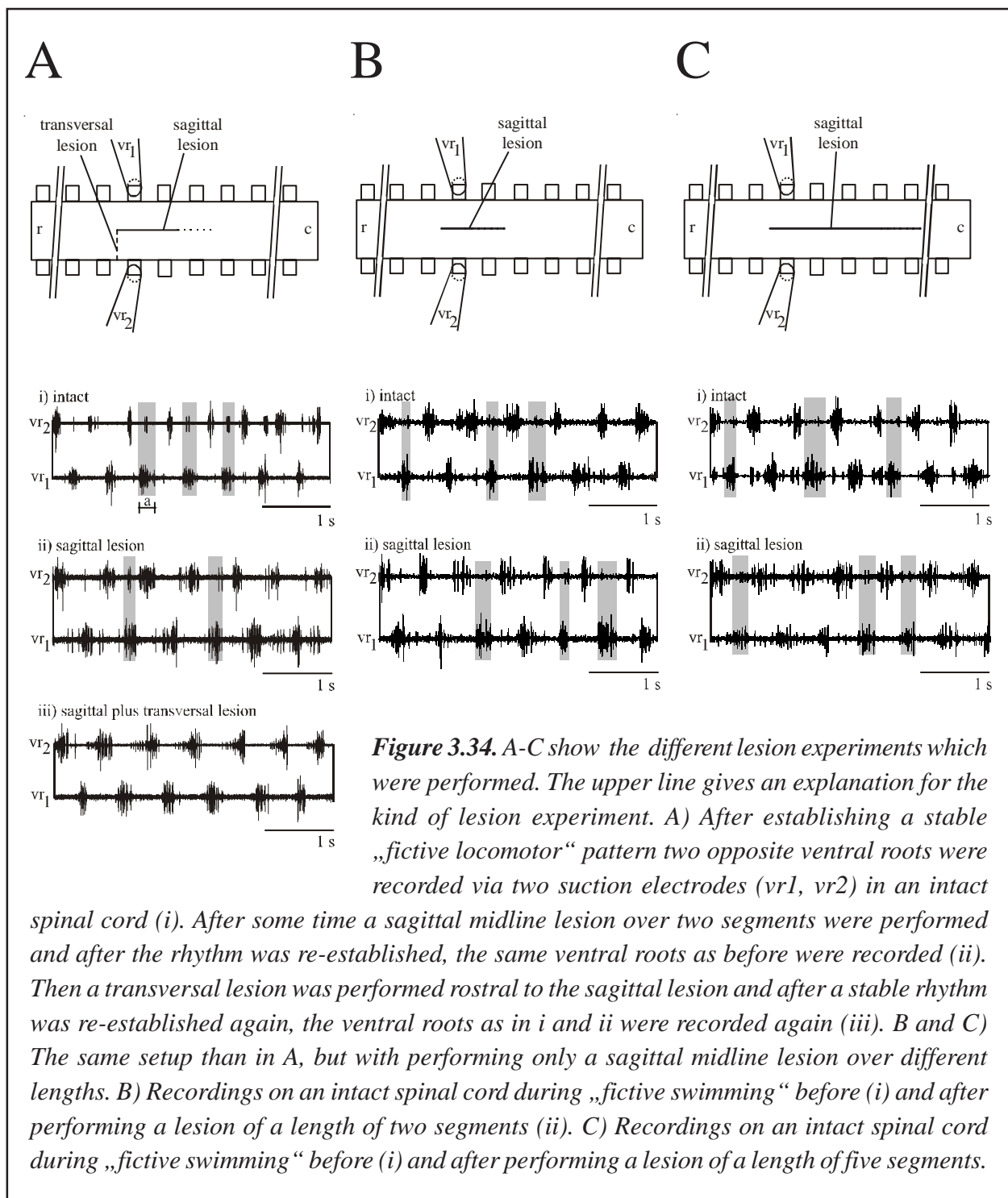
Different extracellular experiments were performed to show the effects of different inputs to the phasic fluctuation of fin motoneurons in antiphase to the myotomal phasic fluctuation. For measuring the activity of fin motoneurons during fictive locomotion the number of extracellular spikes during occurrence of a contralateral myotomal burst were analyzed (see also Fig. 3.34). Shupliakov *et al.* and the above data sets have shown fin motoneurons of the same side to be active in antiphase of myotomal motoneurons, with a peak of activity around the time of the contralateral burst.

In a first set of extracellular experiments we therefore concentrated on these motor units in the ventral root recordings.

3.4.1.1 Sagittal lesion experiments

To investigate the influence of contralateral input for generating fin motoneuron activity two opposite ventral roots of an intact isolated spinal cord were recorded during „fictive swimming“ (N=19). After performing a sagittal midline cut over a length of one (N=6) to two (N=4) segments both ventral roots were recorded again. Before and after the lesion the myotomal motor pattern persisted. Also the motor activity of presumed fin motoneurons (during contralateral myotomal burst activity)

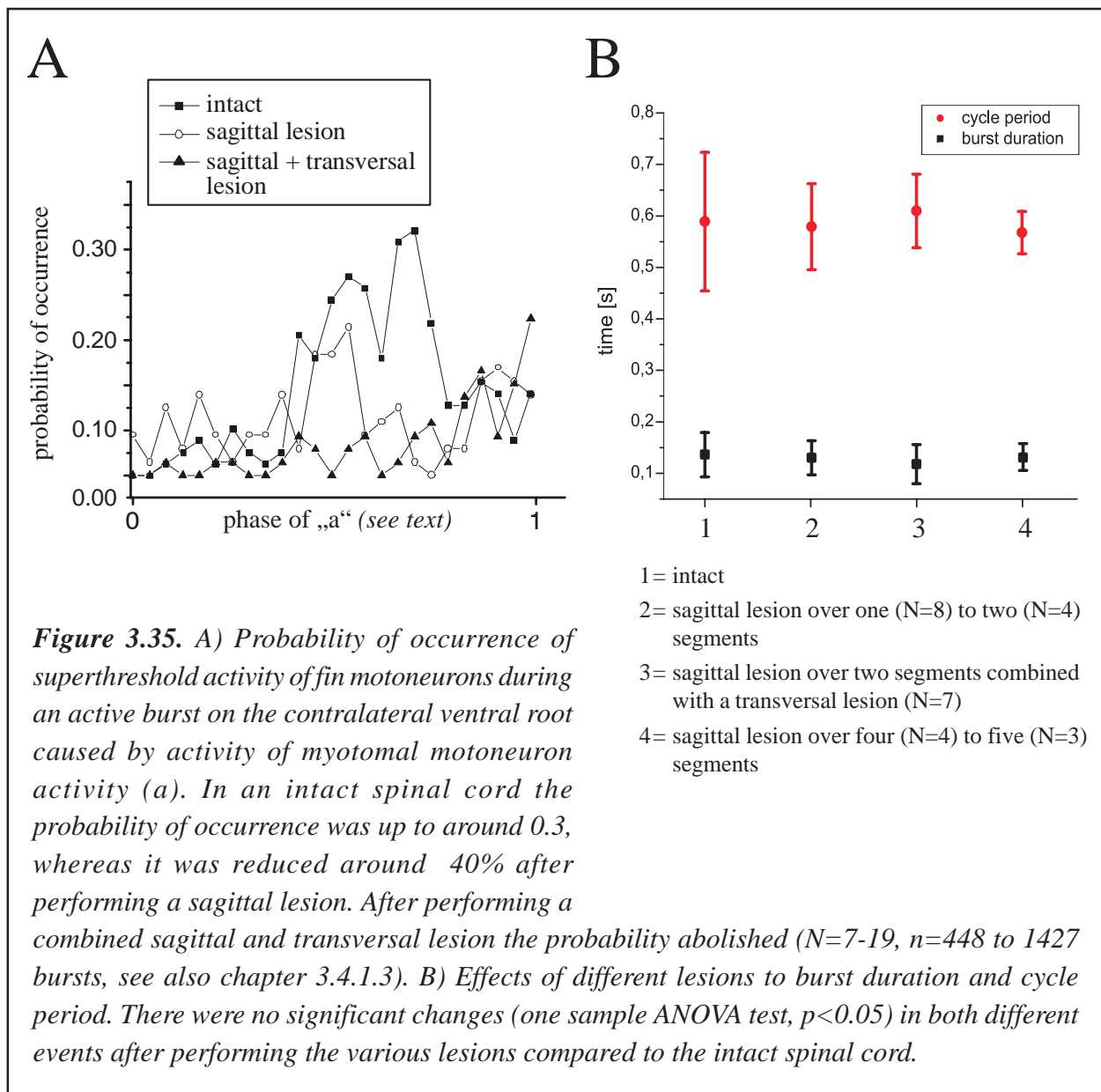
still persisted (Fig. 3.34, A i, ii to C i, ii). Therefore a sagittal midline lesion did not abolish the phasic activity of myotomal motoneurons nor the phasic activity of presumed fin motoneurons. Extending the sagittal midline lesion to a length of four (N=4) to five (N=3) segments caudalwards (Fig. 3.34, C ii) showed that also after performing this longer lesion both phasic activities, the



myotomal motoneuron generated ones and the fin motoneuron generated ones, were still intact. This result suggested that contralateral input to fin motoneurons was not necessary for generating and maintaining its phasic activity, but intracellular recordings had to substantiate this conclusion (see below).

3.4.1.2 Sagittal plus transversal lesion experiments

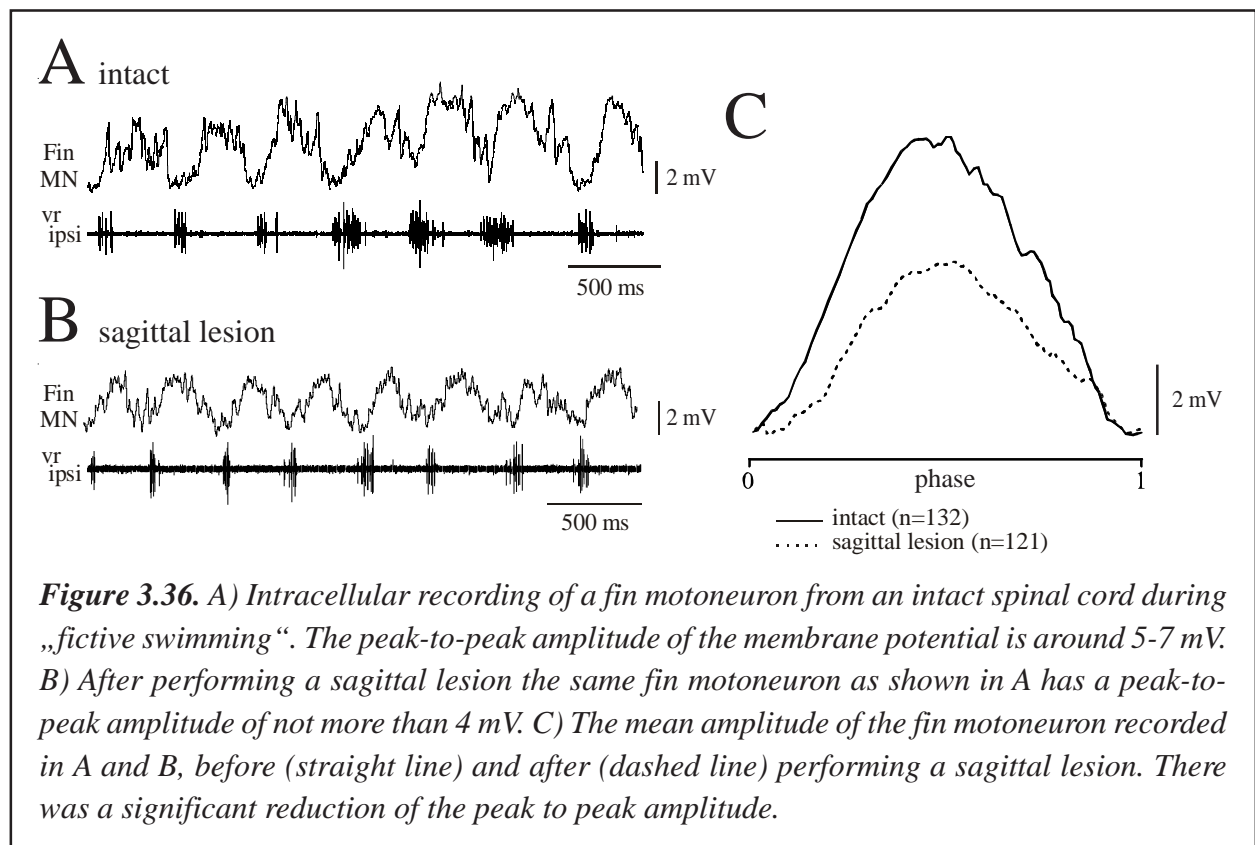
After performing a sagittal midline lesion over a length of two segments during „fictive swimming“ an additional lesion (N=7) was made in a transversal direction rostral from the recorded ventral



roots. After performing the sagittal lesion antiphase motor unit activity was still detectable, but following the second, transversal cut, the antiphase motor unit activity abolished just in contrast to the myotomal burst activity that still persisted (Fig. 3.34 A i-iii). This means that there could be a descending ipsilateral directed input from rostral located segments responsible for activating antiphase activity of fin motoneurons.

3.4.1.3 Summary of the results of extracellular lesion experiments

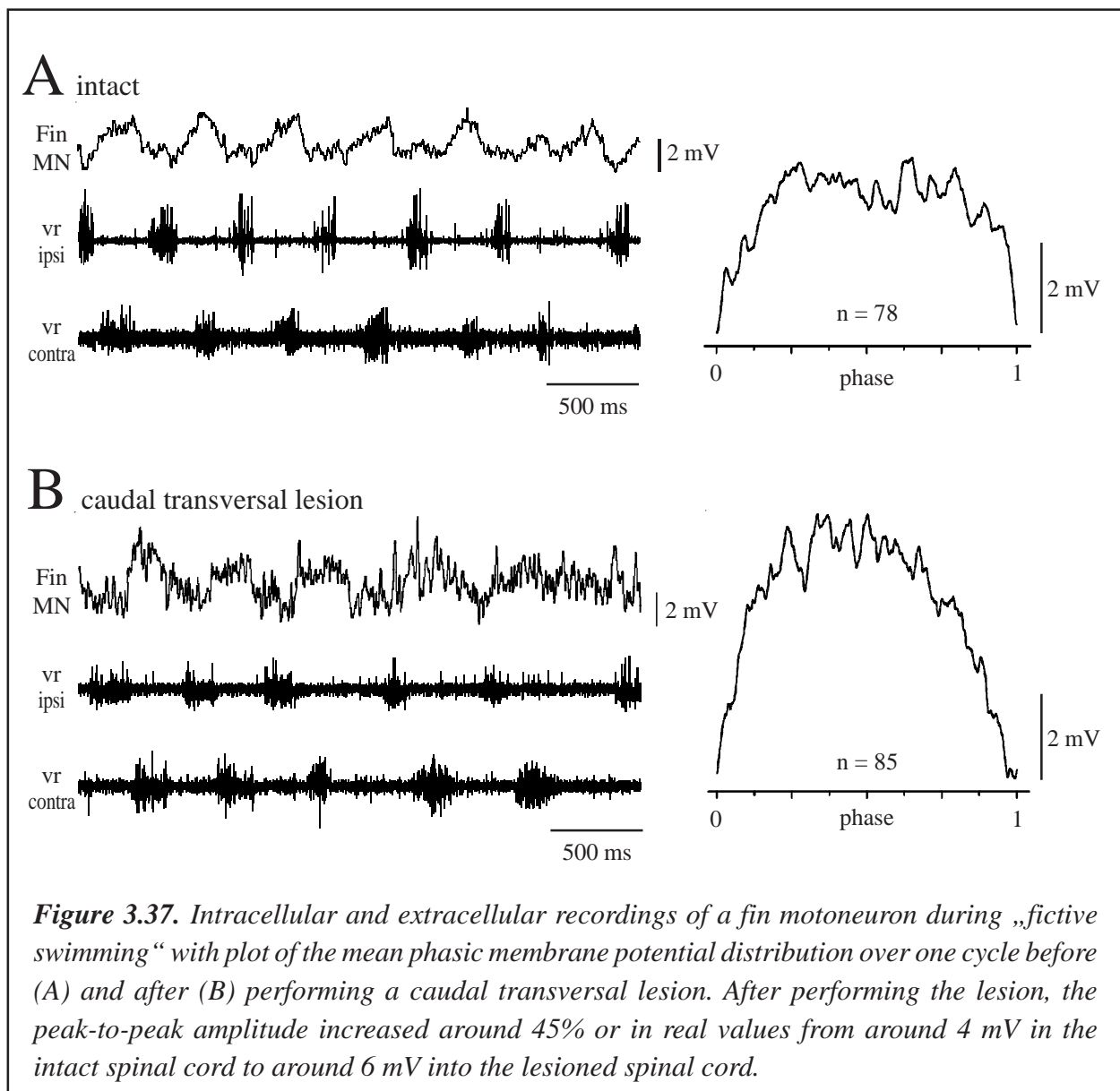
For quantitative analysis of the results of the different lesion experiments, the number of average superthreshold fin motoneuron activity was calculated by counting the spikes on the ipsilateral ventral root during the activity of the myotomal motoneurons on the contralateral ventral root (this time period was called „a“. The spike distribution of „a“ was divided into 25 classes, recalculated and averaged (N=19, n=1427 for the intact spinal cord; N=10, n=786 for the sagittal lesion over a length of one to two segments and N=7, n=448 for the combined sagittal plus transversal lesion of the spinal cord). The results of these spike distributions and also the mean changes to cycle period



and burst duration after performing the lesions compared to those in the intact spinal cord were calculated and plotted (Figure 3.35).

3.4.2 Intracellular recordings

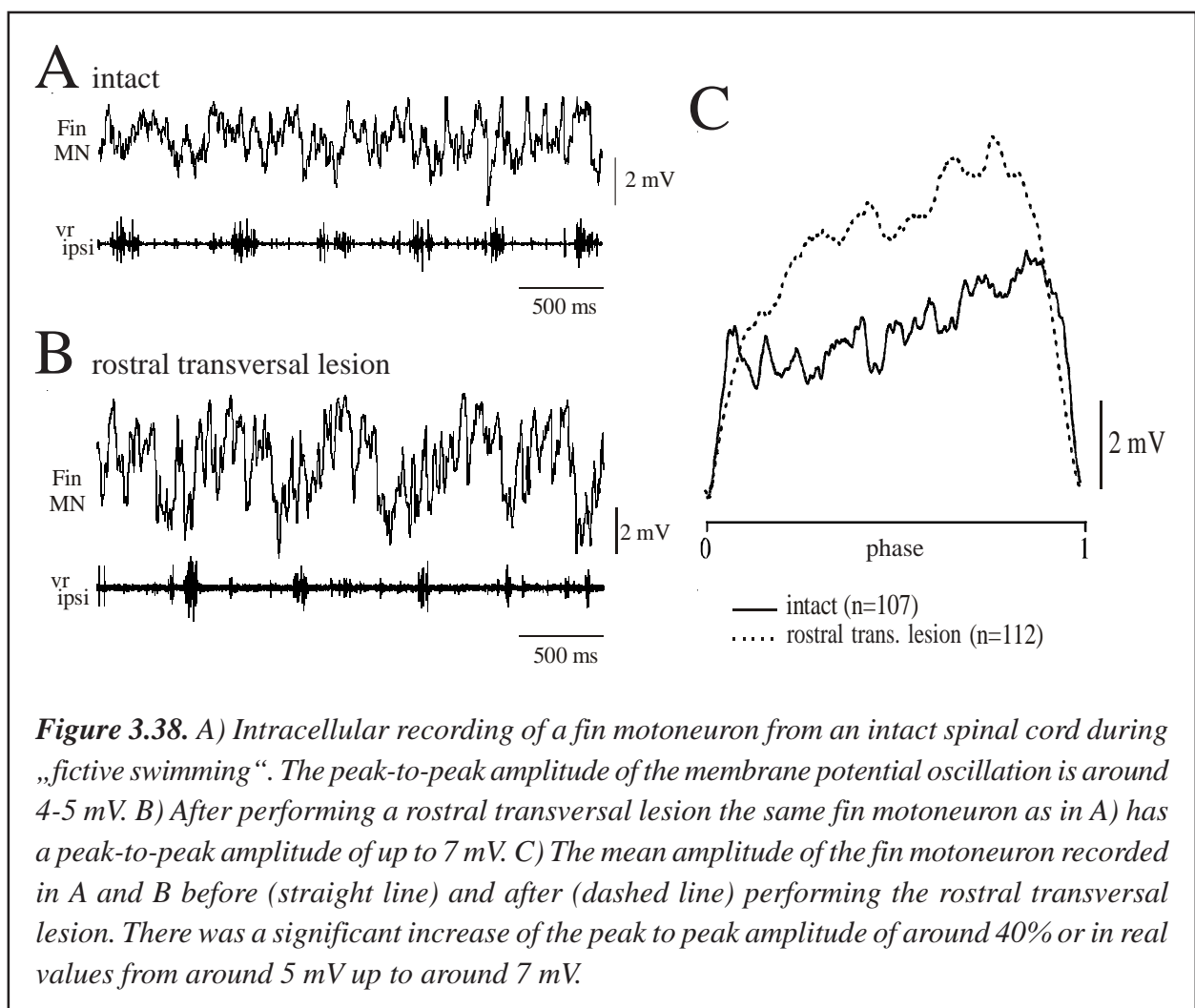
Intracellular experiments were performed to substantiate the results from the extracellular recordings. In order to do so, fin motoneurons were penetrated before and after a lesion was performed in the spinal cord. Due to the fact that no double labelling was performed, recordings from fin motoneurons will be called „presumed“ in case of the same cell being penetrated before and after a lesion. For the



sagittal lesions subsequent double labelling experiments by Tim Mentel have now substantiated the conclusions drawn. For measuring the activity of fin motoneurons during „fictive locomotion“ the same fin motoneurons were recorded in most cases before and after lesioning the spinal cord, to show differences in membrane potential oscillation caused by the lesion.

3.4.2.1 Sagittal lesion experiments

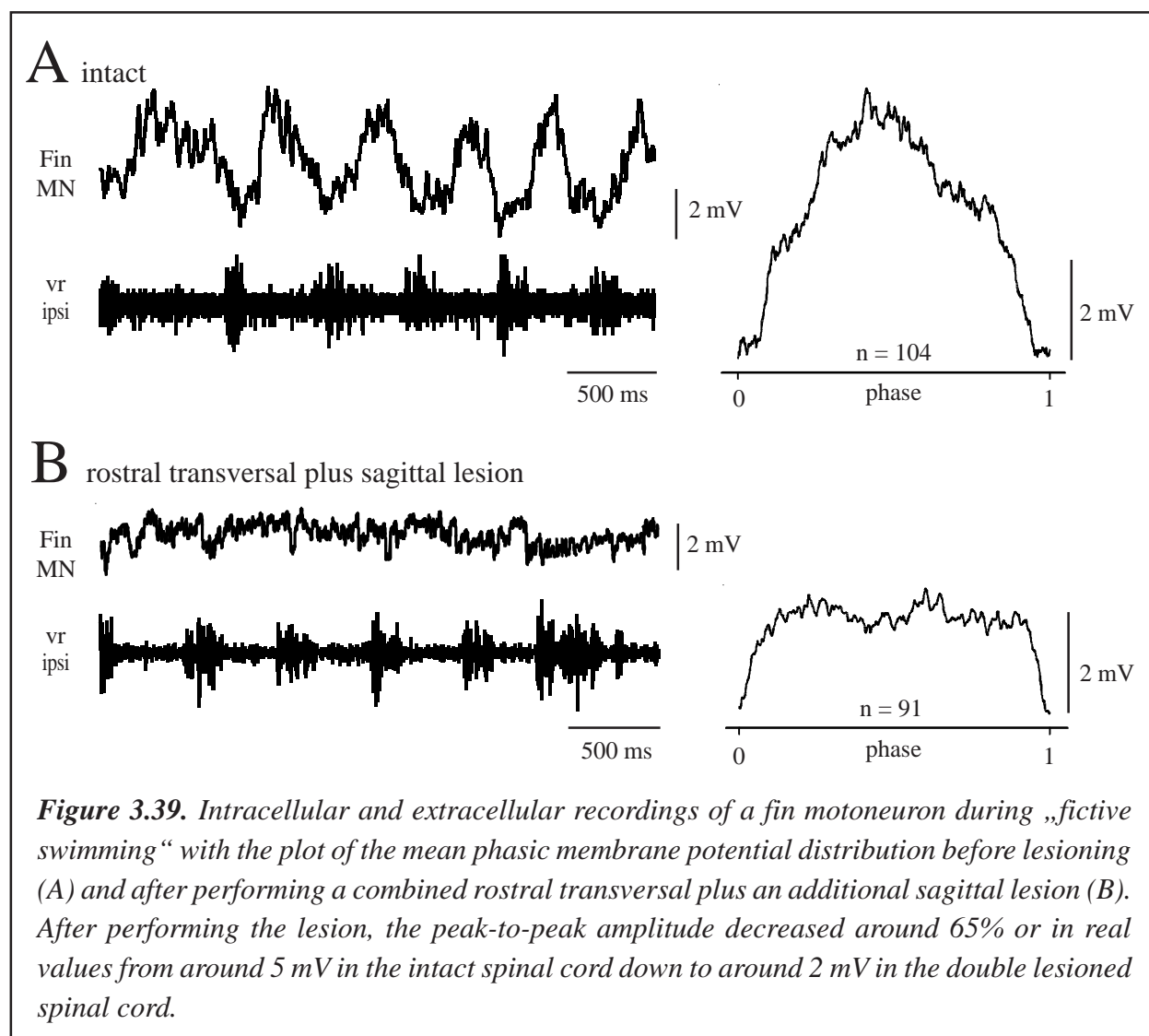
For investigating the influence of contralateral segmental inputs for generating fin motoneuron activity, two opposite ventral roots of an intact isolated spinal cord were recorded extracellularly, as well as, a segmental fin motoneuron intracellularly during „fictive swimming“. After performing a sagittal midline lesion over a length of two segments presumably the same fin motoneuron as before was recorded again (N=4, n=364). Before and after the lesion the myotomal motor pattern



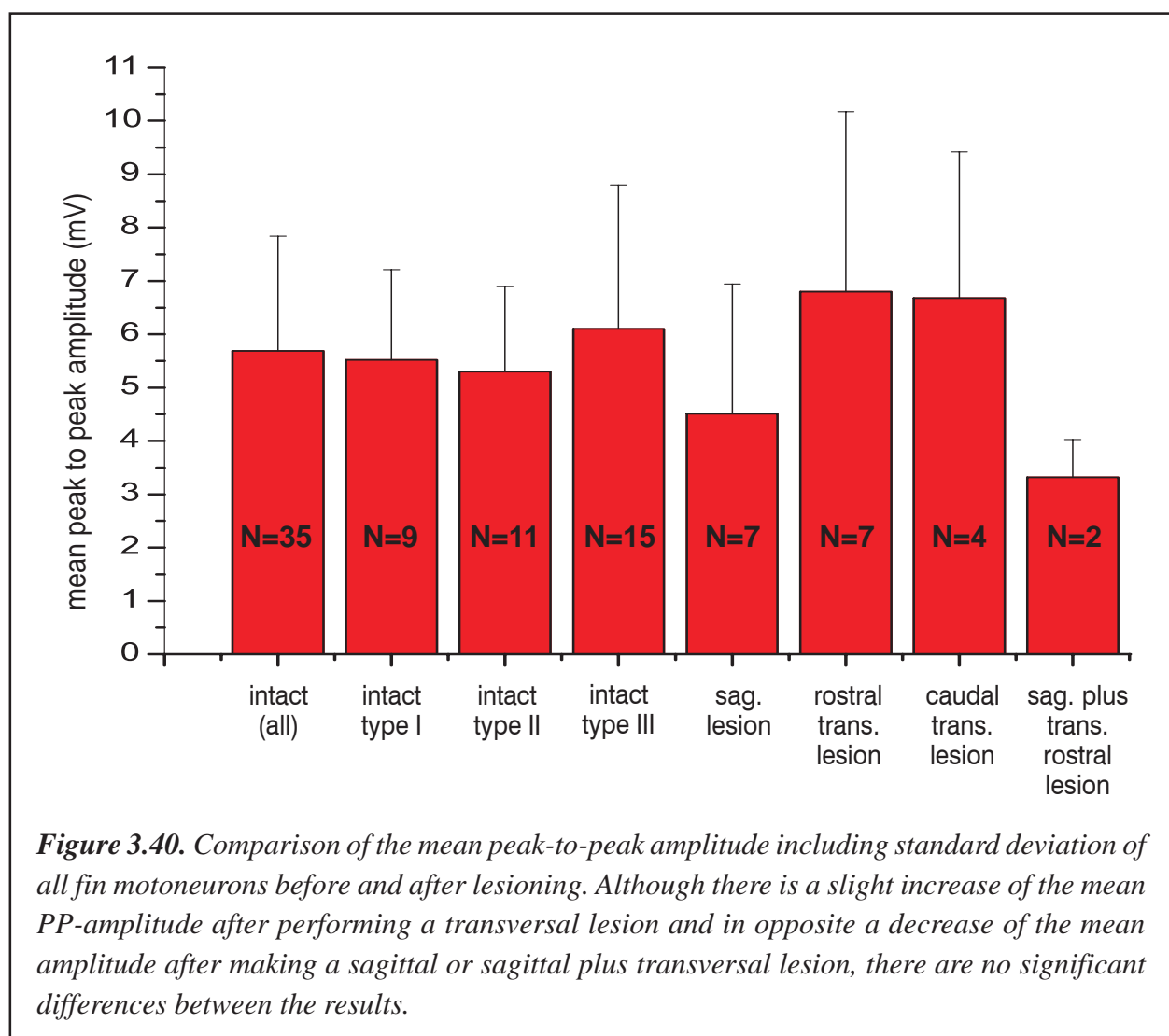
was still present and not changed (see below). The phasic membrane potential oscillation still persisted after the sagittal lesion and the amplitude was reduced by approx. 40 %, ie. the membrane potential oscillation decreased from approx. 7 mV down to approx. 4 mV (Fig. 3.36).

3.4.2.2 Transversal lesion experiments

Studying the influence of descending input for generating fin motoneuron activity, two opposite ventral roots of an intact isolated spinal cord during „fictive swimming“ were recorded extracellularly as well as a fin motoneurons intracellularly. Before and after performing transversal lesions fin motoneurons were penetrated and recorded. Transversal lesions were made rostrally to the penetrated



fin motoneurons (N=7) as well as caudally (N=4). Before and after performing the lesion the myotomal motor pattern was still present (Fig. 3.34, 3.37, 3.38), but in both different lesion experiments the mean intracellular peak-to-peak amplitude persisted after lesioning the spinal cord. On average an increase in amplitude was observed. In case of the caudal transversal lesion the intracellular mean peak-to-peak amplitude increased up to 45%, and the increase after performing a transversal rostral lesion was up to 40% (Fig. 3.40). For performing the rostral transversal lesion in two cases the same fin motoneuron was presumably penetrated before and after lesioning the spinal cord. The peak-to-peak amplitude increased approx. 40% i. e. from approx. 5 mV up to approx. 7 mV (Fig 3.38). These results indicate that there may be a rhythmic drive to fin motoneurons not only from the rostral part of the spinal cord, but also from caudal segments.



3.4.2.3 Sagittal plus transversal lesion experiments

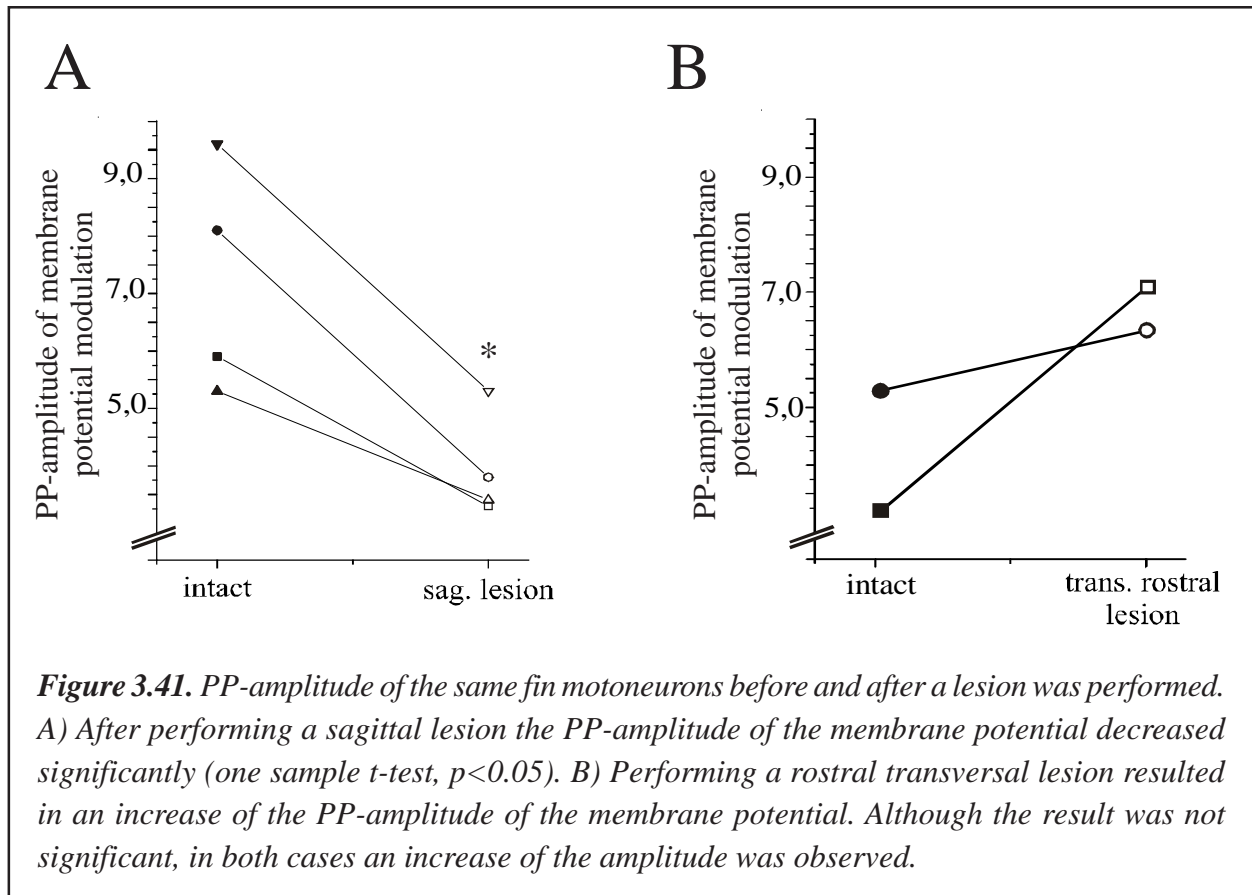
Finally it was tested what would happen with the membrane potential oscillation of fin motoneurons after performing a combined lesion composed of a sagittal lesion plus an additional rostral transversal lesion. Before and after performing the lesions fin motoneurons (N=2) were penetrated and recorded during „fictive swimming“. As shown in 3.4.1.2 the myotomal motor pattern was still present after performing the lesions and also a phasic membrane potential oscillation of the presumed fin motoneurons was still present, but the intracellular peak-to-peak amplitude decreased down to 65% compared to fin motoneurons in the original intact spinal cord, i. e. from approx. 5 mV down to approx. 2 mV (Fig. 3.39).

3.4.2.4 Comparison of intact and lesioned fin motoneuron properties

The results of the lesion experiments were separated into three parts. Firstly, the mean peak-to-peak amplitudes were compared for the different lesions, in a second part the minima and maxima of the amplitude within one phase, and finally changes in burst duration and cycle period were compared.

	min PP-amplitude	max PP-amplitude	mean PP-amplitude +/- SD
all:	1.64 mV	10.28 mV	5.69 mV +/- 2.15 mV
type I:	2.23 mV	8.22 mV	5.52 mV +/- 1.69 mV
type II:	2.32 mV	7.84 mV	5.33 mV +/- 1.62 mV
type III:	2.51 mV	10.31 mV	6.09 mV +/- 2.51 mV
sagittal lesion:	2.13 mV	9.08 mV	4.51 mV +/- 2.44 mV
trans. rostral lesion:	1.74 mV	9.53 mV	6.79 mV +/- 3.38 mV
trans. caudal lesion:	4.13 mV	10.34 mV	6.68 mV +/- 2.74 mV
trans. rostral plus sagittal lesion:	2.81 mV	3.82 mV	3.32 mV +/- 0.71 mV

Table 3.8. Minimum, maximum and mean values (included SD) of the peak-to-peak amplitudes for the different recorded fin motoneurons before and after different lesions were performed (N between 2-15). For more information see text.



3.4.2.4.1 Peak-to-peak amplitude

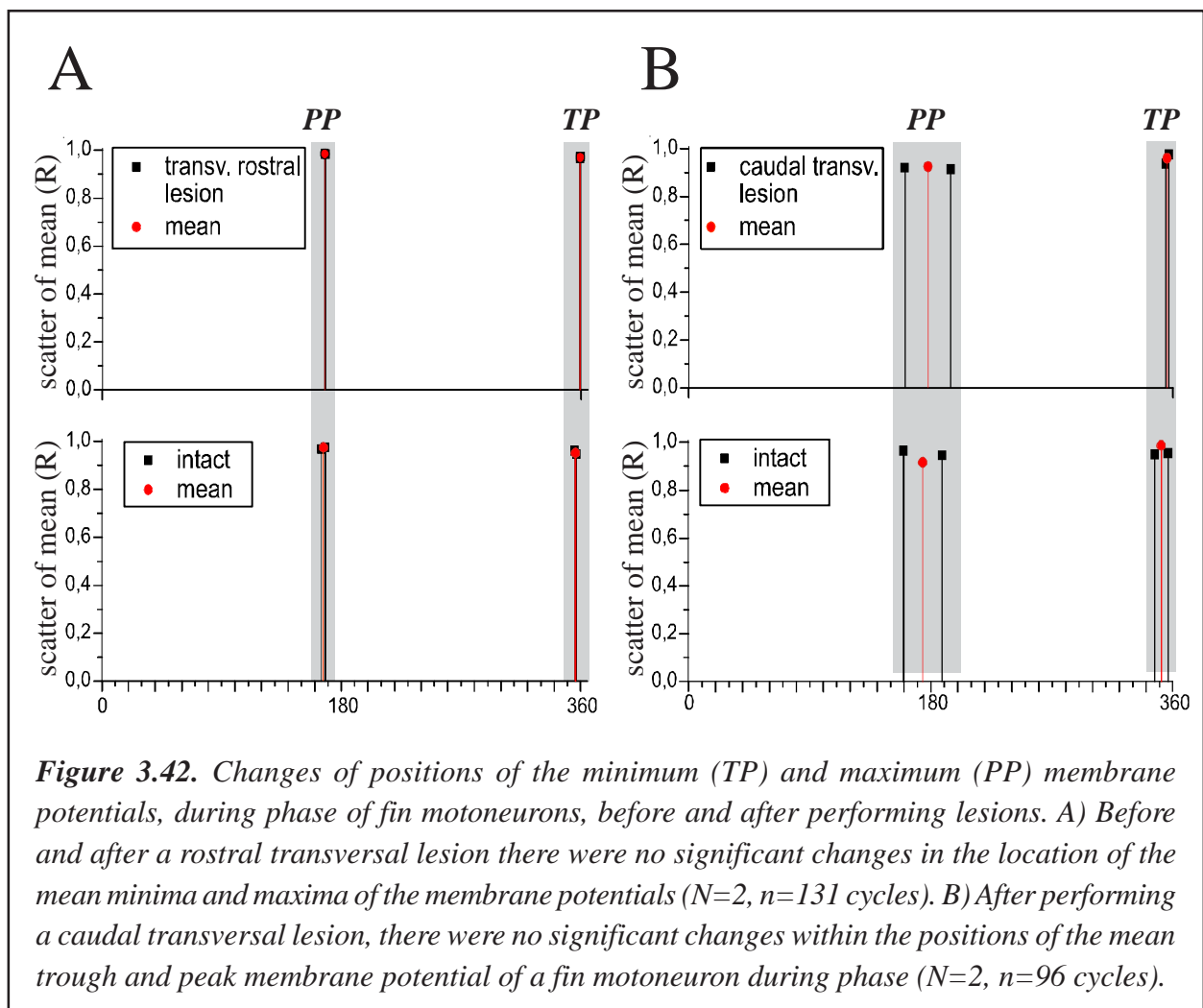
Comparing the mean peak-to-peak amplitude (PP-amplitude) of all examined fin motoneurons did not show significant differences (Fig. 3.40). The mean PP-amplitude for all fin motoneurons was $5.69 \text{ mV} \pm 2.15 \text{ mV}$ ($N=35$) in the intact spinal cord. This result was composed out of nine recordings of type I fin motoneurons ($5.52 \text{ mV} \pm 1.69 \text{ mV}$), 11 recordings of type II fin motoneurons ($5.52 \text{ mV} \pm 1.69 \text{ mV}$) and 15 recordings of type III fin motoneurons ($6.09 \text{ mV} \pm 2.51 \text{ mV}$) (Tab. 3.8).

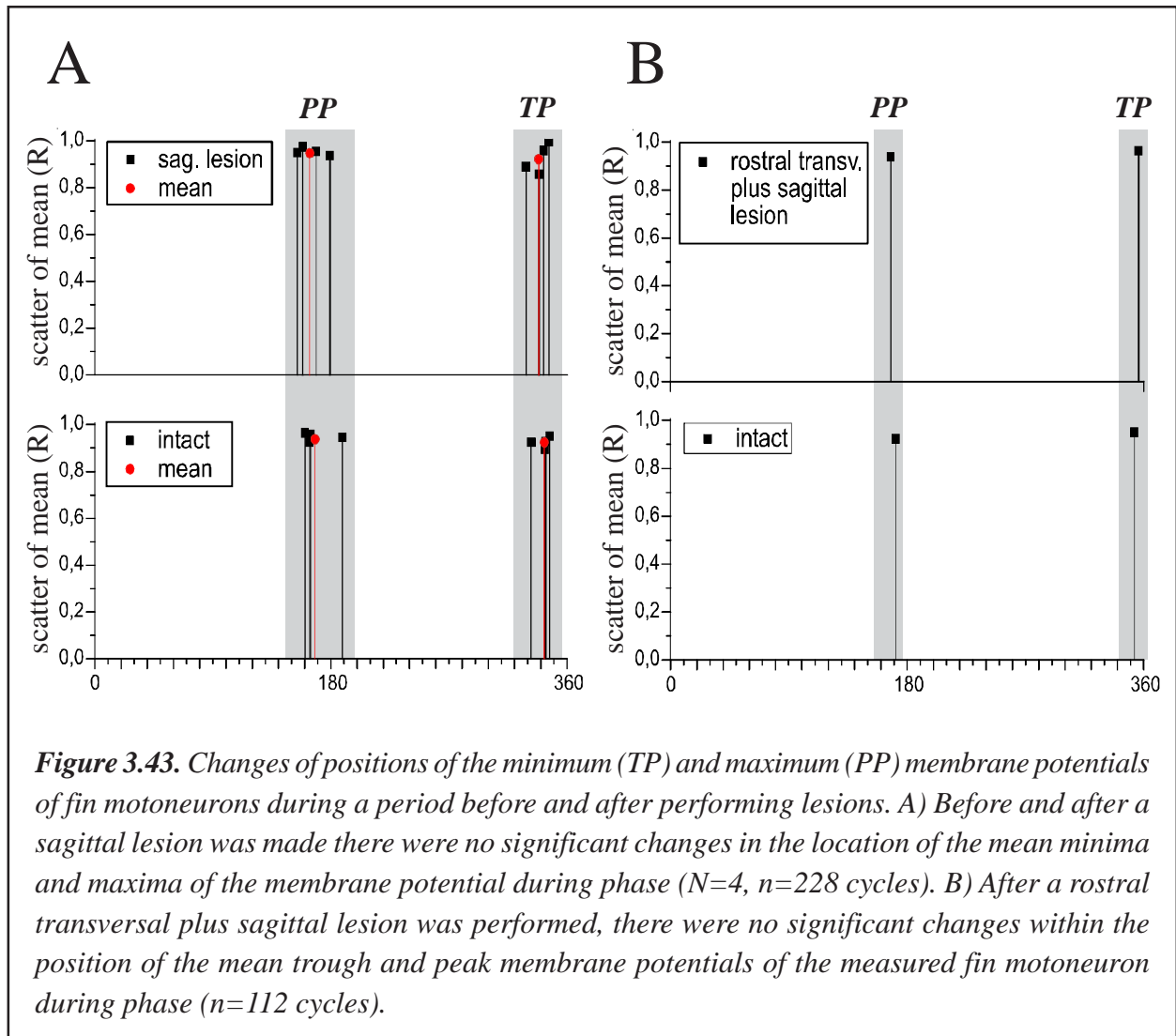
After performing a sagittal lesion the mean PP-amplitude decreased down to $4.51 \text{ mV} \pm 2.44 \text{ mV}$ ($N=7$), whereas after performing a transversal lesion the PP-amplitude increased, regardless of the lesion being rostral ($6.79 \text{ mV} \pm 3.38 \text{ mV}$, $N=7$) or caudal ($6.68 \text{ mV} \pm 2.74 \text{ mV}$, $N=4$) to the recorded presumed fin motoneuron. Following the combined lesion (rostral transversal plus sagittal lesion), the PP-amplitude decreased down to $3.32 \text{ mV} \pm 0.71 \text{ mV}$ ($N=2$). The amplitudes however were not significantly different (one sample t-test, $p < 0.05$) due to their large standard deviations (Tab. 3.8) resulting of different P-P amplitudes measured in the different recordings.

Therefore, to compare the PP-amplitude of the presumably same fin motoneuron it was important to compare the same neurons before and after a lesion was performed (Fig. 3.41). The comparison of PP-amplitude of four different experiments before and after a sagittal lesion indicated a significant decrease (one sample t-test, $p < 0.05$) of the PP-amplitude from $7.93 \text{ mV} \pm 2.04 \text{ mV}$ to $4.19 \text{ mV} \pm 0.93 \text{ mV}$. After the rostral transversal lesion no significant change in peak-to-peak membrane potential (one sample t-test, $p < 0.05$) was observed.

3.4.2.4.2 Phase of membrane potential maxima and minima

An interesting question is to clarify if the phase of occurrence of the maxima and minima of the membrane potential oscillations in fin motoneurons were affected by lesioning the spinal cord. Therefore, the values of each experiment were calculated and also the mean of all experiments





together. The results were plotted as graphs (Fig. 3.42, 3.43). Comparing the different results did not show a phase shift, not before and after a lesion was made nor between the different lesions. The trough and peak potentials of fin motoneurons of type I oscillation in an intact spinal cord were located during a mean phase of 347.91 deg with $R=0.9624$ (range from 341.19 deg with $R=0.9618$ to 357.83 deg with $R=0.9361$) and 169.91 deg with $R=0.8804$ (range from 157.49 deg with $R=0.891$ to 181.42 deg with $R=0.9494$) respectively. Fin motoneurons of type II showed their main minima and maxima in the membrane potential amplitude during a mean phase of 353.41 deg with $R=0.9817$ (range from 340.87 deg with $R=0.9908$ to 358.39 deg with $R=0.9911$) and 163.85 deg with $R=0.8478$ (range from 162.28 deg with $R=0.9615$ to 166.21 deg with $R=0.9414$) respectively (see also Fig. 3.11). The results for the cells after the spinal cord was lesioned ranged in case of minima between 348.83 deg with $R=0.8948$ (range from 328.46 deg with $R=0.8886$ to 346.53 deg with $R=0.8566$)

rostral transversal lesion experiment	intact	minimum	355.32 degree, R=0.9614
		maximum	167.76 degree, R=0.9739
	lesionend	minimum	359.76 degree, R=0.9690
		maximum	167.33 degree, R=0.9844
caudal transversal lesion experiment	intact	minimum	351.77 degree, R=0.9865
		maximum	174.40 degree, R=0.9165
	lesioned	minimum	355.51 degree, R=0.9597
		maximum	177.68 degree, R=0.9259
sagittal lesion experiment	intact	minimum	349.68 degree, R=0.9265
		maximum	165.24 degree, R=0.9165
	lesioned	minimum	348.83 degree, R=0.8948
		maximum	163.84 degree, R=0.9363
sagittal plus rostral transversal lesion experiment	intact	minimum	352.77 degree, R=0.9521
		maximum	171.40 degree, R=0.9234
	lesioned	minimum	355.80 degree, R=0.9632
		maximum	167.61 degree, R=0.9390

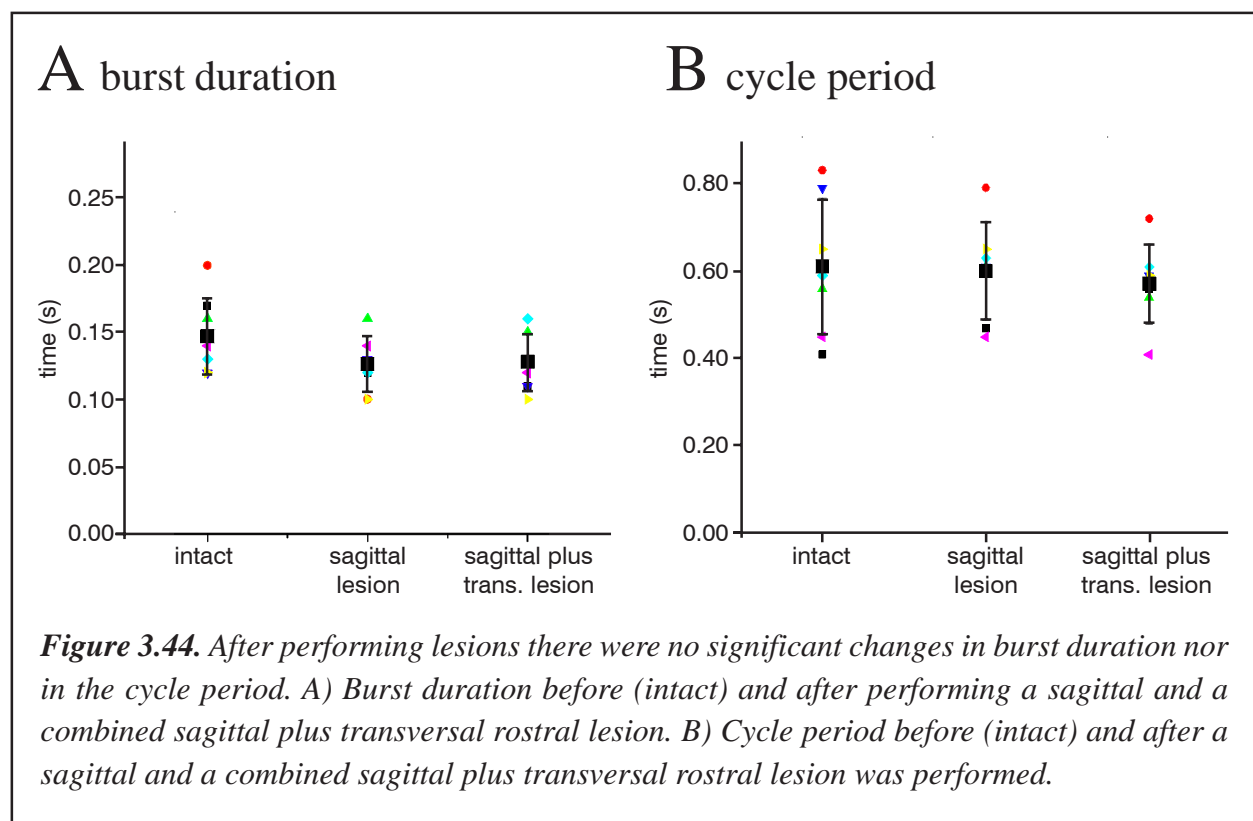
Table 3.9. Mean occurrence of minimum and maximum membrane potential in fin motoneurons within phase before and after the different lesion experiments of the spinal cord were performed.

for the sagittal lesion up to 359.76 deg with R=0.969 (range from 359.74 deg with R=0.9716 to 360.07 deg with R=0.9664) for the rostral transversal lesion. In case of the location of the peak membrane potential during a period the results varied from 163.84 deg with R=0.9363 (range from 154.29 deg with R=0.9479 to 179.17 deg with R=0.937) for the sagittal lesion to 177.68 deg with

$R=0.9259$ (range from 160.62 deg with $R=0.9205$ to 194.75 deg with $R=0.9139$) for the caudal transversal lesion. Comparing the results measured in the presumably same fin motoneurons in the spinal cord before and after lesion the range of the minima and maxima are much closer (Tab. 3.9). There were no significant changes observed in connection with performing the lesions (Fig. 3.42, 3.43).

3.4.2.4.3 Burst duration and cycle period

Comparing the changes in burst duration and cycle period before and after the different lesions were performed did not show significant differences ($N=7$), although the scatter of both was reduced (Fig. 3.44). The mean burst duration in the intact spinal cord during „fictive swimming“ was 0.14 s \pm 0.03 s. After performing the different lesions the burst duration was slightly reduced to 0.13 s \pm 0.02 s in case of the sagittal lesion and to 0.13 s \pm 0.02 s in case of the combined lesion, composed of a sagittal and rostral transversal lesion. The cycle period changed from 0.61 s \pm 0.15 s in the intact spinal cord to 0.60 s \pm 0.10 s in a sagittal lesioned spinal cord to 0.58 s \pm 0.08 s in the



double lesioned one. These results, as well as the results described earlier, indicate that a lesion of the spinal cord does not affect burst duration and cycle period of the fictive locomotion pattern.

4. Discussion

The lamprey spinal network for controlling the motor output for propulsion of the animal is well investigated and understood with respect to the activity of the main trunk- or body wall muscles (Griller *et al.*, 1999). There are however, only a few investigations on the morphology and electrophysiology of motoneurons controlling the fin muscles of the animal (Birnberger and Rovainen, 1971; Rovainen and Birnberger, 1971; Shupliakov *et al.*, 1992; el Manira *et al.*, 1996). In general the role of the fin motoneurons during swimming and its role in positioning the lamprey in the water is not clear at present.

Investigations of the network properties of the „Central pattern generator“ (CPG) have not included the fin motoneurons. Well developed mathematical models of the function of the CPG in lamprey (Grillner *et al.*, 1988; Ekeberg *et al.*, 1991; Buchanan, 1992; Wallén *et al.*, 1992; Williams, 1992) do not include the functions of fin motoneurons during locomotion. Therefore the aim of this thesis was the investigation of fin motoneurons on cellular level (morphologically and electrophysiologically), meaning to describe their different modulation patterns and the synaptic input to fin motoneurons in their activity during „fictive locomotion“, as well as to get a first insight into potential sources of their inputs.

4.1 Different types of fin motoneurons in the lamprey spinal cord

4.1.1 Two morphological different types of fin motoneurons

In this work two morphological different types of fin motoneurons could be shown in the lamprey spinal cord. One type shows ramifications only to the ipsilateral side of the spinal cord called type I (Fig. 3.2) and another one called type II (Fig. 3.6) which has dendritic ramifications to the contralateral side of the spinal cord. Both types are located in the lateral cell column and within the spinal cord the fin motoneurons are arranged rostrally and caudally related to the parental ventral root. Shupliakov *et al.* (1992) showed also two different types of fin motoneurons in the lamprey spinal cord. The shape he described for type I was similar to one type found in this thesis with their elongated triangular or oval shaped somata and a dendritic tree extending in the rostro-caudal

direction, restricted generally to the ipsilateral side. The widespread dendritic tree observed in fin motoneurons of type I was similar to that found in dorsal located myotomal motoneurons (Wallén *et al.*, 1985). The shape of the second type differed to that described by Shupliakov *et al.* (1992). He described a fusiform soma shape with dendritic ramifications that crossed the midline of the spinal cord. Shupliakov *et al.* (1992) did not describe fin motoneurons larger than 35 x 55 µm as I did in this thesis. This could be due to their studies being performed only on *Ichthyomyzon unicuspis* instead on *Lampetra fluviatilis* as in my work. It can be possible that the different types of neurons differ in size and shape within the different species of lamprey.

In one case (not shown) out of eight investigated fin motoneurons adjacent cells in the spinal cord were labelled after intracellular staining of one fin motoneuron of type II, indicating that there exist gap junctions or electrical synapses between fin motoneurons and other neurons located in the spinal cord (similar results for fin motoneurons were found by Sandra Pohler (2005)). Although the dye used, Fluorescein-coupled-dextran-amine (FDA) had a molecular weight of 3000 Daltons and seeming to be rather large in size for crossing gap junctions, it was shown that the dye includes a wide area of different molecular sizes making it possible to be transported across electrical synapses (Chandross *et al.*, 1995). In prior works it was shown that in the lamprey spinal cord electrical synapses exist between various cells of the swimming network. For example Müller cell axons descend ipsilaterally into the spinal cord, where they make combined *en passant* electrical and chemical excitatory synapses upon segmental spinal neurons (Gad *et al.*, 1998). Also the „I2 to giant interneuron synapse“ is functionally a combined electrical and chemical excitatory synapse. Its ultrastructure has been studied by Christensen (1983). In the neonatal rat spinal cord, Kiehn *et al.* (2001) showed that N-methyl-D-aspartate (NMDA) receptor agonists could induce rhythmic synchronous activity in pools of motoneurons, even after blocking of all chemical synaptic transmission. These rhythmic coordinated membrane potential oscillations disappeared after treatment with gap junction blockers, such as carbenoxolone or when the voltage dependent properties of NMDA receptors were suppressed by removing Mg²⁺ from the bath, showing that gap junctions could be important in generating and maintaining rhythmic motor patterns. Therefore the rarely observed dye coupling can be due to the passage of the dye through gap junctions.

4.1.2 Two electrophysiological different types of fin motoneurons

During NMDA induced „fictive swimming“ the results for fin motoneurons of type I compared in trough potential and peak-to-peak amplitude (Fig. 3.10) are similar with those found in lamprey myotomal and fin motoneurons as described before (Hill, 1987; Shupliakov *et al.*, 1992; Wallén *et al.*, 1993). Type II fin motoneurons however have a mean trough potential around 7.5 mV more depolarized than those of type I (Fig. 3.10), indicating that they have a more depolarized membrane potential in general or that they may receive stronger tonic excitatory input during „fictive locomotion“. This could possibly be caused by contralateral excitatory synaptic input depending on their contralateral dendritic ramifications. In addition excitatory input from interneurons located in the ipsilateral part of the spinal cord or from propriospinal neurons seems possible. On the other hand weaker tonic inhibitory influences from the same sources (ipsilateral and contralateral located premotor interneurons) could also be a plausible explanation. At present nothing is known about tonic input to fin motoneurons in the lamprey during „fictive locomotion“.

The mean membrane potential oscillations of fin motoneurons of type I are very similar with a medium fast increase over around 140 to 180 deg of a period reaching its peak potential by around 180 deg followed by a similar fast decay (Fig. 3.4). Type II fin motoneurons showed a very rapidly increase of their depolarization in the locomotor cycle up to 50 to 60 percent of the peak potential within the first 10 deg of the cycle and a similarly fast hyperpolarization at the end of the cycle (Fig. 3.8). The fast depolarization could originate from activation of type II fin motoneurons by excitatory crossed commissural interneurons (eCCINs), which are present in the lamprey spinal cord (Buchanan, 1982). Similar results for both types of motoneurons could be shown by plotting the membrane potential over a time of +/- 200 ms around the middle of its adjacent ventral root burst activity (Fig. 3.5, Fig. 3.9). Fin motoneurons of type I showed a slow continuing hyperpolarization in membrane potential till the middle of the ventral root burst activity, followed by a similar slow steadily depolarization. In opposite, type II fin motoneurons showed a very rapid hyperpolarization during the ipsilateral ventral root burst activity within a time course of around 100 ms.

Although the shape of the membrane potential oscillations differed between the two different morphological types of fin motoneurons, their mean peak- and trough potential over one phase did not differ (Fig. 3.11). This means that both types have their peak depolarization in antiphase to the

myotomal motoneurons as described in literature before (Birnberger and Rovainen, 1972; Rovainen and Birnberger, 1971; Shupliakov *et al.*, 1992).

4.1.3 Different types of fin motoneurons after hierarchical clustering

For checking if the two different types of fin motoneurons could be classified only due to their different membrane potential oscillations without morphologically identification an appropriate method had to be found. Although it would have been possible to classify the different cells just by visual inspection, hierarchical clustering was additionally used as statistical method. It has to be noticed though that this method does not produce quantitative measures of statistical significance. After using hierarchical clustering for classifying the recorded fin motoneurons the two different classes of cells could be confirmed. All the classified motoneurons were in the same clusters as determined morphologically (Fig. 3.12, Fig. 3.13). Therefore hierarchical clustering was also used to classify all recorded fin motoneurons, including cells that were not morphologically distinguished before. The results showed three individual classes of fin motoneurons in case of the membrane potential fluctuation over period (Fig. 3.17) as well as over time (Fig. 3.21). The first two types had membrane potential properties which were quite similar to the morphologically identified fin motoneurons of type I and type II (Fig. 3.11, 3.24), meaning that it seems to be possible that they could be separated just by using a statistical clustering method instead of dyeing them for identification. This would make identification of the different types of fin motoneurons much easier, because it would mean that fin motoneurons of the lamprey had not been to be labelled intracellularly for identification. The third type (type III) had a different type of membrane potential oscillation with its mean peak amplitude at a phase of around 304 deg (Fig. 3.24). Up to three clearly distinguishable maxima could be observed in this type of motoneuron (Fig. 3.16 A, C, E). Membrane potential oscillation similar to type III were never described in literature before and the shape of membrane potential oscillations is not similar to any kind of motoneuron in the spinal swimming network shown before. Type III fin motoneurons are easily identifiable via hierarchical clustering from any other type of fin motoneurons in the lamprey spinal cord.

It was shown by Buchanan (Buchanan and Cohen, 1982; Buchanan and McPherson, 1995), that myotomal motoneurons had their peak depolarization at a phase of 0.2, meaning 72 deg. All other

measured neurons in the lamprey spinal cord (lateral interneurons (LINs), inhibitory crossed commissural interneurons (iCCINs) and edge cells (ECs)) showed their peak depolarization in a phase ranged from around 0.05 (18 deg) in case of CCINs up to around 0.35 (126 deg) measured for ECs. It is important to notify that Buchanan defined the cycle period from the start of one ipsilateral ventral root burst to the start of the next one, instead of the middle from one ventral root burst to the middle of the next being used in my study as well as most recent studies of other researchers. Therefore all data mentioned above have to be shifted in phase by about 0.18 to compare them with the results in this work. After correcting the values reported by Buchanan and McPherson, the mean peak depolarizations of the different neurons were in a phase range of between 0.23 (83 deg) for CCINs and 0.53 (191 deg) for ECs.

Another type of interneurons located in the spinal cord of the lamprey are giant interneurons (GINs). GINs have been considered as second-order sensory relay neurons (Rovainen, 1974). Buchanan and Cohen showed that they were mostly (6 out of 13) not modulated during fictive locomotion and that their mean peak-to-peak membrane potential modulation in fictive locomotion was only around 2 mV. The types of GINs that exhibited rhythmic modulation showed various peak depolarizations. Four of them had their peak depolarisation during the ipsilateral ventral root burst, but two others had peak depolarizations in antiphase to the ventral root burst. This may indicate that they could serve in generating the antiphasic activity of fin motoneurons provided that they project onto fin motoneurons. The corrected phase of the GINs peak depolarization was around 0.8 (288 deg), meaning that in case of them being connected to fin motoneurons they could contribute to the modulation of type III fin motoneurons as well. Also the fact that GINs are only located in the caudal part of the spinal cord, that there are two different types (one that has its peak depolarization during activity of the ipsilateral ventral root burst and another type that has its peak depolarization during antiphase of the ipsilateral ventral root activity) and that they have contralateral and rostral projecting axons (Rovainen, 1967) make it conceivable to hypothesize that GINs may play a role in controlling fin motoneurons.

Moreover, as GINs can be excited by mechanical stimulation of the fin and body skin (Teräväinen and Rovainen, 1971) and that GINs receive monosynaptic and polysynaptic excitatory inputs from dorsal cells (Rovainen, 1974) raises the possibility there exist two different types of GINs, one

involved in controlling myotomal motoneurons and another type in controlling of fin motoneurons. Type III fin motoneurons have their peak depolarization at a very late stage in the cycle period defined from the middle of one ipsilateral ventral root burst to the next one, later than any other rhythmically modulated neuron located in the spinal cord of the lamprey (cf. Grillner *et al.*, 2002).

4.2 Synaptic input to the three different types of fin motoneurons

It is known that during locomotion lamprey myotomal motoneurons receive phasic excitatory and inhibitory synaptic input in an alternating fashion (Kahn, 1982; Russel and Wallén, 1983; Wallén and Shupliakov, 1991) from excitatory and inhibitory interneurons that are components of the segmental network (Grillner *et al.*, 1991; Grillner, 2003), but nothing is known about fin motoneurons. In this thesis several experiments have been made by injecting chloride ions via negative current into the recorded three different types of fin motoneurons to invert the inhibitory postsynaptic potentials (IPSPs) to depolarized potentials. Cells which received a phase of inhibition could be determined because their relative hyperpolarization was inverted and became a phase of relative depolarization, they were reversed (Coombs *et al.*, 1955; Araki *et al.*, 1961).

There are several different possibilities for the synaptic drive that fin motoneurons receive for producing their phasic membrane potential oscillation. Firstly, there is the possibility of phasic inhibition during ipsilateral ventral root burst activity superimposed on a tonic excitation or secondly a phasic excitation during contralateral ventral root burst activity could be superimposed on a tonic excitation. Also possible could be a phasic inhibition alternating with phasic excitation. The results (Fig. 3.26-3.29) for type I and type II fin motoneurons showed that the peak-to-peak amplitude increased after negative current injection, also showing a reversal of the hyperpolarized phase (Fig. 3.26, 3.28). This reversal with negative current showed that there has to be an active phasic inhibition. Therefore the hypothesis of getting phasic excitation superimposed on a tonic excitation does not fit. To clarify if there is a also phasic excitation, the amplitude of the synaptic noise 100 ms around the ipsilateral (PPi) and contralateral (PPc) ventral root burst activity was measured. It could be shown that during negative current injection the PPi was initially reduced but after increasing of negative current the amplitude became larger, whereas the PPc behave nearly unaffected of any negative current injection (Fig. 3.27, 3.29). This may indicate that there is not only a phasic inhibition

in fin motoneurons during the ipsilateral ventral root activity, because it could be shown that the IPSPs could be reversed after negative current injection. However, given that the PPc was mostly unaffected it could also be concluded that fin motoneurons of type I and type II also get phasic excitatory input.

These results are similar to those found in myotomal motoneurons of the lamprey. Myotomal motoneurons receive a phasic inhibitory input during the contralateral ventral root burst activity together with a phasic excitatory drive during the activity of the ipsilateral ventral root burst (Russel and Wallén, 1983).

This type of controlling motoneuron membrane potential oscillation by alternating phases of excitation and inhibition appears to be a common system in vertebrate rhythmic locomotor systems. For example, similar results were found in tadpole (Roberts *et al.*, 1981) and cat (Edgerton *et al.*, 1976; Jordan, 1981).

Compared to myotomal motoneurons in the lamprey spinal cord, fin motoneurons show a membrane potential oscillation with a phase shift of almost 180 deg (Shupliakov *et al.* 1992). Therefore they can not be coupled directly to the same premotor interneurons located in the CPG generating the myotomal motoneuron activity, mainly the ipsilateral located excitatory interneurons (EINs) and the contralateral located inhibitory crossing commissural interneurons (iCCINs). One possibility could be an activation of fin motoneurons via excitatory crossed commissural interneurons (eCCINs) and a phasic inhibition by ipsilateral located inhibitory interneurons. There could be a possible influence from lateral inhibitory interneurons (LINs) to fin motoneurons. It was found that LINs could inhibit motoneurons, but it is not known if they affect myotomal or fin motoneurons and also if they connect to motoneurons in general (Rovainen, 1982). Also their receiving of polysynaptic excitatory and inhibitory input from dorsal cells (Rovainen, 1974) could make the LINs to a possible candidate for having strong influences of controlling fin motoneurons.

Modulation of fin motoneurons of type III during „fictive locomotion“ was not examined in sufficient extent. Therefore it is not possible to make a conclusion about the input these motoneurons receive.

4.3 Connectivity of fin motoneurons

Extracellular recordings from ventral roots before and after performing sagittal lesions over a length of one up to five segments caudally of the recorded segment did show a small reduction of presumed fin motoneuron activity, but activity was still present (Fig. 3.34, 3.35). In contrast the activity abolished after performing a transversal lesion additionally to the sagittal one, anyhow if the length of the sagittal hemisection was prolonged up to five segments (Fig. 3.34, 3.35). Before and after the lesions the cycle period and burst duration of myotomal motoneurons in fictive swimming did not change (Fig. 3.35).

For better understanding of the internal cellular processes intracellular recordings were carried out before and after the different lesions were performed. The membrane potential oscillations of fin motoneurons showed a reduction of around 40% of its amplitude after performing a sagittal lesion (Fig. 3.36) and an increase of up to 45% after performing a rostral- or a caudal directed transversal lesion (Fig 3.37, 3.38). A strong decrease of around 65% in the amplitude of the membrane potential was observed after carrying out a combined transversal plus sagittal lesion (Fig. 3.39). Due to the small number of experiments (N=2) the data of the latter experiment has to be confirmed in future. These results are similar to that found during extracellular recordings, because there it was also shown that after performing a sagittal lesion the superthreshold activity of fin motoneurons was reduced up to 33% (Fig. 3.35, A).

This may suggest, that depending on the three different types of fin motoneurons located in the lamprey spinal cord it could be possible that only special types of them would be recruited during swimming. It could be possible that, depending on the present situation of the spinal cord, the different types of fin motoneurons could be recruited and activated, just as they would be necessary for the present state of swimming. This means that, during swimming, for example some cells of type I could be active if the animal would be in a stable position, but after the bearing of the animal changes to a special degree, additional fin motoneurons of one type or of another could be activated for re-establishing the former position of the animal. Therefore the results of the recordings after performing an extracellular sagittal lesion are not fully comparable with those found during the intracellular ones.

For sure it could be shown that after a sagittal and transversal (rostral or caudal) lesion the phasic membrane potential oscillation persisted and that neither the excitatory- nor the inhibitory phase was abolished. This means that ipsilateral ascending and descending input to fin motoneurons as well as contralateral input do affect the membrane potential oscillation of fin motoneurons, but none of them are necessary for maintaining the rhythmic membrane potential fluctuation during „fictive swimming“. Similar results could be shown in lamprey for myotomal motoneurons (Wallén *et al.*, 1993). However after disrupting descending plus contralateral inputs by performing a combined sagittal plus rostral transversal lesion the membrane potential of fin motoneurons was reduced down to around 65%. This result was also shown during extracellular recordings of ventral roots, because after performing the combined lesion the superthreshold activity of most antiphasic active motoneurons was abolished.

Therefore it seems that the ascending input to a segment is not strong enough to depolarize motoneurons to the needed threshold for generating their action potentials. Wallén *et al.* (1993) showed during „fictive swimming“ that myotomal motoneurons showed a marked reduction in the amplitude of the membrane potential fluctuation after performing a rostral transversal lesion and therefore they concluded that myotomal motoneurons need to receive a strong ipsilateral excitatory drive. In contrast to myotomal motoneurons it was shown in this thesis that the amplitude of fin motoneurons increased after performing a rostral transversal lesion by repenetrating presumably the same cell, meaning that there has to be a strong descending rhythmic drive to fin motoneurons, which may be caused by iCCINs.

On the other hand it seems possible that there has to be an excitatory drive from the contralateral part of the spinal cord to fin motoneurons, because it was shown that the amplitude of the membrane potential was reduced when a midline lesion was carried out and the same cell was recorded before and after the lesion was performed. Due to a similar resting potential before and after the lesion was performed it was assumed that the cell was not injured and therefore both recordings were comparable. The seen reduction of the amplitude of the membrane potential could be caused by eCCINs. Figure 3.40 shows the mean peak-to-peak amplitude for the identified three different types of fin motoneurons plus the lesion experiments that were performed. In this bar diagram all the different

cells were taken together and their mean was calculated. Although there were no significant changes, probably caused by the variations in the different peak-to-peak potentials of the same type of cells, the results are tending to those shown for the single cells (Fig. 3.41).

Due to the remaining phasic membrane potential fluctuations after performing the different lesions it is unlikely that the phase values for the occurrence of the membrane potential minima and maxima would have been changed. Indeed there are no changes in the positions of the minima and maxima of the membrane potential before and after the different lesions were carried out (Fig. 3.42, 3.43). Also the burst duration and the cycle period were unaffected by the lesions (Fig. 3.44). Therefore it seems that there has to be a strong coupling between the rhythmic membrane potential fluctuation of fin motoneurons and myotomal motoneurons during „fictive swimming“.

4.4 Possible mechanisms for controlling fin motoneurons

Taking the results from my work plus the known data from literature together I may suggest a hypothetical model system for possible synaptic input to fin motoneurons during „fictive swimming“: Müller cells, located in the lamprey brainstem, receive a rhythmic modulation in their membrane potential during fictive swimming, with a tendency to be co-active with rostral ipsilateral myotomal motoneurons (Kasicki and Grillner, 1986; Kasicki *et al.*, 1989). It is also known that stimulation of Müller cells of types M_3 and I_1 causes a flexion of the fin to the opposite direction in small adult lampreys of *Petromyzon marinus* (Rovainen, 1967) via a polysynaptic pathway through unidentified excitatory interneurons, activating contralateral located fin motoneurons (Rovainen, 1967). Müller cells of types M_3 and I_1 are receiving a pattern of inputs consisting of inhibition from the ipsilateral vestibular nerve and excitation from the contralateral vestibular nerve. These two types of cells also show consistent excitation to downward rolls to the contralateral side and to nose-up rotation suggesting that they are involved in specific vestibulospinal reflexes (Rovainen, 1979). Also this could be an evidence for controlling activity of fin motoneurons (FMNs), which are appropriate for righting the animal following downward rotation of the contralateral side, via type M_3 and I_1 Müller cells. In summary, it is known for Müller cells of type M_3 and I_1 that they excite monosynaptically ipsilateral located myotomal motoneurons and polysynaptically contralateral located fin motoneurons (Rovainen, 1974b).

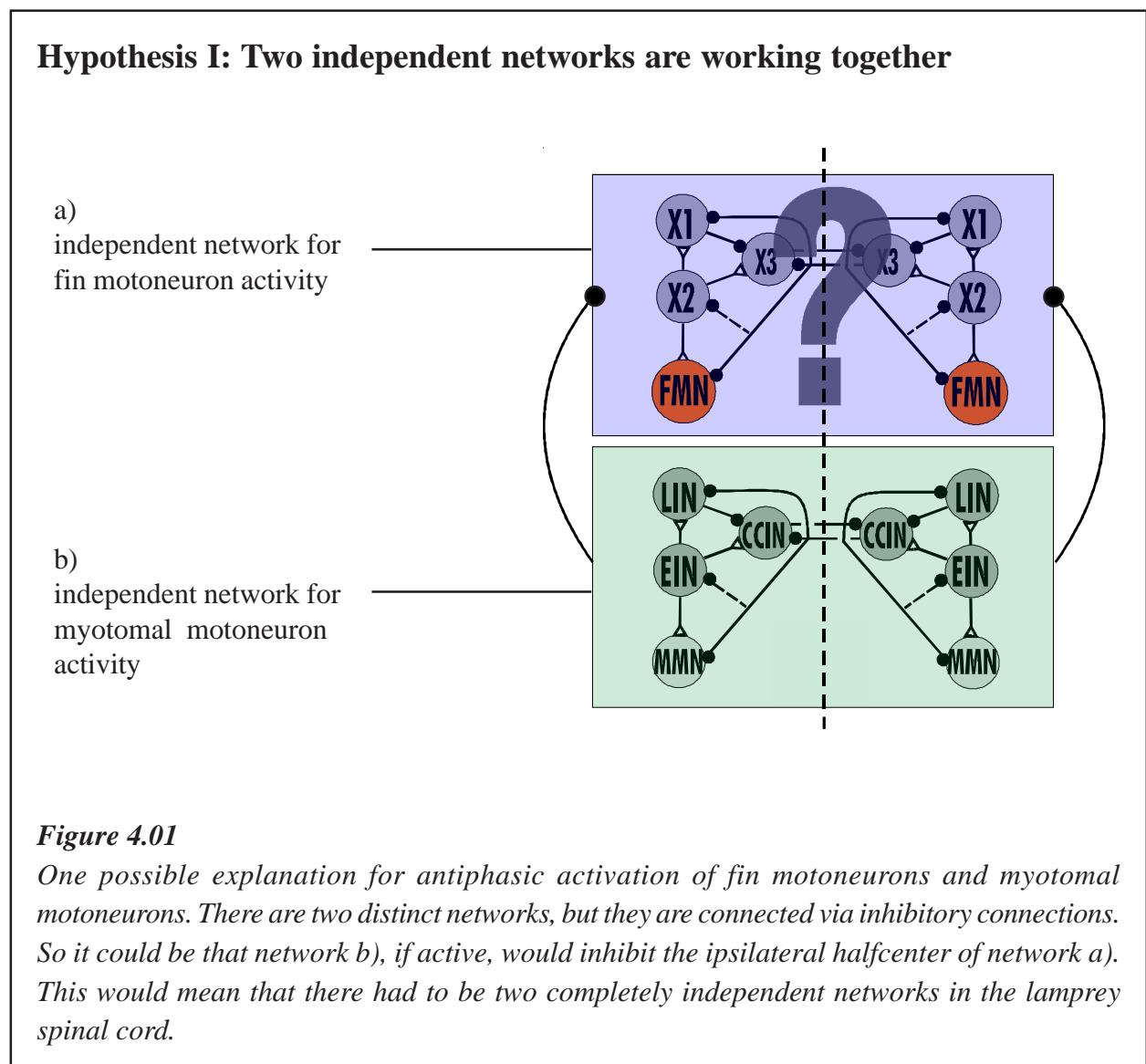
There are different types of neurons located in the spinal cord of the lamprey that could be involved in coordination of fin motoneurons. Following is a description of propriospinal neurons and their possible connections to fin motoneurons.

Lateral inhibitory interneurons (LINs) can project till the tail region of the spinal cord (Rovainen, 1974) and their synaptic output causes an inhibition of ipsilateral crossed commissural interneurons (CCINs) (Buchanan, 1982). It is also known that LINs can inhibit motoneurons (Rovainen, 1982). LINs receive direct input from contralateral located CCINs (Buchanan, 1982) and also from ipsilateral located excitatory interneurons (EINs) (Buchanan and Grillner, 1987). Additionally they receive polysynaptic excitatory and inhibitory input from dorsal cells (DCs) (Rovainen, 1974). At present it is not known whether LINs have in addition to connections to inhibitory CCINs also connections to excitatory CCINs. This could be an important question for finding a possible mechanism for activation of fin motoneurons (FMNs).

Research over the last years made CCINs the most important neuron class responsible for coordination of myotomal motoneuron activity, but at present nothing is known about influences of the two individual classes of CCINs on FMNs. Knowing that 10-20% of motoneurons and CCINs have contralateral directed dendrites (Buchanan, 1982; Wallén *et al.*, 1985) and that the number of motoneurons per segment are not more than 140 (*Ichthyomyzon unicuspis*) to 200 (*Petromyzon marinus*) (Rovainen and Dill, 1984), could also be a sign that those 10-20% of cells having dendrites crossing the midline may have connections to FMNs, because their number is only around 10-20% of those of myotomal motoneurons (Pohler, 2005). There are three different classes of CCINs, two of them show inhibitory connections and one class with sparse contralateral directed dendrites shows excitatory synaptic connections to contralateral neurons. The latter class receives disynaptic inhibition from the ipsilateral positioned I₁ Müller cells. Inhibitory CCINs are twice as numerous as excitatory ones (Buchanan, 1982). CCINs have output synapses on the opposite side of the spinal cord and their postsynaptic targets include motoneurons, LINs and other CCINs (Buchanan, 1982). As mentioned above it seems possible that excitatory CCINs (eCCINs) may have connections to FMNs. After performing a sagittal lesion the peak-to-peak membrane potential of presumed FMNs decreased (*Fig. 3.36*).

Excitatory Interneurons (EINs) can excite not only LINs and CCINs (Buchanan and Grillner, 1987), but also other EINs (Buchanan *et al.*, 1989). Opposite to EINs there are also inhibitory interneurons (IINs) located in the spinal cord. They are much less common than EINs and they inhibit nearby CCINs. Their modulation during „fictive swimming“ is in phase with nearby motoneurons (Buchanan and Grillner, 1988).

Edge cells (ECs), known as intraspinal stretch receptors (Rovainen, 1974) can be separated in two different classes. Contralaterally projecting ECs are inhibitory and have been shown to inhibit other ECs, LINs, and CCINs (Rovainen, 1974; Di Prisco *et al.*, 1990). Ipsilaterally projecting edge cells are excitatory and have been shown to excite motoneurons and CCINs (Di Prisco *et al.*, 1990).



Giant interneurons (GINs) can be excited by mechanical stimulation of the fin and body skin (Teräväinen and Rovainen, 1971) and they receive monosynaptic and polysynaptic excitatory inputs from dorsal cells (DCs) (Rovainen, 1974). Due to their direct dorsal cell input and their ascending axons that can reach the brainstem, GINs have been considered to be second-order sensory relay neurons (Rovainen, 1974).

DCs correspond to the Rohon-Beard cells of larval teleosts and amphibians (Clarke *et al.*, 1984; Nakao and Ishizawa, 1987) and the peripheral process of DCs innervate the skin and enter the

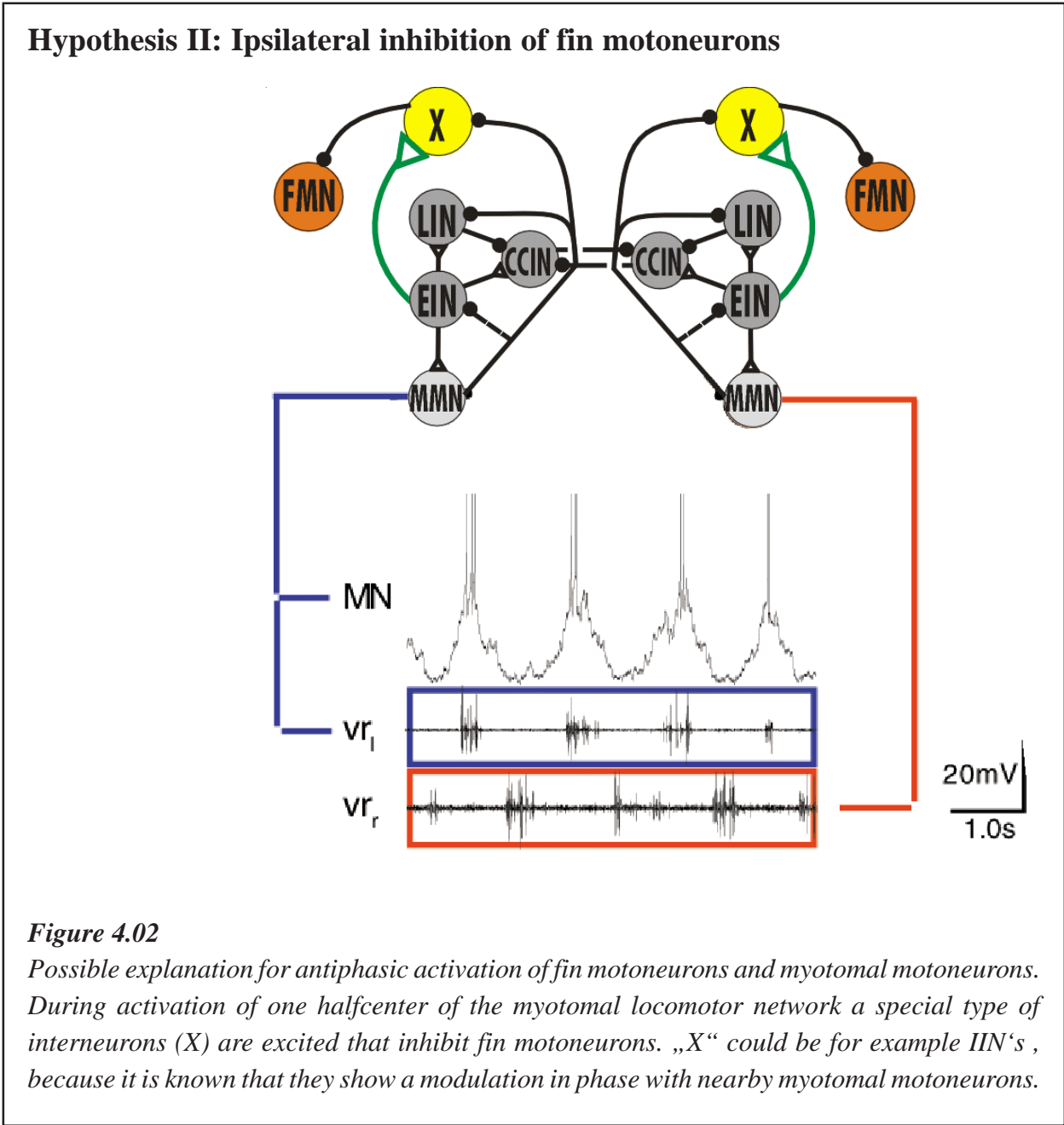
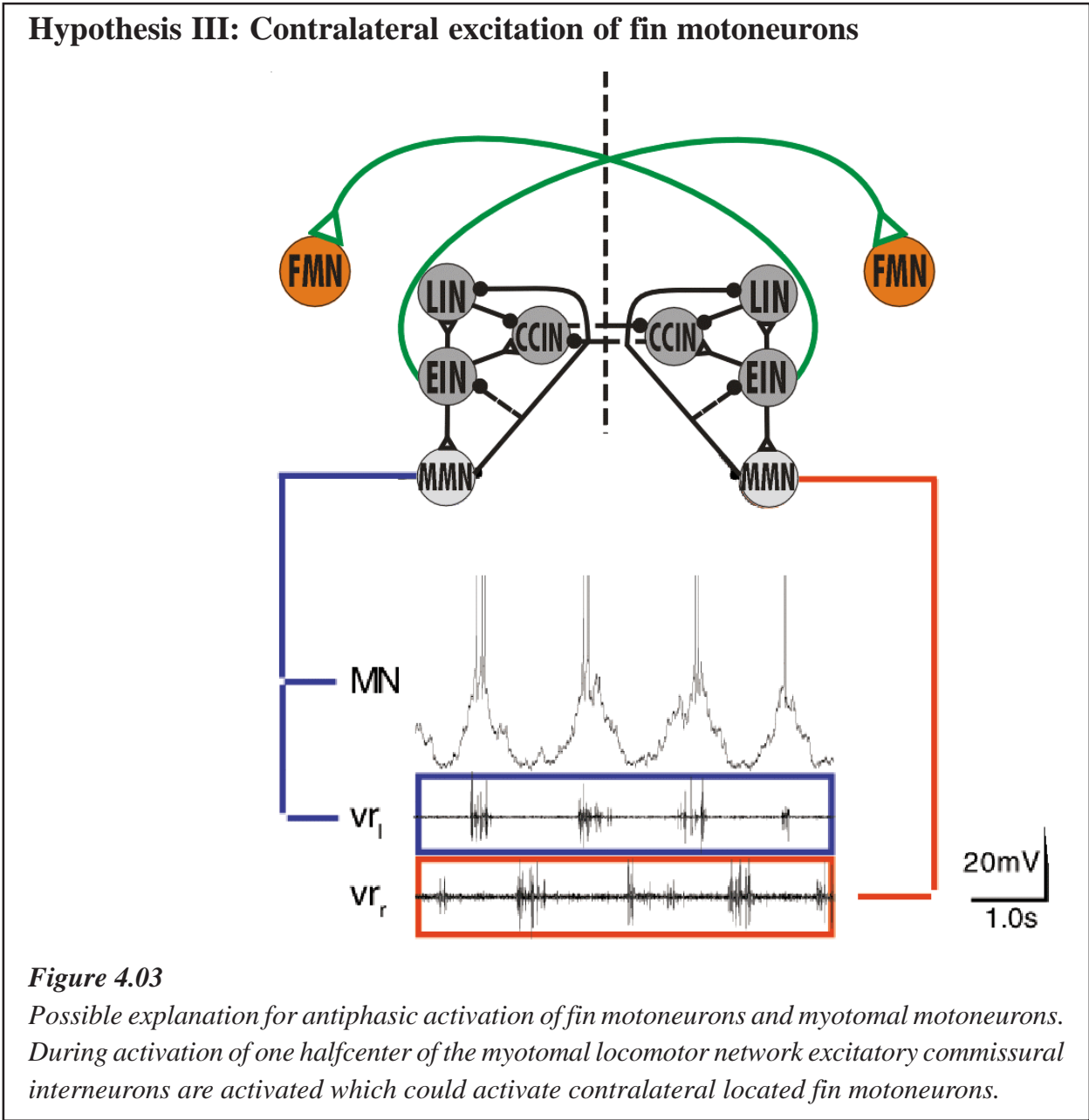
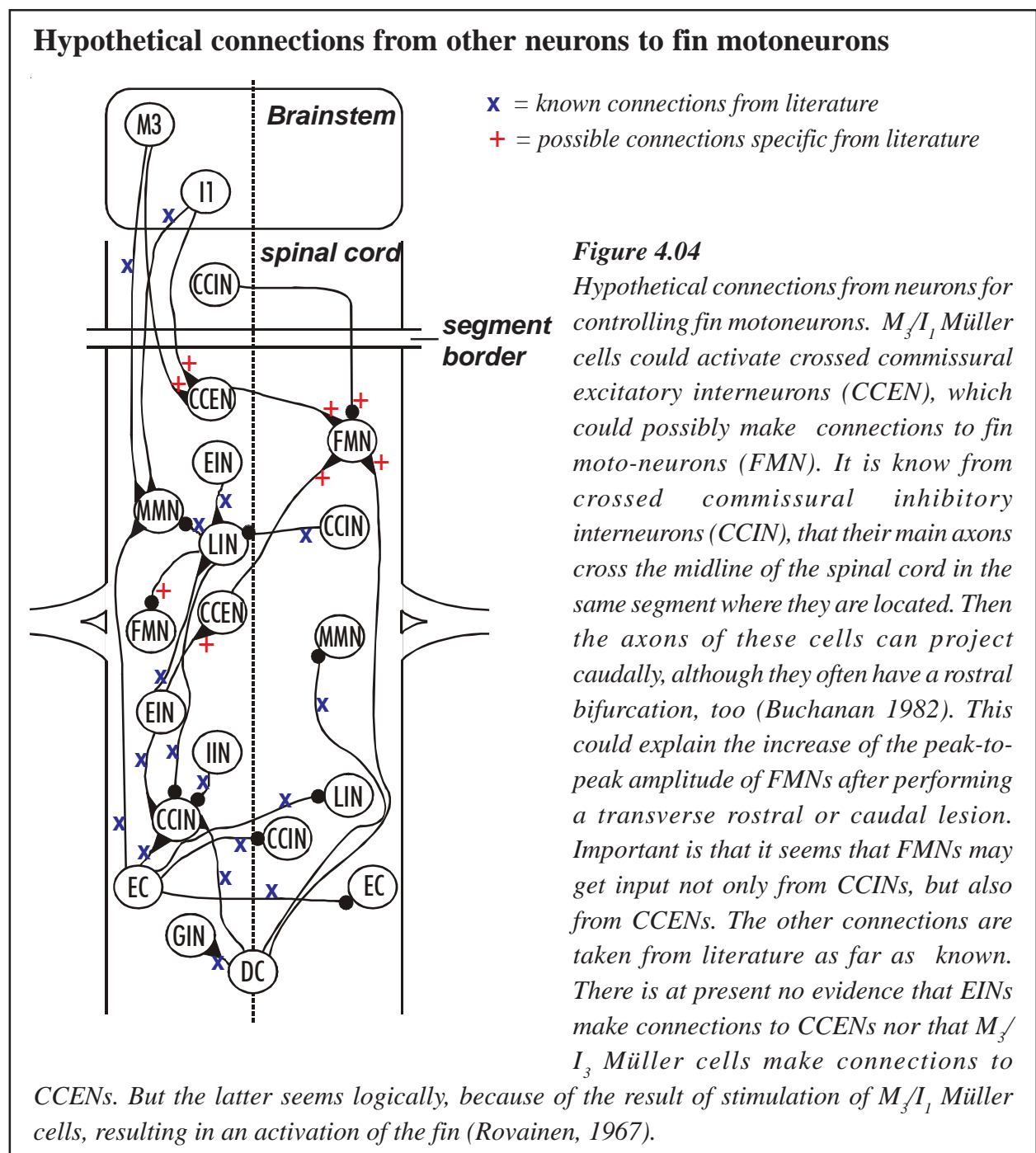


Figure 4.02
Possible explanation for antiphasic activation of fin motoneurons and myotomal motoneurons. During activation of one halfcenter of the myotomal locomotor network a special type of interneurons (X) are excited that inhibit fin motoneurons. „X“ could be for example IIN's , because it is known that they show a modulation in phase with nearby myotomal motoneurons.

spinal cord via a dorsal root. They can produce monosynaptic EPSPs in GINs and polysynaptic EPSPs and IPSPs in motoneurons, LINs, ECs, and CCINs (Rovainen, 1974; Buchanan, 1982). DCs participate in local reflexes (Teräväinen and Rovainen, 1971), and they can have powerful effects on „fictive swimming“ when electrically stimulated, but their membrane potentials show little or no modulation (Buchanan and Cohen, 1982; Buchanan and Kasicki, 1995; el Manira *et al.*, 1996). It has been shown in several vertebrates that all these individual classes of neurons are important for coordination of myotomal motoneurons, but so far no hypothesis was developed including fin motoneurons to this model.



There are three different explanations for the antiphasic activation of fin motoneurons during fictive swimming. First there could be a separate network co-ordinating fin motoneuron activity, activated by the ipsilateral halfcenter of the myotomal motoneuron network that could inhibit the ipsilateral located halfcenter of the fin motoneuron network (Fig. 4.01). At present there is no evidence for two different networks in the lamprey spinal cord coordinating myotomal motoneurons and fin motoneurons independently.



Two models are shown in Fig. 4.02 and Fig. 4.03. Both are based on the hypothesis that fin motoneurons are integrated in the „myotomal“ locomotion network. One possibility is that FMNs are getting inhibitory drive from a special type of ipsilateral IINs, but that those IINs only receive excitatory drive, if the ipsilateral half center is active. This means that if the ipsilateral locomotor network would be active the IINs connected to FMNs would be activated, inhibiting the ipsilateral located FMNs. Due to the fact that IINs are modulated in phase with nearby motoneurons (Buchanan and Grillner, 1988), it could be an indication that such a connection could exist. On the other hand there is so far no evidence that there are connections from IINs to motoneurons.

Finally, the third possibility exists that the activation of contralaterally located FMNs via excitatory crossed commissural interneurons could occur meaning that by activation of the ipsilateral halfcenter of the myotomal locomotor network contralateral located fin motoneurons would be activated. This could potentially happen through excitatory crossed commissural interneurons. At present this seems to be the most logical explanation, for example due to the reduction of the peak-to-peak amplitude of fin motoneurons after performing a sagittal lesion. Also there could be some descending and ascending inhibitory drive possibly caused by IINs or by inhibitory CCINs. A hypothetical model for neuronal connections to fin motoneurons is shown in Fig. 4.04. Of course other influences including unidentified neurons have to be considered.

At the present state of research it seems that fin motoneurons could be part of the myotomal locomotor network, integrated by a combination of the models shown in Fig. 4.02 and Fig. 4.03. On the other hand the results of the lesion experiments show that neither ascending/descending- nor contralateral inputs are necessary for generating the membrane potential oscillation of FMNs. This results suggest, that there could be a separate neural oscillator in each hemisegment of the spinal cord.

5. References

- ARAKI T., ITO M. AND OSCARSSON O. (1961) Anion permeability of the synaptic and non-synaptic motoneurone membrane. *J. Physiol.* 159:410-435.
- ARSHAVSKY YU.I., BELOOZEROVA I. N., ORLOVSKY G. N., PANCHIN YU. V., PAVLOVA G. A. (1985a) Control of locomotion in marine mollusc *Clione limacina*. I. Efferent activity during actual and fictitious swimming. *Exp. Brain Res.* 58(2):255-62.
- ARSHAVSKY YU.I., BELOOZEROVA I. N., ORLOVSKY G. N., PANCHIN YU. V., PAVLOVA G. A. (1985b) Control of locomotion in marine mollusc *Clione limacina*. II. Rhythmic neurons of pedal ganglia. *Exp. Brain Res.* 1985;58(2):263-72.
- ARSHAVSKY YU.I., BELOOZEROVA I. N., ORLOVSKY G. N., PANCHIN YU. V., PAVLOVA G. A. (1985c) Control of locomotion in marine mollusc *Clione limacina*. III. On the origin of locomotory rhythm. *Exp. Brain Res.* 1985;58(2):273-84.
- BARBEAU H. AND ROSSIGNOL S. (1987) Recovery of locomotion after chronic spinalization in the adult cat. *Brain Res.* 412(1):84-95.
- BÄSSLER U. (1983) *Neural Basis of Elementary Behavior in Stick Insects*. Berlin: Springer Verlag.
- BÄSSLER U. AND WEGNER U. (1983) Motor output of the denervated thoracic ventral nerve cord in the stick insect *Carausius morosus*. *J. Exp. Biol.* 105:127-145.
- BÄSSLER U. AND BÜSCHGES A. (1998) Pattern generation for insect walking movements - multisensory control of a locomotor program. *Brain Research Reviews*; 27:65-88.
- BATSCHLET E. (1981) *Circular statistics in biology*. Academic Press.

- BEKOFF A, NUSBAUM M. P., SABICHI A. L., CLIFFORD M. (1987) Neural control of limb coordination. I. Comparison of hatching and walking motor output patterns in normal and deafferented chicks. *J. Neurosci.* 7(8):2320-2330.
- BEKOFF A., KAUER J. A., FULSTONE A., SUMMERS T. R. (1989) Neural control of limb coordination. II. Hatching and walking motor output patterns in the absence of input from the brain. *Exp. Brain Res.* 74(3):609-617.
- BIRNBERGER K. L. AND ROVAINEN C. M. (1971) Behavioral and intracellular studies of a habituating fin reflex in the sea lamprey. *J. Neurophysiol.* 34(6):983-989.
- BRODIN L. AND GRILLNER S. (1986) Effects of magnesium on fictive locomotion induced by activation of N-methyl-D-aspartate (NMDA) receptors in the lamprey spinal cord in vitro. *Brain. Res.* 380(2):244-252.
- BUCHANAN J. T. (1982) Identification of interneurons with contralateral, caudal axons in the lamprey spinal cord: synaptic interactions and morphology. *J. Neurophysiol.* 47(5):961-975.
- BUCHANAN J. T. (1999) The roles of spinal interneurons and motoneurons in the lamprey locomotor network. *Prog. Brain Res.* 123:311-21.
- BUCHANAN J. T. (2001) Contributions of identifiable neurons and neuron classes to lamprey vertebrate neurobiology. *Prog. Neurobiol.* 63(4):441-466.
- BUCHANAN J. T. AND COHEN A. H. (1982) Activities of identified interneurons, motoneurons, and muscle fibers during fictive swimming in the lamprey and effects of reticulospinal and dorsal cell stimulation. *J. Neurophysiol.* 47(5):948-960.
- BUCHANAN J. T. AND GRILLNER S. (1987) Newly identified 'glutamate interneurons' and their role in locomotion in the lamprey spinal cord. *Science.* 236(4799):312-314.

- BUCHANAN J. T. AND GRILLNER S. (1988) A new class of small inhibitory interneurons in the lamprey spinal cord. *Brain Res.* 438:404-407.
- BUCHANAN J. T., GRILLNER S., CULLHEIM S., RISLING M. (1989) Identification of excitatory interneurons contributing to generation of locomotion in lamprey: structure, pharmacology, and function. *J. Neurophysiol.* 62(1):59-69.
- BUCHANAN J. T. AND KASICKI S. (1995) Activities of spinal neurons during brain stem-dependent fictive swimming in lamprey. *J. Neurophysiol.* 73(1):80-87.
- BUCHANAN J. T. AND MCPHERSON D. R. (1995) The neural network for locomotion in the lamprey spinal cord: Evidence for the involvement of commissural interneurons. *J. Physiol.* 89: 221-233.
- BÜSCHGES A., SCHMITZ J. AND BÄSSLER U. (1995) Rhythmic patterns in the thoracic nerve cord of the stick insect induced by pilocarpine. *J. Exp. Biol.*; 198: 435-456.
- BUTT S. J., LEBRET J. M., KIEHN O. (2002) Organization of left-right coordination in the mammalian locomotor network. *Brain Res. Brain Res. Rev.* 40(1-3):107-117.
- CANGIANO L. AND GRILLNER S. (2003) Fast and slow locomotor burst generation in the hemispinal cord of the lamprey. *J. Neurophysiol.* 89(6):2931-2942.
- CAZALETS J. R., SQALLI-HOUSSAINI Y., CLARAC F. (1992) Activation of the central pattern generators for locomotion by serotonin and excitatory amino acids in neonatal rat. *J. Physiol.* 455:187-204.
- CHANDROSS K. J., C JANSON M., SPRACY D. C., KESSLER J. A. (1995) Transforming growth factor-beta 1 and forskolin modulate gap junctional communication and cellular phenotype of cultured Schwann cells. *J. Neurosci.* 15:262-273.

- CLARKE J. D., HAYES B. P., HUNT S. P., ROBERTS A. (1984) Sensory physiology, anatomy and immunohistochemistry of Rohon-Beard neurones in embryos of *Xenopus laevis*. *J. Physiol.* 348:511-525.
- COHEN A. H. AND WALLÉN P. (1980) The neuronal correlate of locomotion in fish. „Fictive swimming“ induced in an in vitro preparation of the lamprey spinal cord. *Exp. Brain Res.* 41(1):11-18.
- COOMBS J. S., ECCLES J. C. AND FATT P. (1955) The specific conductances and the ionic movements across the motoneuronal membrane that produce the inhibitory postsynaptic potential. *J. Physiol.* 130(2):326-373.
- CRUSE H. (1990) What mechanisms coordinate the leg movements in walking arthropods? *Trends Neurosci.* 13:15-21.
- CURRIE S. N. AND STEIN P. S. (1988) Electrical activation of the pocket scratch central pattern generator in the turtle. *J. Neurophysiol.* 60(6):2122-2137.
- DALE N. (1986) Excitatory synaptic drive for swimming mediated by amino acid receptors in the lamprey. *J. Neurosci.* 6(9):2662-2675.
- DELCOMYN F. (1980) Neural basis of rhythmic behavior in animals; *Science* 210(4469):492-498.
- DELCOMYN F. (1985) Factors regulating insect walking. *A. Rev. Ent.* 30, 239–256.
- DELIAGINA T. G., GRILLNER S., ORLOVSKY G. N., ULLÉN F. (1993) Visual input affects the response to roll in reticulospinal neurons of the lamprey. *Exp. Brain Res.* 95(3):421-428.
- DI PRISCO G. V., WALLÉN P., GRILLNER S. (1990) Synaptic effects of intraspinal stretch receptor neurons mediating movement-related feedback during locomotion. *Brain Res.* 530(1):161-166.

- EDERER M., SAUTER T., BULLINGER E., GILLES E., ALLGOEWER F. (2003) An approach for dividing models of biological reaction networks into functional units. *Simulation* 709:703-716.
- EDGERTON V. R., GRILLNER S., SJÖSTRÖM A., ZANGGER P. (1976) Central generation of locomotion in vertebrates. In: *Neural control of locomotion* (ed. R. Herman, S. Grillner, P. Stein and D. Stuart), Vol. 18, pp. 439-464. Plenum Press, New York.
- EL MANIRA A., SHUPLIAKOV O., FAGERSTEDT P., GRILLNER S. (1996) Monosynaptic input from cutaneous sensory afferents to fin motoneurons in lamprey. *J. Comp. Neurol.* 369(4):533-42.
- EL MANIRA A., TEGNER J., GRILLNER S. (1997) Locomotor-related presynaptic modulation of primary afferents in the lamprey. *Eur. J. Neurosci.* 9(4):696-705.
- FORSSBERG H., GRILLNER S., HALBERTSMA J. (1980) The locomotion of the low spinal cat. I. Coordination within a hindlimb. *Acta Physiol. Scand.* 108(3):269-281.
- GETTING P. A. (1981) Mechanisms of pattern generation underlying swimming in *Tritonia*. I. Neuronal network formed by monosynaptic connections. *J. Neurophysiol.* 46(1):65-79.
- GETTING P. A. and Dekin M. S. (1985) Mechanisms of pattern generation underlying swimming in *Tritonia*. IV. Gating of central pattern generator. *J. Neurophysiol.* 53(2):466-480.
- GEWECKE M. AND WENDLER G. (1985) *Insect Locomotion*. Verlag Paul Parey Hamburg.
- GRILLNER S. (1974) On the generation of locomotion in the spinal dogfish. *Exp. Brain Res.* 20(5):459-470.
- GRILLNER S. (1975) Locomotion in vertebrates: central mechanisms and reflex interaction. *Physiol. Rev.* 55(2):247-304.
- GRILLNER S. (1985) Neurobiological bases of rhythmic motor acts in vertebrates. *Science.* 228(4696):143-149.

- GRILLNER S. (2000) From egg to action. *Brain Res. Bull.* 53 (2000) 473–477.
- GRILLNER S. (2003) The motor infrastructure: from ion channels to neuronal networks. *Nat. Rev. Neurosci.* 4(7):573-86.
- GRILLNER S., McCLELLAN A., SIGVARDT K., WALLÉN P., WILEN M. (1981) Activation of NMDA-receptors elicits „fictive locomotion“ in lamprey spinal cord in vitro. *Acta Physiol. Scand.* 113(4):549-551.
- GRILLNER S., WILLIAMS T., LAGERBACK P. A. (1984) The edge cell, a possible intraspinal mechanoreceptor. *Science.* 223(4635):500-503.
- GRILLNER S. AND ZANGGER P. (1984) The effect of dorsal root transection on the efferent motor pattern in the cat’s hindlimb during locomotion. *Acta Physiol. Scand.* 120(3):393-405.
- GRILLNER S. AND MATSUSHIMA T. (1991) The neural network underlying locomotion in lamprey. *Neuron*, vol.7, 1-15.
- GRILLNER S. AND ORLOVSKY G. N. (1991) Locomotion, neural networks. *Encyclopedia of human biology*, vol 4; academic press, 769-781.
- GRILLNER S., WALLÉN P., BRODIN L. AND LANSNER A. (1991) Neuronal network generating locomotor behavior in lamprey: circuitry, transmitters, membrane properties, and simulation. *Ann. Rev. Neurosci.* 14:169-199.
- GRILLNER S., DELIAGINA T., EKEBERG Ö., (1995) Neural networks that coordinate locomotion and body orientation in lamprey. *TINS* vol. 18, no 6.
- GRILLNER S., GEORGOPOULOS A. P., JORDAN J. M. (1997) Selection and Initiation of Motor behaviour
In: P. Stein, D. Stuart, A. Selverston, S. Grillner, (Eds.) *Neurons, Network, and motor behaviour*, MIT Press, Cambridge, MA, p3-19.

- GRILLNER S., CANGIANO L., HU G., THOMPSON R., HILL R., WALLÉN P. (2000) The intrinsic function of a motor system—from ion channels to networks and behavior. *Brain Res.* 886:224-236.
- GRILLNER S AND WALLÉN P. (2002) Cellular bases of a vertebrate locomotor system-steering, inter-segmental and segmental co-ordination and sensory control. *Brain Res. Brain Res. Rev.* 40(1-3):92-106.
- HARRIS-WARRICK R. M., MARDER E., SELVERSTON A. I., MOULINS M (1992) Dynamic biological networks. The stomatogastric nervous system, p. 328. Cambridge, MA: MIT.
- JOHNSON B. R., PECK J. H., HARRIS-WARRICK R. M. (1992) Elevated temperature alters the ionic dependence of amine-induced pacemaker activity in a conditional burster neuron. *J. Comp. Physiol.* 170(2):201-209.
- JORDAN L. M. (1981) Comment: Gating effects and constraints on the central pattern generators for rhythmic movements. *Can. J. Physiol. Pharmacol.* 59:727-732.
- JORDAN L. M., BROWNSTONE R. M., NOGA B. R. (1992) Control of functional systems in the brainstem and spinal cord. *Curr. Opin. Neurobiol.* 2(6):794-801.
- JOVANOVIĆ K., PETROV T., STEIN R. B. (1999) Effects of inhibitory neuro-transmitters on the mudpuppy (*Necturus maculatus*) locomotor pattern in vitro. *Exp. Brain Res.* 129:172-184.
- KAHN J. A. (1983) Patterns of synaptic inhibition in motoneurons and interneurons during „fictive swimming“ in the lamprey, as revealed by Cl⁻ injections. *J. Comp. Physiol.* 147:189-194.
- KAHN J. A. AND ROBERTS A. (1982) The central nervous origin of the swimming motor pattern in embryos of *Xenopus laevis*. *J. Exp. Biol.* 99:185-196.

- KASICKI S. AND GRILLNER S. (1986) Müller cells and other reticulospinal neurons are phasically active during fictive locomotion in the isolated nervous system of the lamprey. *Neurosci. Lett.* 69:239-243.
- KASICKI S., GRILLNER S., OHTA Y., DUBUC R. AND BRODIN L. (1989). Phasic modulation of reticulospinal neurones during fictive locomotion and other types of spinal motor activity in lamprey. *Brain Res.* 484:203-216.
- KATZ P. S. AND HARRIS-WARRICK R. M. (1991) Recruitment of crab gastric mill neurons into the pyloric motor pattern by mechanosensory afferent stimulation. *J. Neurophysiol.* 65(6): 1442-1451.
- KIEHN O., KJAERULFF O. (1998) Distribution of central pattern generators for rhythmic motor outputs in the spinal cord of limbed vertebrates. *Ann. NY Acad. Sci.* 860:110-129.
- KIEHN O., KJAERULFF O., TRESCH M., HARRIS-WARRICK R. M. (2001) Contributions intrinsic motor neuron properties to the production of rhythmic motor output in the mammalian rat spinal cord. *Brain Res. Bull.* 53:649-659.
- MACKAY-LYONS M. (2002) Central pattern generation of locomotion: A review of the evidence. *Physical Therapy* Vol. 82 No. 1.
- MAGNUSON D. S., TRINDER T. C. (1997) Locomotor rhythm evoked by ventrolateral funiculus stimulation in the neonatal rat spinal cord in vitro. *J. Neurophysiol.* 77(1):200-206.
- MANN K., GUPTA S., RACE A., MILLER M. A., CLEARY R. J. (2003) Application of circular statistics in the study of crack distribution around cemented femoral components. *J. Biomech.* 36:1231-1234.
- MARDER E. (2001) Moving rhythms. *Nature* 410(6830):755.

- MARDER E. AND CALABRESE R. L. (1996) Principles of rhythmic motor pattern generation. *Physiol. Rev.* 76(3):687-717.
- MATSUSHIMA T. AND GRILLNER S. (1992) Neural mechanisms of intersegmental coordination in lamprey: local excitability changes modify the phase coupling along the spinal cord. *J. Neurophysiol.* 67(2):373-388.
- MAYNARD D. M. AND DANDO M. R. (1974) The structure of the stomatogastric neuromuscular system in *Callinectes sapidus*, *Homarus americanus* and *Panulirus argus* (Decapoda Crustacea). *Philos. Trans. R. Soc. Lond. B. Biol. Sci.* 268(892):161-220.
- MCLEAN D. L., MERRYWEST S. D., SILLAR K.T. (2000) The development of neuromodulatory systems and the maturation of motor patterns in amphibian tadpoles. *Brain Res. Bull.* 53:595-603.
- MORTIN L. I. AND STEIN P. S. (1989) Spinal cord segments containing key elements of the central pattern generators for three forms of scratch reflex in the turtle. *J. Neurosci.* 9(7):2285-2296.
- MULLONEY B., SKINNER F. K., NAMBA H., HALL W. M. (1998) Intersegmental coordination of swimmeret movements: mathematical models and neural circuits. *Ann. N. Y. Acad. Sci.* 860:266-280.
- NAKAO T. AND ISHIZAWA A. (1987) Development of the spinal nerves in the lamprey: I. Rohon-Beard cells and interneurons. *J. Comp. Neurol.* 256(3):342-355.
- NISHIMARU H., KUDO N. (2000) Formation of the central pattern generator for locomotion in the rat and mouse, *Brain Res. Bull.* 53:661-669.
- OHTA Y., DUBUC R., GRILLNER S. (1991) A new population of neurons with crossed axons in the lamprey spinal cord. *Brain Res.* 564(1):143-148.
- PARKER D. (2001) Spinal cord plasticity. *Mol. Neurobiol.* 22(1-3):55-80.

- PAUL D. H. AND MULLONEY B. (1986) Intersegmental coordination of swimmeret rhythms in isolated nerve cords of crayfish. *J. Comp. Physiol.* 158: 215–224.
- PEARSON K. G. (1993) Common principles of motor control in vertebrates and invertebrates. *Annu. Rev. Neurosci.* 16:265-297.
- PEARSON K. G. (2000) Motor systems. *Curr. Opin. Neurobiol.* 10:649-654.
- PENNARTZ C. M. , DE JEU M. T., GEURTSSEN A. M., SLUITER A. A., HERMES M. L. (1998) Electrophysiological and morphological heterogeneity of neurons in slices of rat suprachiasmatic nucleus. *Journal of Physiol.* 506(Pt. 3):775-793.
- ROBERTS A., SOFFE S. R., PERRINS R. (1997) Spinal networks controlling swimming in hatchling *Xenopus* tadpoles. pp83-89 in *Neurons, Networks and Motor Behaviour*. Eds Stein, PSG, Grillner S., Selverston A. I. and Stuart D. G.; MIT Press, Boston.
- ROBERTS A. (2000) Early functional organisation of spinal neurons in developing lower vertebrates. *Brain. Res. Bull.* 53:585–593.
- ROBERTS A. AND CLARKE J. D. W. (1982) The neuroanatomy of an amphibian embryo spinal cord. *Phil. Trans. R. Soc.* 296:195–212.
- ROSSIGNOL S., CHAU C., BRUSTEIN E., GIROUX N., BOUYER L., BARBEAU H., READER T. A. (1998) Pharmacological activation and modulation of the central pattern generator for locomotion in the cat. *Ann. N. Y. Acad. Sci.* 860:346-59.
- ROVAINEN C. M. (1967) Physiological and anatomical studies on large neurons of central nervous system of the sea lamprey (*Petromyzon marinus*). II. Dorsal cells and giant interneurons. *J. Neurophysiol.* 30(5):1024-1042.
- ROVAINEN C. M. (1974) Synaptic interactions of identified nerve cells in the spinal cord of the sea lamprey. *J. Comp. Neurol.* 154(2):189-206.

- ROVAINEN C. M. (1974b) Synaptic interactions of reticulospinal neurons and nerve cells in the spinal cord of the sea lamprey. *J. Comp. Neurol.* 154:207-223.
- ROVAINEN C. M. (1979) Neurobiology of lampreys. *Physiol. Rev.* 59(4):1007-1077.
- ROVAINEN C. M. (1982) Neurophysiology. In: Hardisty, M.W., Potter, I.C (Eds.), *The Biology of Lampreys*. Vol. 4A. Academic Press, London, pp. 1-136.
- ROVAINEN C. M. AND BIRNBERGER K. L. (1971) Identification and properties of motoneurons to fin muscle of the sea lamprey. *J. Neurophysiol.* 34(6):974-982.
- ROVAINEN C. M., DILL D. A. (1984) Counts of axons in electron microscopic sections of ventral roots in lampreys. *J. Comp. Neurol.* 225:433-440.
- RUSSEL D. F. AND WALLÉN P. (1983) On the control of myotomal motoneurons during „fictive swimming“ in the lamprey spinal cord in vitro. *Acta Physiol. Scand.* 117:161-170.
- SELZER M. E. (1979) Variability in maps of identified neurons in the sea lamprey spinal cord examined by a wholemount technique. *Brain Res.* 163(2):181-193.
- SHUPLIAKOV O., WALLÉN P., GRILLNER S. (1992) Two types of motoneurons supplying dorsal fin muscles in lamprey and their activity during fictive locomotion. *J. Comp. Neurol.* 321(1):112-123.
- SMITH J. C. AND FELDMAN J. L. (1987) In vitro brainstem-spinal cord preparations for study of motor systems for mammalian respiration and locomotion. *J. Neurosci. Methods.* 21(2-4):321-33.
- SOFFE S. R. (1993) Two distinct rhythmic motor patterns are driven by common premotor and motor neurons in a simple vertebrate spinal cord. *J. Neurosci.* 13:4456-4469.
- STEIN P. S., McCULLOUGH M. L., CURRIE S. N. (1998) Spinal motor patterns in the turtle. *Ann. NY Acad. Sci.* 860:142-154.

- SUN Q. Q., DALE N. (1999) G-proteins are involved in 5-HT receptor-mediated modulation of N- and P/Q- but not T-type Ca^{2+} channels, *J. Neurosci.* 19:890-899.
- TANG D., SELZER M. E. (1979) Projections of lamprey spinal neurons determined by the retrograde axonal transport of horseradish peroxidase. *J. Comp. Neurol.* 188(4):629-645.
- TERÄVÄINEN H. AND ROVAINEN C. M. (1971) Fast and slow motoneurons to body muscle of the sea lamprey. *J. Neurophysiol.* 34(6):990-998.
- TRESCH M. C., KIEHN O. (2000) Motor coordination without action potentials in the mammalian spinal cord, *Nature Neurosci.* 3:593-599.
- TRETIKOFF D. (1909) Das Nervensystem von Ammocoetes. I. Das Rückenmark. *Arch. Mikrosk. Anat.* 73:607-680.
- ULLÉN F., DELIAGINA T. G., ORLOVSKY G. N., GRILLNER S. (1995) Spatial orientation in the lamprey. I. Control of pitch and roll. *J. Exp. Biol.* 198(Pt 3):665-673.
- WADDEN T., HELLGREN J., LANSNER A., GRILLNER, S. (1997) Intersegmental coordination in the lamprey: simulations using a network model without segmental boundaries. *Biol. Cybern.* 76:1-9.
- WALLÉN P. AND WILLIAMS T. L. (1984) Fictive locomotion in the lamprey spinal cord in vitro compared with swimming in the intact and spinal animal. *J. Physiol.* 347:225-239.
- WALLÉN P. AND LANSNER A. (1984) Do the motoneurons constitute a part of the spinal network generating the swimming rhythm in the lamprey? *J. Exp. Biol.*, 113:493-497.
- WALLÉN P., GRILLNER S., FELDMAN J. L., BERGELT S. (1985) Dorsal and ventral myotome motoneurons and their input during fictive locomotion in lamprey. *J. Neurosci.* 5(3):654-661.

WALLÉN P., EKEBERG Ö., LANSNER A., BRODIN L., TRAVÉN H., GRILNER S. (1992) A computer-based model for realistic simulations of neural networks. II. The segmental network generating locomotor rhythmicity in the lamprey. *J. Neurophysiol.* 68:1939-1950.

WALLÉN P., SHUPLIAKOV O., HILL R. H. (1993) Origin of phasic synaptic inhibition in myotomal motoneurons during fictive locomotion in the lamprey. *Exp. Brain Res.* 96:194-202.

ZAR J. H. (1998) *Biostatistical analysis*. 4th edition, Prentice Hall.

Danksagung

An erster Stelle möchte ich mich ganz besonders bei meinem Betreuer Prof. Dr. Ansgar Büschges für die Überlassung des Themas, seiner unendlichen Geduld was die Fertigstellung dieser Arbeit anging, seiner bedingungslosen Unterstützung und Förderung, und für die wertvollen Diskussionen und hilfreichen Anregungen im Verlauf dieser Arbeit danken.

Prof. Dr. Peter Kloppenburg danke ich herzlichst für die Übernahme des Zweitgutachtens.

Bei Prof. Dr. Sten Grillner und Prof. Dr. Abdel el Manira am Stockholmer Karolinska Institut bedanke ich mich herzlichst für die Möglichkeit der zwei sehr lehrreichen Forschungsaufenthalte dort und für viele Tipps, Anregungen und Diskussionen. Dr. Peter Wallén, Dr. David Parker und Dr. Lorenzo Cangiano danke ich für all die Geduld, Tipps und Hilfen bei der Suche nach den richtigen „Motoneuronen“. Dr. Dietmar Heß und seiner Frau Yvonne sehr herzlich für die Wohnmöglichkeit während meines ersten Stockholmaufenthaltes und für die vielen netten Gespräche.

PD Dr. „Jochen“ Schmidt danke ich besonders für die Durchsicht und Korrektur des Rohmanuskriptes dieser Arbeit und für Tipps und Diskussionsbereitschaft. Dr. Tim Mentel, Dr. Dirk Bucher und Dr. Hanno Fischer für Anleitungen, Hilfe, Motivation, Ideen und Diskussionen. Dr. Hans Scharstein für fruchtbare Diskussionen vor allem statistischer Fragen, namentlich zu nennen ist hier vor allem die „Kreisstatistik“.

Bei den ehemaligen und jetzigen Mitarbeitern der Arbeitsgruppe möchte ich mich ganz herzlich für das gute Arbeitsklima bedanken. Namentlich nennen möchte ich hier vor allem Dr. Turgay Akay, Jens Gabriel, Anke Borgman, Gabriel Knop, Lutz Körschgen und natürlich Violetta Weiler. An die gemeinsame Zeit denke ich oft und gerne zurück.

Hans-Peter Bollhagen danke ich besonders für die wertvolle Hilfe bei allen technischen Fragen und für viele anregende Gespräche. Christa Graef und Sherylane Marasigan für die unermüdliche Hilfe bei Ansetzung von vielen vielen Litern Neunaugenringer.

Michael Dübbert und Michael Schöngen danke ich herzlichst für die Bereitschaft mir bei Elektronikproblemen zu helfen und für Diskussionen und Gespräche.

Prof. Dr. Milan Höfer und Dr. Vladimir Vacata danke ich sehr herzlich für die Hilfe bei der Durchsicht und Korrektur meiner Arbeit, Dr. Udo Hölker und Dr. Jürgen Lenz von der bioreact GmbH für das Verständnis das sie für mich aufbrachten wenn alles mal wieder „ein wenig länger“ gedauert hat.

Bedanken möchte ich mich auch bei Dr. Nicole Lindemann und Helmut Wratil für unzählige Kaffeestunden gefüllt mit vielen lustigen aber auch traurigen Geschichten und Ereignissen.

Dr. Kai Pata von der Universität Tartu in Estland danke ich herzlichst für ihre Hilfe bei der Erklärung der Methode des „hierarchical clustering“ und für Korrekturen am Manuskript. Ausserdem danke ich ihr für die vielen wundervollen Stunden die wir gemeinsam hatten und hoffentlich noch haben werden.

Publikationen und Teilpublikationen

KRAUSE A. AND BUSCHGES A. (2001) Generation and control of fin motoneuron activity in the lamprey spinal locomotor network. 6th International Congress of Neuroethology, Bonn.

KRAUSE A., RIEWE D., BUSCHGES A. (2002) Generation and control of fin motoneuron activity in the lamprey spinal locomotor network. Abstracts of the 95th Annual Meeting of the Deutsche Zoologische Gesellschaft Halle/Saale.

KRAUSE A., MENDEL T. AND BUSCHGES A. (2003) Contribution of intra- and intersegmental signals to the generation of fin motoneuron activity in the lamprey spinal locomotor network. Proceedings of the 29th Neurobiology Conference, Göttingen.

KRAUSE A. AND MENDEL T. (2003) Mechanisms mediating coordination between myotomal and fin motoneurons in the lamprey spinal cord during fictive locomotion. Neurovisionen, Düsseldorf.

MENDEL T., POHLER S., KRAUSE A. AND BUSCHGES A. (2004) Distribution of fin motoneurons in the spinal cord of the lamprey and their activity pattern during NMDA induced fictive swimming. 7th International Congress of Neuroethology, Nyborg..

MENDEL T., KRAUSE A. AND BUSCHGES A. (2005) Generation of fin motoneuron activity during NMDA-induced „fictive swimming“ in the isolated lamprey spinal cord. Proceedings of the 30th Neurobiology Conference, Göttingen.

Erklärung

Ich versichere, dass ich die von mir vorgelegte Dissertation selbständig angefertigt, die benutzten Quellen und Hilfsmittel vollständig angegeben und diejenigen Stellen der Arbeit - einschließlich Tabellen, Karten und Abbildungen -, die anderen Werken im Wortlaut oder dem Sinn nach entnommen sind, in jedem Einzelfall als Entlehnung kenntlich gemacht habe; dass diese Dissertation noch keiner anderen Fakultät oder Universität zur Prüfung vorgelegen hat; dass sie - abgesehen von unten angegebenen Teilpublikationen - noch nicht veröffentlicht worden ist sowie, dass ich eine solche Veröffentlichung vor Abschluss des Promotionsverfahrens nicht vornehmen werde. Die Bestimmungen dieser Promotionsordnung sind mir bekannt. Die von mir vorgelegte Dissertation ist von Prof. Dr. Ansgar Büschges betreut worden.

Köln den 22. 9. 2005

Curriculum Vitae

Persönliche Daten:

Name: Alexander Krause
Geburtsdatum: 13. Februar 1970
Geburtsort: Remagen, Rheinland Pfalz
Familienstand: ledig
Staatsangehörigkeit: Deutsch

Schulbildung:

09/1976-07/1980 Grundschule in Remagen
08/1980-06/1986 Staatliche Realschule Remagen
09/1986-05/1989 „Amos-Comenius-Gymnasium“ in Bonn-Bad Godesberg
mit Abschluß der Allgemeinen Hochschulreife

wissenschaftliche Ausbildung:

10/1991-05/1996 Studium der Biologie an der Universität Bonn
06/1996-07/1997 Diplomarbeit an der Universität Bonn mit Abschluß zum Diplom-Biologen.
Hauptfach: Mikrobiologie, Nebenfächer: Zellbiologie, Physik.
Titel der Diplomarbeit: „Elektrophysiologische Untersuchung des Ionen-
transportes in Protoplasten verschiedener Stämme der Hefe
Saccharomyces cerevisiae“.
Diplom am 11. 7. 1997
08/1997-03/1999 wissenschaftlicher Mitarbeiter an der Universität Bonn in der
Arbeitsgruppe von Prof. Dr. Milan Höfer
seit 04/1999 Promotionsstudiengang an der Universität zu Köln in der
Arbeitsgruppe von Prof. Dr. Ansgar Büschges